MOBILE PROPELLER DYNAMOMETER

VALIDATION

By

MASON WADE MORRIS

Bachelor of Science in Mechanical Engineering

Bachelor of Science in Aerospace Engineering

Oklahoma State University

Stillwater, Oklahoma

2012

Submitted to the Faculty of the
Graduate College of the
Oklahoma State University
in partial fulfillment of
the requirements for
the Degree of
MASTER OF SCIENCE
December, 2013

MOBILE PROPELLER DYNAMOMETER

VALIDATION

Thesis Approved:

Dr. Jamey D. Jacob

Thesis Adviser

Dr. Andrew S. Arena

Dr. Rick Gaeta

Name: MASON WADE MORRIS

Date of Degree: DECEMBER, 2013

Title of Study: MOBILE PROPELLER DYNAMOMETER VALIDATION

Major Field: MECHANICAL AND AEROSPACE ENGINEERING

ABSTRACT: With growing interest in UAVs and OSU's interest in propeller performance and manufacturing, evaluating UAV propeller and propulsion system performance has become essential. In attempts to evaluate these propellers a mobile propeller dynamometer has been designed, built, and tested. The mobile dyno has been designed to be cost effective through the ability to load it into the back of a test vehicle to create simulated forward flight characteristics. This allows much larger propellers to be dynamically tested without the use of large and expensive wind tunnels. While evaluating the accuracy of the dyno, several improvements had to be made to get accurate results. The decisions made to design and improve the mobile propeller dyno will be discussed along with attempts to validate the dyno by comparing its results against known sources. Another large part of assuring the accuracy of the mobile dyno is determining if the test vehicle will influence the flow going into the propellers being tested. The flow into the propeller needs to be as smooth and uniform as possible. This is determined by characterizing the boundary layer and accelerated flow over the vehicle. This evaluation was accomplished with extensive vehicle aerodynamic measurements with the use of full-scale tests using a pitot-rake and the actual test vehicle. Additional tests were conducted in Oklahoma State University's low speed wind tunnel with a 1/8-scale model using qualitative flow visualization with smoke. Continuing research on the mobile dyno will be discussed, along with other potential uses for the dyno.

TABLE OF CONTENTS

Chapter Page

LIST OF FIGURES

Figure Page

Figure Page

Figure Page

CHAPTER I

INTRODUCTION

Testing and evaluating aircraft propeller performance has been important since the early 1900's; but with the rise of the jet age the propeller research focus shifted to turbine performance. However, with the rapid growth of the UAV industry, finding efficient ways to measure propeller/engine performance is as important as ever. When determining an aircraft's endurance, range, and climb/takeoff performance it is essential to have the propulsion system characterized. With the aircraft spending almost all of its time in a forward flight regime it is necessary to test propellers dynamically since propellers behave very different dynamically than statically. With this in mind, a propeller/engine dynamometer that can take not only static, but also dynamic measurements of the thrust and torque, are essential.

With many UAVs having very special flight profiles you may not be operating within a manufacturer's published performance data range or performance data simply may not be available, in addition, very often in the UAV industry propellers are bought from small companies that do not have the resources to test and evaluate the performance of their propellers. The data from the manufacture may need validation before flight-testing on an expensive research aircraft. These are all reasons why developing a propeller dyno to accurately measure propulsion system flight performance is vital. The research in custom-built composite propellers at OSU also shows an additional need for determining propeller flight performance.

A wind tunnel dyno can produce forward flight characteristics, but this is often expensive. On the other hand, the wind tunnel available may not be large enough to fit the desired propeller, or wind tunnel blockage effects may be too large to correct. With ongoing research in UAV propellers and engine design at Oklahoma State University, a mobile propeller and engine test unit was developed. This system will allow accurate dynamic propeller and engine performance measurements in a cost effective manner.

After designing the mobile dyno, it is validated against a known source to assure that the system is accurate in computing performance characteristics. In addition to validation, the flow going into the propeller must be smooth and uniform as to not affect the propeller's aerodynamics. To assure the vehicle's aerodynamics are not causing errors in measurements the inflow into the propeller is measured to assure that the boundary layer and accelerated flow over the vehicle are not within the propeller plane.

Thesis Goals and Objectives

The purpose of this thesis is to discuss the design of the mobile dyno and the renderings made to alleviate problems encountered while running initial tests. To assure the accuracy of the mobile dyno it is validated against a known source. The comparison used for the mobile dyno is the wind tunnel dyno designed at OSU and published data from University Illinois at Urbana-Champaign (UIUC). Although the validation is not finished due to the needed renovation of the wind tunnel dyno, the validation process and the completed testing results will be discussed.

Another large part of the research is determining the flow over the test vehicle to assure it does not influence the propeller's aerodynamics. Much like when testing in a wind tunnel the tunnel is measured for its airflow characteristics to assure the flow is smooth, uniform, and as close to laminar as possible. The process taken while characterizing the flow over the test vehicle and the results will be discussed in great detail.

CHAPTER II

REVIEW OF LITERATURE AND PREVIOUS WORK

Before designing any type of dynamometer, there must first be an understanding of what measurements are needed to fully characterize the propeller or engine. When designing a propeller dyno, a discussion of how a propeller is characterized and what parameters are needed to acquire the overall performance of the propeller is required.

While mobile dyno research has been conducted, most of the mobile dyno designs are not available in literature. However, previous work in static dynos or dynos mounted in wind tunnels are very useful and references are plentiful. Previous work at Oklahoma State University was the development of a wind tunnel dyno to conduct measurements of small propellers in the University's low-speed wind tunnel. The University Multispectral Laboratories has also developed a dyno to examine the static performance of many small UAV engines.

Since the dyno will be mobilized by a test vehicle, the vehicle must be shown to not influence results from the propeller. To assure this is not the case, determining the flow into the propeller plane is essential. To fully measure and understand the vehicle's aerodynamics, boundary layer flow must be discussed and understood to allow us to compute the variables that help describe the airflow.

Propeller Performance

To understand how to design a propeller dynamometer, we must first understand what defines a propeller's performance and how to accurately measure these parameters. By looking at *Theory of Propellers*, a propeller must produce thrust to allow the aircraft to counter the drag produced by the vehicle. Unfortunately, the thrust production comes with the penalty of requiring a certain amount of torque or power to turn the propeller. Obviously, both of these parameters are heavily influenced by the propeller's rpm and forward velocity. While these are the most important measurements, much like a wing, the performance is also affected by the density of the air in the propellers airstream. We quickly see that a propeller can be fully characterized by measuring its thrust, torque, rpm, and velocity.

However, this does not allow us to compare different propellers against one another effectively. To make comparisons, we must first use dimensional analysis to find some very important parameters. These parameters take the propeller's measured outputs and make new terms that are non-dimensional. The factors used to define a propeller's performance can be found in the dimensionless terms found below (Theodorsen, T.).

$$J = \frac{V}{nd} \qquad C_T = \frac{T}{\rho n^2 d^4} \qquad C_P = \frac{P}{\rho n^3 d^5} \qquad \eta = \frac{TV}{P} = \frac{C_T V}{C_P n d}$$

Since these terms are dimensionless, it allows a person to compare several propellers of different diameters, pitches, and airfoil cross-section. When looking at Thrust Coefficient, C_T, it shows that propeller thrust and rotational speed are the only conditions that change and must be measured throughout testing to accurately define this term. Similarly, you need to measure torque and rotational speed in order to produce a Power Coefficient or C_P. Then Advanced Ratio J is a function of velocity and rotational speed, which allows us to plot a propeller's performance on one plot to show the effects of both forward velocity and rotational speed on the propeller. After

looking at the dimensionless terms, it is obvious that thrust, torque, rotational speed, and velocity must be measured in real time to produce accurate propeller performance data. Also, note that the ambient air conditions must be measured before or during each test, but can be assumed to be constant; so these conditions only need to be measured once. Although the parameters discussed earlier are the only parameters that are needed to define a propeller's performance, additional parameters will be needed on the mobile dyno to assure accuracy in each of these components.

Boundary Layer Flow

When characterizing the flow over the test vehicle, the boundary layer flow will be defined using help from *Viscous Fluid Flow*. This book proves to be very useful in the assumptions and approximations of boundary-layer theory. When describing the boundary layer over the vehicle, flow will be assumed to boundary-layer flow past a flat plate. When looking at boundary layer integrals notice that boundary layer thickness δ is only a function of the downstream distance and velocity of the free-stream. Other terms used in describing boundary layer flow will be displacement thickness and momentum thickness, both shown below (White, F. M., 2009).

$$\delta^* = \int_0^\infty \left(1 - \frac{u}{U}\right) dy \qquad \theta = \int_0^\infty \frac{u}{U}\left(1 - \frac{u}{U}\right) dy$$

However, when looking at the laminar Blasius solution, these terms simplify to the versions found below. These calculations are, unfortunately, not very useful, due to the large Reynolds number proving that the flow is turbulent.

$$\delta = \frac{5.0x}{\sqrt{Re}} \qquad \delta^* = \frac{1.7208x}{\sqrt{Re}} \qquad \theta = \frac{0.664x}{\sqrt{Re}}$$

Since these relations will not be very useful, an alternative approach will need to be used to solve for displacement and momentum thickness. The approach used in this paper will be curve

fitting the measured boundary layer profile using a turbulent approximated power-law, shown below. Once we have this equation we can solve for the displacement and momentum thickness as functions of δ.

$$\frac{u}{U} = \left(\frac{y}{\delta}\right)^{\frac{1}{n}}$$

These boundary-layer relations will be used to help define the vehicle's aerodynamics later in this paper.

Experimental Study of Pickup Truck Aerodynamics

Research on pickup truck aerodynamics of the wakes created behind the truck were studied by the University of Michigan (Abdullah, 2009). While this paper is more focused on the flow behind the cab and truck bed instead of the flow over the truck cab, there can still be a lot of valuable information taken from this study. Much like the experimental setup used and the PIV measurements give good insight of what the flow looks like above the cab.

The University of Michigan study was conducted on a very generic pickup model mounted in a wind tunnel with several pressure ports on the vehicle to get actual pressure measurements from the flow around the vehicle. The vehicle was also mounted a large flat plate that was displaced a specified distance from the wind tunnel floor to simulate the ground moving beneath the vehicle, or ground effect. Along with the pressure measurements, PIV measurements were taken by shining a laser sheet into the wind tunnel and seeding smoke into the wind tunnel. A high-speed camera will take images that can then analyze the smoke particle velocity and path utilizing an image shifting algorithm.

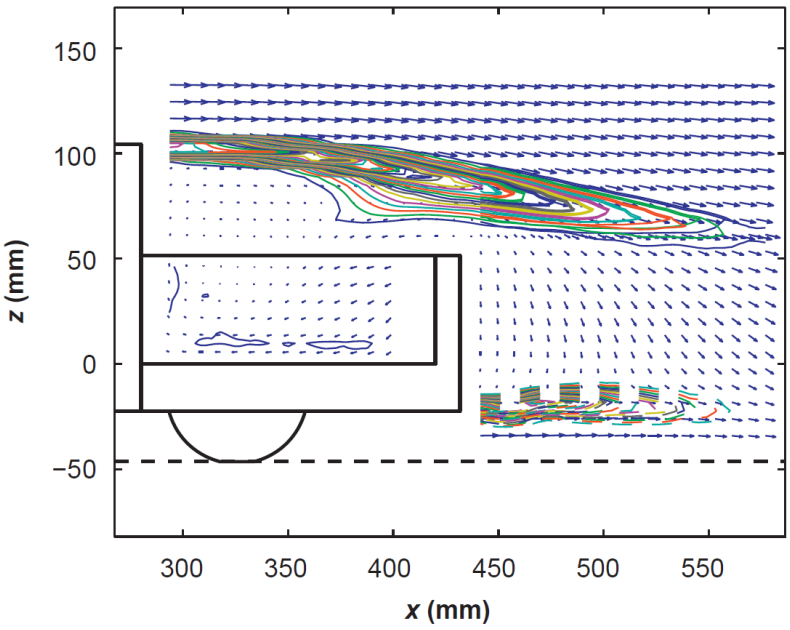

Figure 1-Mean velocity and vorticity fields in the symmetry plane of the wake of a pickup truck (Abdullah,2009)

Although the study does not focus entirely on the flow over the truck cab, we can still gather a lot of information about the flow over the cab by looking at the PIV plots, Figure 1 shows an example. By looking at this figure, you see that except for the flow within 25mm above the cab of the model the flow is uniform and parallel to the cab. Unfortunately, we cannot tell if the flow has been accelerated over the model.

Wind Tunnel Dynamometer

The goal when designing the wind tunnel dyno was to develop a low-cost system that would use the OSU wind tunnel to accurately test small UAV propulsion systems. While there have been several propeller dynos developed, most are very costly to build and operate. Since the wind tunnel dynamometer was such a success in producing a low-cost system, it proved to be a good foundation for the design of the dynamometer portion of the mobile dyno.

Since the OSU wind tunnel is used for the discussion of the wind tunnel dyno and the scaled vehicle aerodynamics testing portion of this paper, giving a wind tunnel layout is

appropriate. The OSU wind tunnel is a low-speed open-return wind tunnel that uses a 125hp motor to turn a fan that draws air into the wind tunnel. The air comes into the wind tunnel through a honeycomb air straightening screen at the inlet and is contracted through a 15:1 contraction section then pulled through a 3-foot-by-3-foot test section. A basic schematic of the wind tunnel is shown in Figure 2 below.

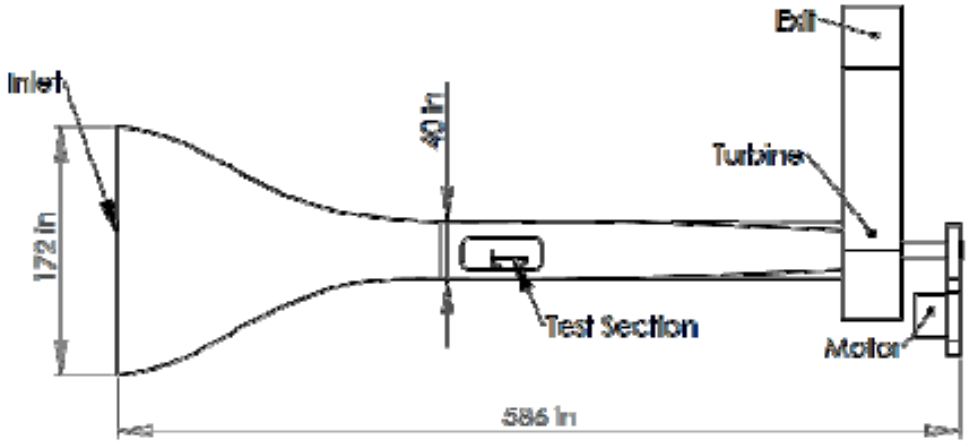

Figure 2-Oklahoma State University Low Speed Wind Tunnel Schematic

The dyno is constructed of mostly aluminum to be lightweight and easily machined. It is mounted inside the wind tunnel on a stand that is bolted down through the bottom of the tunnel using four bolts. The stand simply serves as a way to mount the dynamometer to the wind tunnel and place the propeller center at the center of the wind tunnel section. By utilizing a four-bar linkage system the dyno is allowed to pivot in the thrust direction by using four low-friction bearings. With low cost in mind, the wind tunnel dyno utilizes beam style load-cells to measure torque, instead of a costly torque sensor that would require a sophisticated mounting system. It proves much cheaper and simpler to have the motor and propeller system mounted to a shaft that rides on two low-friction bearings. The shaft then transmits any torque from the propulsion system to a beam-load-cell that fixes the shaft from rotating. The thrust is also measured using a cost effective beam load-cell. The thrust load-cell is mounted to the top portion of the stand and

then fixes the dyno from pivoting in the thrust direction, thereby transmitting all forces in the longitudinal direction through the load-cell (Conner, J. and Arena, A., 2002).

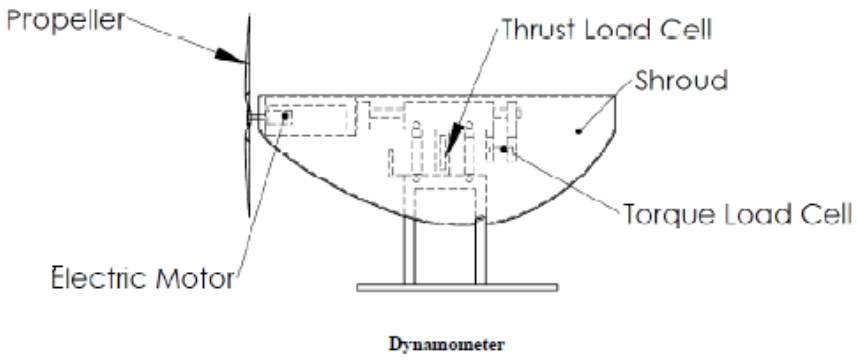

Figure 3-Wind Tunnel Dyno Schematic (Conner, J. and Arena, A., 2002)

Measuring rotational speed is achieved by using a simple optical sensor that reads from reflective tape mounted to one of the propeller blades. This creates a pulse each time the propeller blade completes a full revolution sends a signal to a display containing a signal conditioner. The wind tunnel velocity is measured with a small pitot-static tube that is mounted upstream with pressure readings being sent by a pressure transducer. A composite fairing stops any drag not induced by the propeller by completely shielding the dynamometer from the airflow.

Figure 4-Custom 5-Blade Propeller mounted on Wind Tunnel Dyno

Overall this has proven to be a very effective way to produce performance data for propellers up to 18 inches without blockage effects. The design methods used to make this dynamometer have heavily influenced dynos designed at OSU including the mobile dyno.

Automated Dynamic Propeller Testing

In the past, to allow more precision and rapid testing of multiple propellers, the wind tunnel dyno has been set up to be completely autonomous. For example, just mount the desired propulsion system, set the wind tunnel speed and rpm limits, press a button, and a Labview program will control the wind tunnel speed and propeller rotational rate through a range that will accurately record propeller performance data (Gamble, 2009).

A future goal is to use this information to make the mobile dyno system more autonomous so that when testing propellers the forward velocity is held as constant as possible with the truck accelerator and a Labview program runs the propeller at several different rotational speeds to get an entire range of advanced ratio values. Then simply change the truck speed and record data through another range of propeller rotational speeds. All of the data acquisition would be autonomous along with propeller rpm control. This will make the testing process more efficient and consistent and allow multiple propellers to be tested more rapidly.

High Energy Density Propulsion Systems and Small Engine Dyno

This research has proven useful in the different aspects of the engine dynamometer design. Since the mobile dyno will be fitted with small engines for a complete propulsion system performance analysis, the research in developing the small engine dynamometer will assist with successful integration (Hays, T., 2009).

The energy density research could also be continued with the mobile dyno to create dynamic tests, instead of strictly static engine test with a constant load. When running a small

engine with a propeller, the air speed of the system will heavily impact the performance of the system, along with the performance dynamics.

University Multispectral Labs UAS Engine Study

With a goal to reduce overall aircraft weight without reducing performance, the UML undertook research of several typical UAS engines. Another major focus of this research was fuel injection improvements on non-fuel injected engines and acoustic signatures on engines in different exhaust configurations. A total of 69 engines within the 5-100 horsepower range were tested during this study. To successfully evaluate these different engines, a new engine dynamometer was designed using some of the design aspects from the wind tunnel dyno discussed earlier.

The dynamometer design shown in Figure 5below consisted of a 5.625-inch diameter steel tube that rotates on two low-friction deep groove bearings called a spindle design. The spindle is mounted to a very large and heavy frame to allow up to 100-hp engines to be tested. The torque tube is fixed with a chain in series with an s-type tension load-cell attached to the torque bar, which allows all the torque to go through the load-cell. The engine is mounted to the opposite side of the steel tube on a plate which allows all torque to be transmitted through the spindle housing. The dyno measured rpm using an optical sensor and reflective tape, much like the wind-tunnel dyno, and fuel flow was measured as well to determine the fuel efficiency of the engines. The engines were put under load by installing a propeller and varying rpm (UML, 2009).

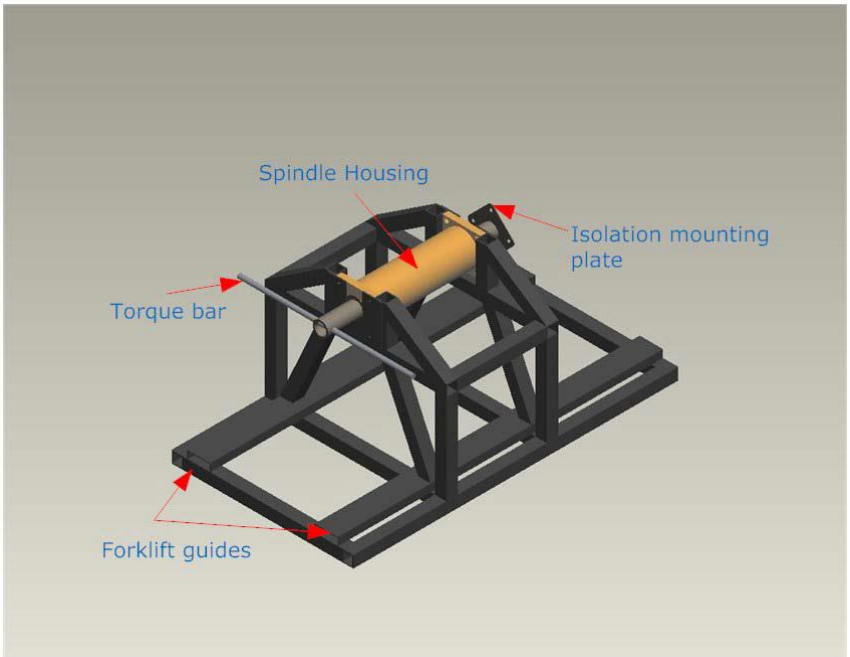

Figure 5-UMLSmall Engine Static Dynamometer Schematic (UML, 2009)

The dynamometer portion of the mobile dyno uses the same spindle housing used for this dyno, but is made more versatile by adding a way to measure thrust. This modification allows measurement of propeller performance, as well as engine performance. The way the modification to thrust was made will be discussed in detail later.

Designing and Manufacturing of Mobile Dyno

The design and manufacturing of the mobile dyno was a senior design project for graduating Oklahoma State University seniors in Mechanical Engineering. Once OSU had decided to design a mobile dyno used for propeller and propulsion system testing, the students' design requirements were to properly size and manufacture a system that could dynamically test propellers in an effective, accurate manner. The original design criterion for this project was that engines up to 100 horsepower and propellers up to 6 feet in diameter should be the largest testable setup during simulated flight conditions. The parameters measured would be thrust, torque, and rpm of the engine/motor (McGovney, 2010).

It was decided that a truck would be the best solution to produce forward flight characteristics since research trucks are readily available and capable of traveling the required test flight speeds. Once this was established, the next major design decision was where to install the dyno relative to the truck. The dyno installation was narrowed down to three obvious options: attached to the front, in the truck bed, or on a trailer pulled from behind, as shown in Figure 6. Each of these options has pros and cons. While in front would offer the most undisrupted, smooth airflow, a front mount would have to be designed to attach it to the front of the truck which would make it difficult to see when driving. A trailer would be convenient for transportation, but would create extra cost for the purchase of a trailer and the propeller would get dirty flow from the truck. The final decision was to design a dyno to fit in the back of the test vehicle with the dynamometer mounted high above the truck cab to allow clean flow into the propeller. While loading and unloading would be undesirable, truck bed installation is the cheapest and safest option for clean flow. Since the dyno will be installed in a truck bed, it is sized so that it is mounted high above the cab to put the propeller in undisrupted flow; but not to interfere with traffic lights and power lines. For stability during testing the dyno was made with a very heavy base to prevent shifting. For versatility, the dyno was designed to fit in the designated test vehicle with an 8-foot bed, as well as almost any full-size truck with a standard size bed.

Figure 6-Different Mobile Dyno Location Design Options

After determining that the dyno would be mounted in a truck bed, making the dyno easily transportable was the next consideration. The dyno needs to be able to be unassembled or collapsible to make it more stable and easier for transportation during loading and unloading as

well as driving to the test location. The dyno is designed to be user friendly by hinging the legs allowing the back legs to fold inward and the front legs to fall back allowing it to collapse in half. Because of its large size and weight, a winch and a large 12-volt deep-cycle battery mounted to the dyno is used to assist in folding and unfolding the mobile dyno. The mobile dyno is also fitted with large c-channel to allow a forklift to lift the dyno into and out of the test vehicle. The two different dyno positions are shown in Figure 7 below.

Figure 7-Mobile Dyno in Collapsed and Test Position (McGovney, 2010)

Figure 8-Mobile Dyno Installed in Test Vehicle (McGovney, 2010)

Data acquisition is achieved with a laptop and a custom Labview program that records data from a National Instruments Data Acquisition (DAQ) unit. The raw voltages come from the display box shown in Figure 9 below and are wired into the DAQ. All of the sensors for the dyno plug into the display box using 15-pin connector to allow the display boxes to filter and condition the sensor signals while also allowing the operator see outputs in real time. The display box is powered by the 12-volt accessory plug in the truck cab and gives excitation voltage to all of the sensors. The sensors used are rpm with an optical sensor, thrust with a beam-type load-cell, and torque with a beam-type load-cell. As will be discussed later, other sensors are added to accurately assess the propeller's performance.

Figure 9-Mobile Dyno Display and Signal Conditioner Box (McGovney, 2010)

For initial testing, the dyno is fitted with a large out-runner Hacker motor powered by four 12-volt deep-cycle batteries wired in series to produce 48-volts. This motor is capable of testing propellers around 25 inches in diameter. For propellers much larger than this, an internal combustion engine will be fitted to meet the propeller's power requirements.

CHAPTER III

DYNAMIC PROPELLER DYNO

After the manufacturing of the mobile dyno, several preliminary propeller tests were conducted. The preliminary tests revealed several shortcomings that needed to be addressed and corrected before the dyno could be used to obtain accurate results. The overall experimental setup for the dynamic dyno will be discussed, along with all modifications made to improve the overall performance.

The mobile dyno will also be validated against known sources of data to assure that the dyno is supplying accurate and reliable results. The iteration process of running tests and upgrades, along with attempts to validate the propeller dyno, are discussed in detail below.

Experimental Setup

The dynamic dyno design, as discussed earlier, is a large, collapsible propeller/engine dyno that fits in the back of a test vehicle. When the dyno is in the test configuration, it is erected to place the propeller dynamometer portion high above the test vehicle's cab so that there is no influence from the vehicle's aerodynamics. A smooth, relatively flat road is needed to help keep the data from being "noisy" from vibrations caused by the road and truck suspension. A road with little traffic and a speed limit of at least the propeller test speeds is required to get the range of data needed. A vacant airport would be the best test location, but these are difficult to find and use; however, if possible, may be used in the future. In our case, the tests were performed with a single cab ¾-ton Chevrolet truck on a relatively straight and smooth highway on the outskirts of

Stillwater.

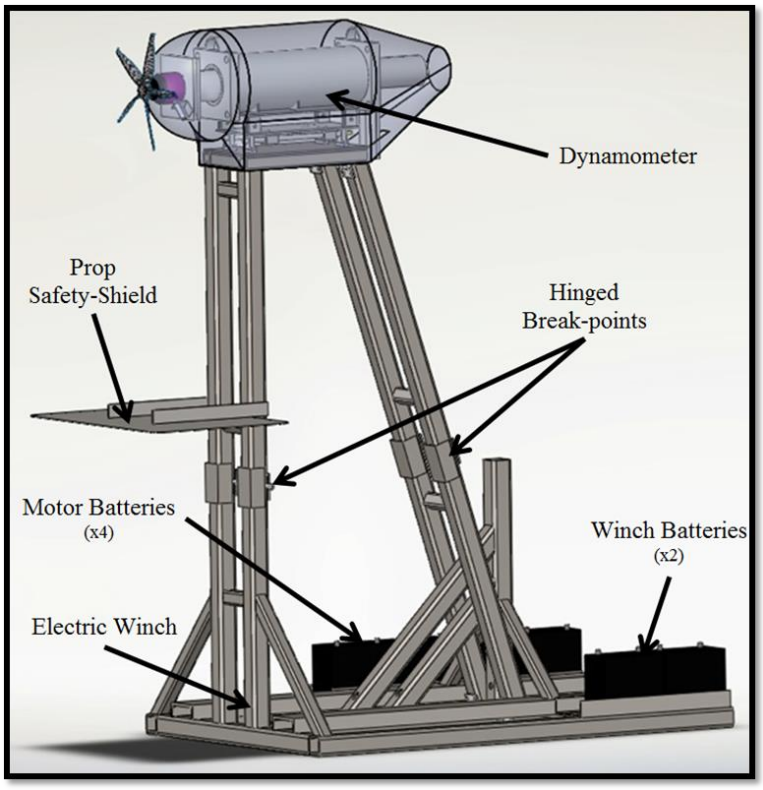

Figure 10-Overall Mobile Dyno Schematic

The mobile dyno unit consists of the large collapsible frame with the dynamometer mounted to the very top. A schematic is shown in Figure 10 above. The dyno is made collapsible by hinging the rear legs in the middle and bottom of the section allowing the legs to fold in on themselves, while the front legs are only hinged in the middle allowing the dyno to fold over 90 degrees, which drastically reduces its overall size. This helps improve stability during loading/unloading and transportation to the testing site. Due to the dyno's large size, an electric cable winch is used to collapse and raise the dyno from each position.

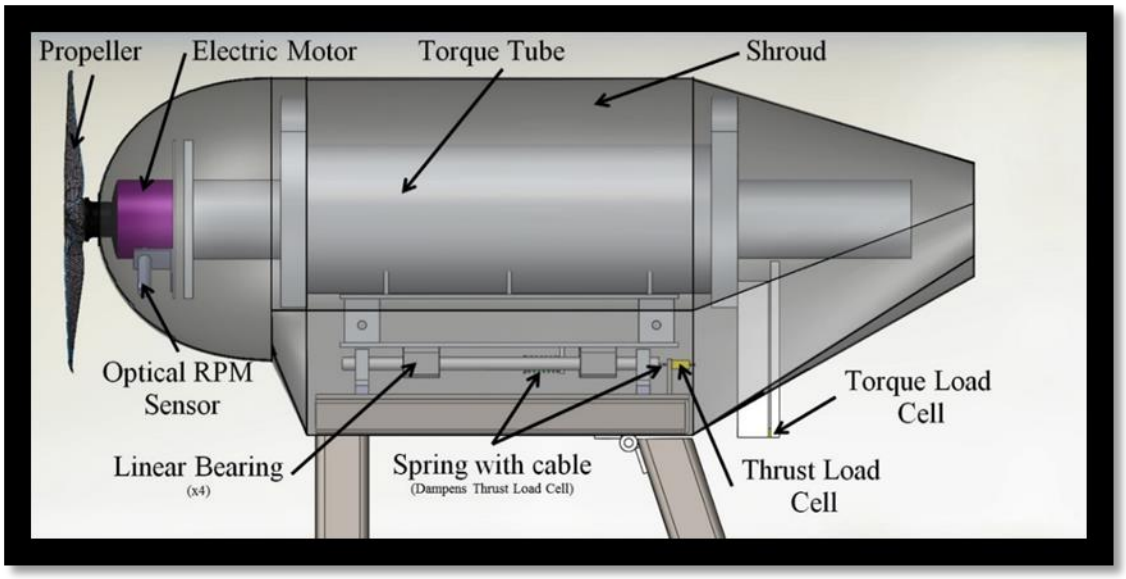

Figure 11-Overall Mobile Dyno Dynamometer Schematic

The dynamometer consists of the torque tube and housing, or spindle system, which is a steel tube mounted inside of two low-friction, deep-groove, and cylindrical-roller bearings. The motor and propeller are mounted to the front of the torque tube where a flat plate has been welded as a motor mount. The torque tube is fixed by bolting a beam type load-cell to an aluminum bracket that is bolted to the spindle housing and having another aluminum bracket bolted to the torque tube with a machined slot just large enough to fit the load-cell width. This allows all of the torque to be transmitted to the load-cell through a moment arm at the opposite end of the motor/propeller. To allow thrust measurements, the torque tube system is mounted to two rails via four low-friction linear bearings that are free to move forward and backward, or left and right when looking at Figure 11. The torque tube rail system is held in place with another beam type load-cell that is mounted to a steel tab welded to the mobile dyno mounting pad. An all-thread with a stiffener is bolted to the bottom of the dynamometer rail system by another welded steel tab and then bolted to the load-cell on the other end allowing thrust loads to be transmitted to the sensor. Rpm measurement is taken by an optical sensor that reads from reflective tape mounted to the out-runner motor. The propeller motor is powered by four 12-volt deep-cycle batteries wired

in series to produce 48-volts. The winch that collapses and raises the dyno is powered by two 12-volt deep-cycle batteries.

Improvements

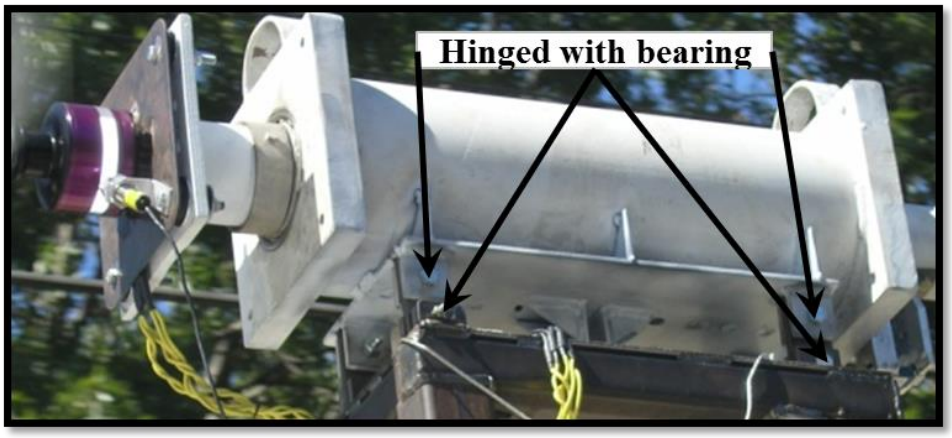

Figure 12-Original Four-bar Linkage System Used to Measure Thrust

The first improvement was a different design to measure thrust. The original 4-bar linkage system shown above caused large errors in the thrust reading due to the geometry shown in Figure 13. The four-bar system allows travel in an arc path. As a result, if the torque tube is not perfectly balanced on the top of the arc, a component of the dynamometer's weight rests on the thrust load-cell. This design is very similar to the wind tunnel dyno and works well with the wind tunnel since the weight of the dyno is much less than on the mobile dyno. However, since the dynamometer of the mobile dyno weighs over 100 pounds, not only are the errors very large and compounded with any angle of incline, the load-cells are also very easily overloaded and damaged during testing.

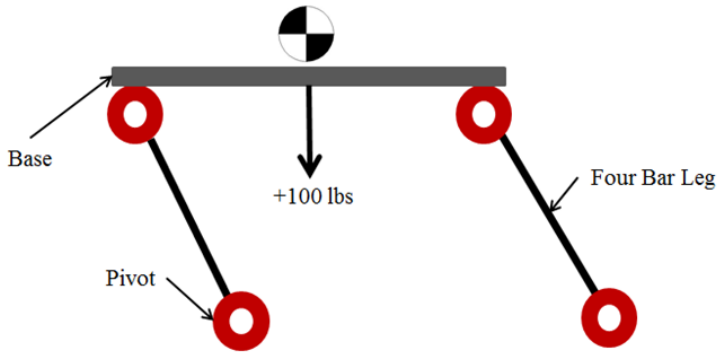

Figure 13-Four-bar Linkage System Geometry

To correct this problem, a new rail system was designed to allow the dynamometer to only move in the thrust direction. A cross-section view is shown in Figure 14. The rails used are two pieces of ¾-inch polished stainless steel rod mounted to four aluminum pillow blocks which are bolted to the mobile dyno mounting platform. The four low-friction linear bearings are bolted to the bottom of the dynamometer and glide on the rails. When the rail system was designed, the thrust load cell was moved out from under the dynamometer to the back edge to allow easy access. The load-cell is now held to the dynamometer by a ¼-inch all-thread with a stiffener sleeve. When the dyno is collapsed, the thrust load-cell can be loosened and four shaft collars can be tightened against the linear bearings to lock the dynamometer in place.

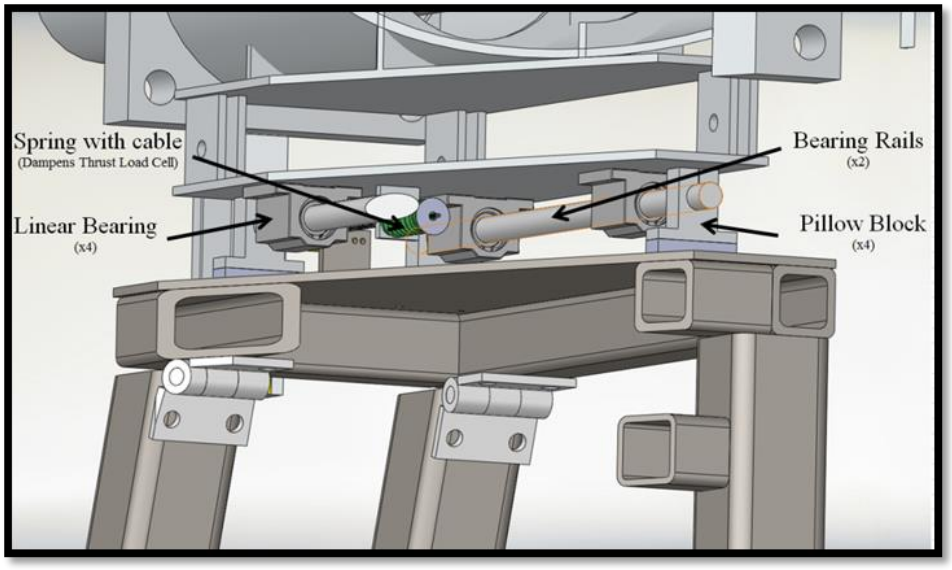

Figure 14-New Rail-System Design for Thrust Measurements

Another anticipated problem encountered during testing was the influence of drag on the dynamometer. Figure 15 is a graph of the results of a test run without a propeller, traveling at a constant 30mph using the truck speedometer as a reference. The constant low spots around 250 seconds in the data show the drag on the dynamometer. As shown in the graph, at 30mph the drag will be roughly a half pound and will obviously get worse as speeds increase. The spikes in the graph are indications of the test vehicle going through inclines and the sensors reading a weight component of the dynamometer's weight, and will be discussed later.

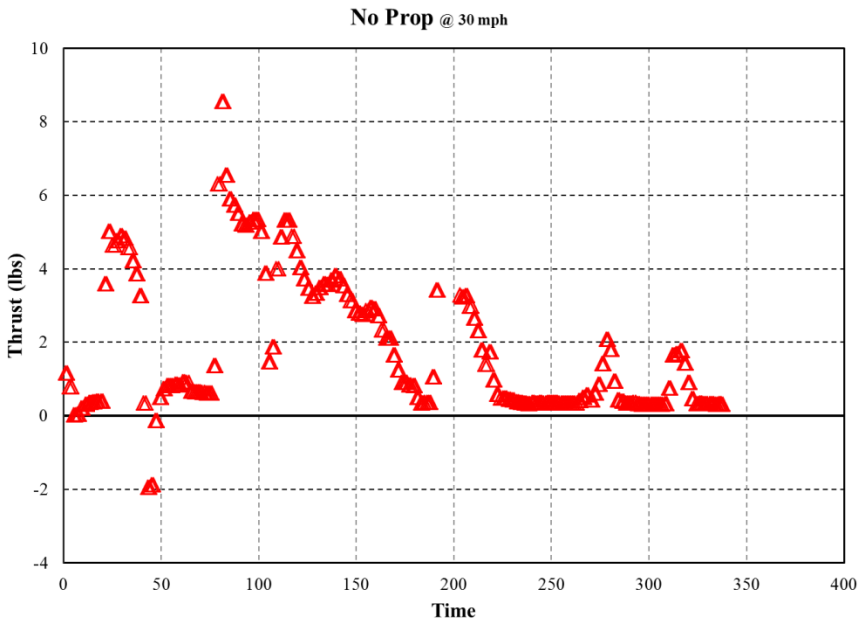

Figure 15-Thrust Variations Due to Inclines and Drag

A fairing was fabricated to shield the dynamometer from the oncoming airflow. The fairing is shown in Figure 16 and encloses the entire dynamometer section by bolting to the mobile dyno mounting base. The fairing is a two piece fiberglass structure, nose cone and fairing body, and was made using the plug-mold-part construction method. The first step of the fairing fabrication was to design the fairing in Solidworks, with the fairing enclosing the entire dynamometer, but not interfering with the dyno which would cause thrust measurement errors. The fairing is also designed as streamlined as possible to reduce any backflow problems. The plug was made using a CNC milling table to cut several two dimensional cross-sections throughout the fairing length, gluing foam between each cross section. Then using a foam cutting hot-wire, cut the foam to the overall fairing outer dimensions using the cross-sections as guides. After the outer mold-lines have been sanded and leveled to satisfaction using a filler epoxy, the three molds were made by simply laying tooling coat with several layers of epoxy and heavy fiberglass one plug at a time. After the molds are cured and separated from the plugs, five layers of 10oz fiberglass and epoxy were laid up inside the mold, put under vacuum to release any air

bubbles, and left to cure. Since weight was not a factor, five layers of 10oz fiberglass were used so that it would be very rigid and cheap. The fairing has proved to successfully remove the drag on the torque tube caused by the oncoming airstream and prop wash. The fairing also shielded the optical sensor and reflective tape curing disruptions to rpm measurements when the reflective tape was in direct sunlight.

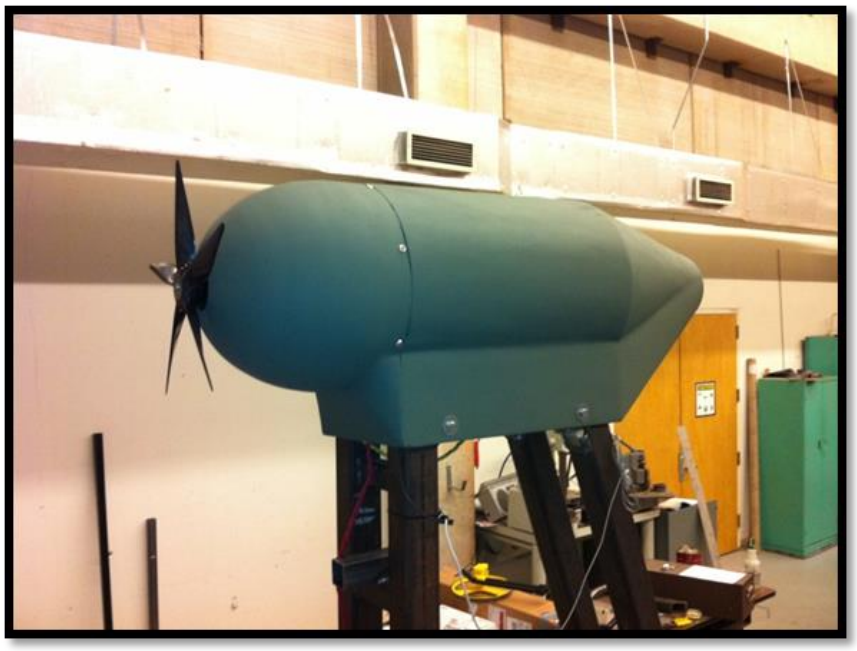

Figure 16- Dynamic Dyno Finished Fairing Installed

A very simple, yet essential, addition to the mobile dyno was a reference pitot-probe to record airspeed during testing instead of relying on the truck's speedometer as a reference. For initial testing, a small Eagle Tree pitot-static probe was used with a pressure transducer to give raw voltage to the DAQ. The probe is fixed to the dyno with square tubing welded to a piece of strut channel that allows you to adjust the height of the probe within the channel, very similar to the pitot-rake used in the first full-scale test discussed later. The strut channel is tall enough to allow the probe to be placed as high as the centerline of the propeller. The larger piece of square tubing is welded to the side of the mobile dyno to allow the square tubing that is welded to the c-

channel to slide to different positions so that the probe can be moved left or right, allowing the probe to be moved further away from the dyno to allow for larger propeller clearance. The square tubing is locked in place at a specified location with nuts welded on the outside of the square tubing over a hole into which a large bolt can be threaded wedging the tubing in place.

As seen in Figure 15, the spikes in the data during the test with no propeller installed occurs as a result of the vehicle driving up and down inclines and having the dynamometer's weight affect the thrust readings. If we are able to determine the angle of the incline and the weight of the dynamometer, we can simply subtract the additional weight from the raw data and obtain true thrust values. Adding an inclinometer will allow angle measurements to be taken during testing. Also, dismounting and weighing the dynamometer will allow us to know the weight component measured by the thrust load-cell. The angle measurements can then be added to the program and be used to subtract the error from the thrust data or post process the data, if desired.

To assure that the inclinometer can accurately remove the errors in thrust caused by the weight of the dynamometer, there were tests ran with the angle and thrust measured. Each test was ran with the fairing installed, no propeller, and roughly at 40mph using the truck's speedometer as a reference. The results are shown in both Figure 17 and Figure 18.

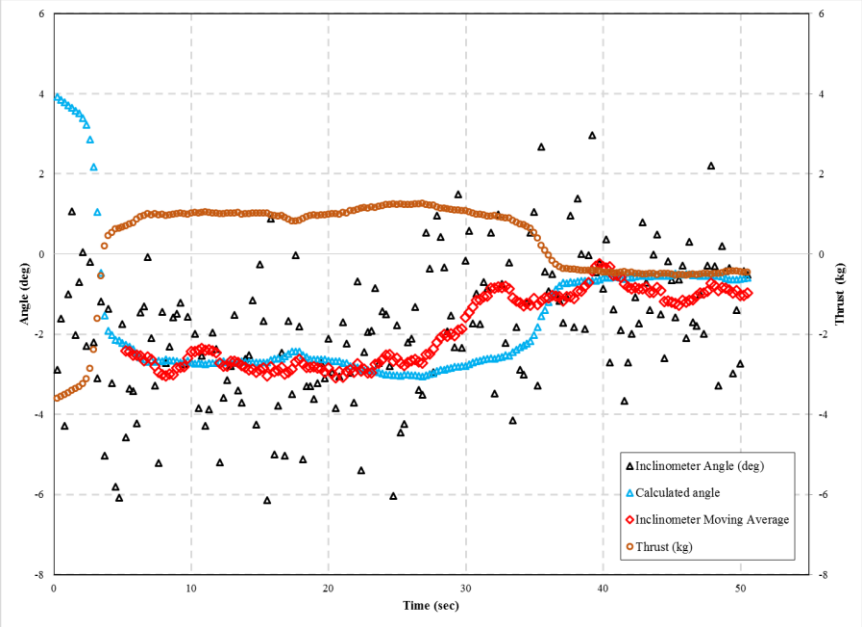

Figure 17-Northbound Inclinometer and Thrust Data

As shown in both the Northbound and Southbound plots, the inclinometer did not produce usable raw data due to all of the noise produced by the vibrations of the truck going over the road's surface. However, thrust shows to be very smooth with not a lot of noise, so when an angle can be accurately measured, the data should be easily corrected. When looking at the moving average of the inclinometer values, the data shows to be more useful. Even though the average is with 20 data points, the results seem to be very similar to the calculated angle values needed to actually remove all thrust errors. So after looking at both plots, the inclinometer might be usable, but removing some of the noise would also prove to be useful. Also, since the average inclinometer data does equal the calculated angle to produce zero thrust, the thrust system may have hysteresis. Possibly other methods of calibrating both thrust and inclinometer together may be needed. Calibrating both sensors together would allow the zero thrust reading to be at the zero angle position.

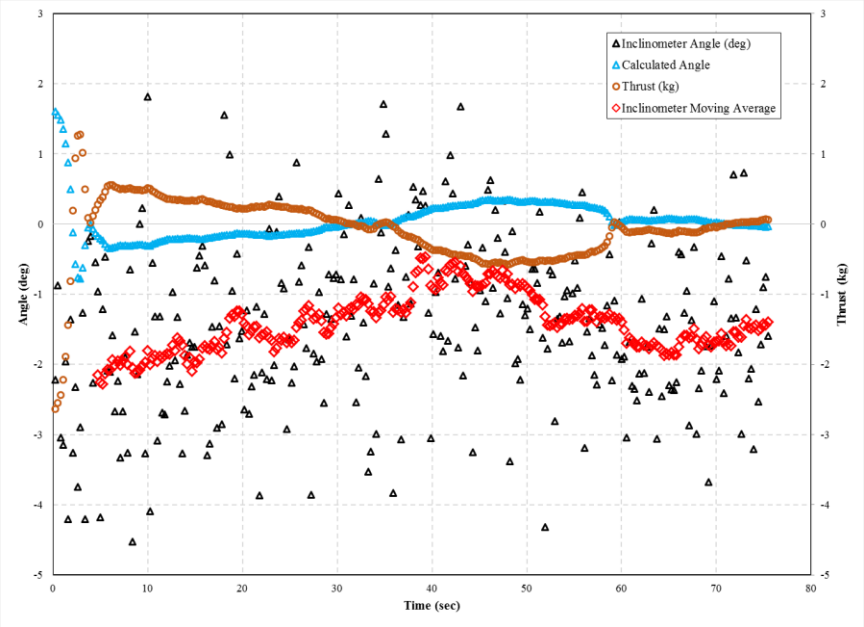

Figure 18-Southbound Inclinometer and Thrust Data

One method used to attempt to reduce or even eliminate the noise was to insert a vibration-dampening polyurethane spacer between the inclinometer and the mounting plate. This was to eliminate some of the noise by absorbing vibrations created by the truck going over the road's surface. The results of the testing with the insulator are shown in the appendix. Unfortunately, the insulator did not appear to help the noisy inclinometer measurements since the same amount of data points had to be used in the moving average to produce usable data.

The development of a new calibration method for thrust and torque increased the accuracy of the calibration curves. The old method was very unreliable and consisted of using a threaded tension gauge, much like a fish-scale, threading the scale into the front of the motor, having someone pull at a constant force while another person took voltage readings with the laptop at a couple of different loads. The same method was used for torque measurement by threading the scale into the torque load-cell bracket.

Now the new process for calibrating thrust is accomplished by manufacturing a piece of square tubing with a low-friction bearing mounted on one end and the other end mounted to the frame of the mobile dyno. The square tubing is welded together in such a way that it puts the pulley at the exact center point of the propeller. Once mounted, a bolt with an eyelet is threaded into the motor and fitted with a thin steel cable. The cable is draped over the pulley with weights hung off the opposite end of the cable. Using calibration weights, you can go through a very fine range of weights to get a good mesh to use to create a calibration curve fit.

Torque calibration is now achieved by concentrically sliding a 1-foot long piece of 3.5-inch pvc drainage pipe over the end of the torque tube and securing with a bolt so that only about half of the pipe covers the torque tube. The other half of the pvc pipe has a 3/8-inch hole drilled all the way through the diameter of pipe parallel to the ground. This allows a 3/8-inch piece of steel rod to slide through the holes and creates a place to hang calibration weights. By hanging the weights at different distances from the center of the torque tube and with changing the weight, different torque values are obtained and plotted with raw voltages to create a fine mesh calibration curve.

Validation

Validation of the mobile dyno has been attempted with several different propellers in static cases (V_∞=0). The results of two of the propellers are shown in Figure 19 below in the thrust versus rpm and torque versus rpm graphs. A 3-blade Mejzlik 22x12 and a custom 3-blade 18x18 propeller manufactured at OSU were used in this test. These propellers were chosen because an experimental aircraft built at OSU was using each propeller to assess differences in acoustic readings. The custom propeller's theoretical performance also needed to be validated before use in flight trials.

When comparing the static thrust between the wind tunnel dyno (open symbols) and the mobile dyno (closed symbols) in the plots below, the data matches up very well throughout the entire rpm range. The wind tunnel dyno was only plotted to 5000 rpm due to limits in the power available to the motor. The maximum standard deviation for the two propellers tested in the wind tunnel was 0.234 for thrust. The standard deviation for the mobile dyno tests could not be calculated due to the values being recorded by reading the display. Unfortunately, this data was taken a couple of years ago and more recent data shows that the wind tunnel may need to be restored to give better results as shown later.

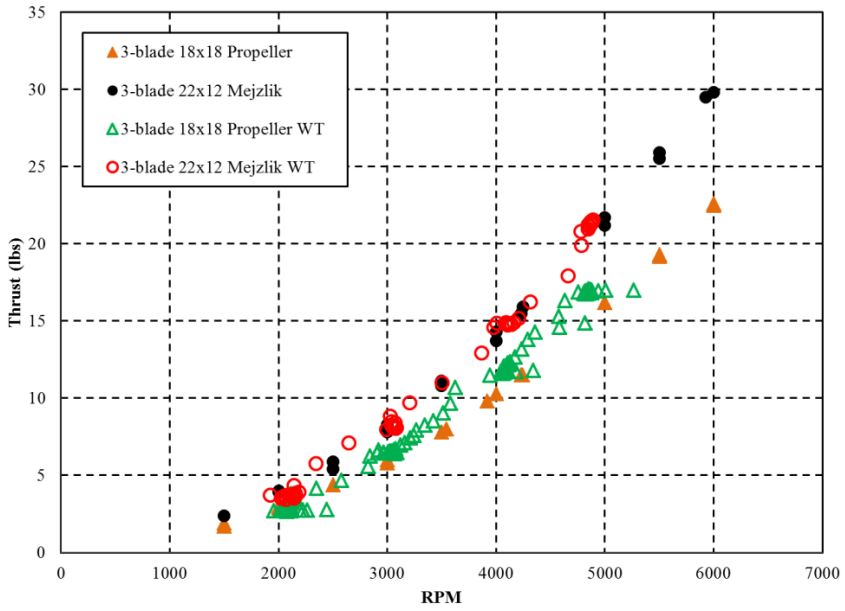

Figure 19-Thrust vs. RPM of Two Different Propellers on the Wind Tunnel Dyno and Mobile Dyno

Looking at the torque plot shown in Figure 20 below the data does not match as well as the thrust plot. However, they still show to be close enough to be within reason. Again, the wind tunnel results only go to 5000 rpm due to the limits in power supplied. Standard deviation for the wind tunnel results of this plot was 0.035 in torque and the standard deviation for the mobile dyno could not be calculated since the data was read from the display.

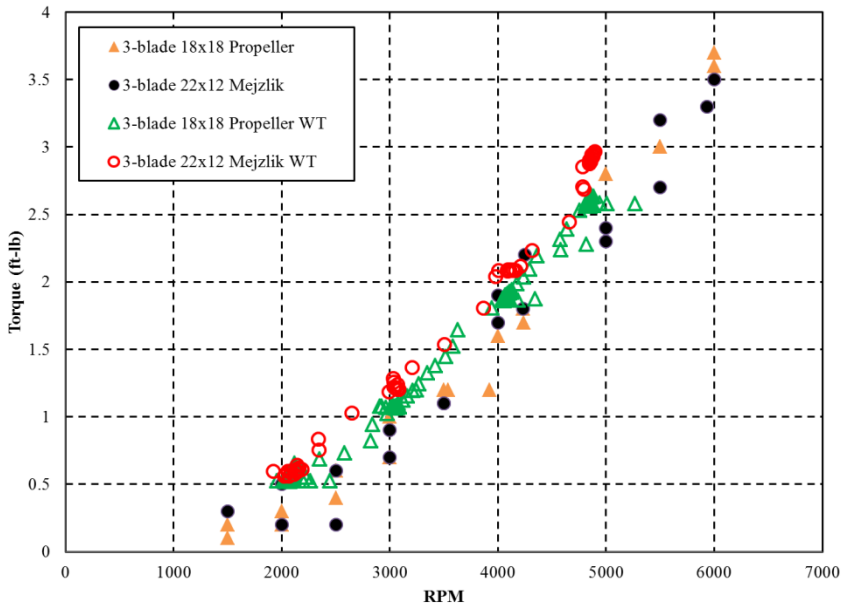

Figure 20- Torque vs. RPM of Two Different Propellers on the Wind Tunnel Dyno and Mobile Dyno

After comparing static data, naturally, dynamic validation would be the next step. So before running mobile dyno tests, the wind tunnel would be validated against UIUC data; and if successful, the wind tunnel dyno would be compared to mobile dyno results. Simply comparing the mobile dyno with UIUC data is not very useful since UIUC did not publish results of propellers above a 19-inch diameter and tested at very low rotational speeds, which in turn produced very small amounts of thrust and torque, and therefore, the thrust and torque measurements are not within the sensitivity of the mobile dyno.

When comparing data to the UIUC propeller database, we were not as fortunate as we were with the larger propeller tests shown earlier. The data shown in Figure 21 below is not a very good match. However, several tests were run, and they show that as the thrust values approach 4 to 5 pounds, C_T levels out and matches the UIUC data very well. This could be the reason why the previous test gave good results, since the propellers tested initially were of much larger diameter and produced a minimum thrust of about 3 pounds. Interestingly, if UIUC data is

assumed to have constant C_T as it goes to higher rpm the higher C_T will match very well. This is a good assumption since statically the coefficients of thrust and power should remain constant. Since the UIUC data is at very low rpm, we must make this assumption. The wind tunnel dyno in the current configuration is not able to give reliable results below 4 to 5 pounds of thrust as it should. This is possibly due to the dyno needing to be rebuilt.

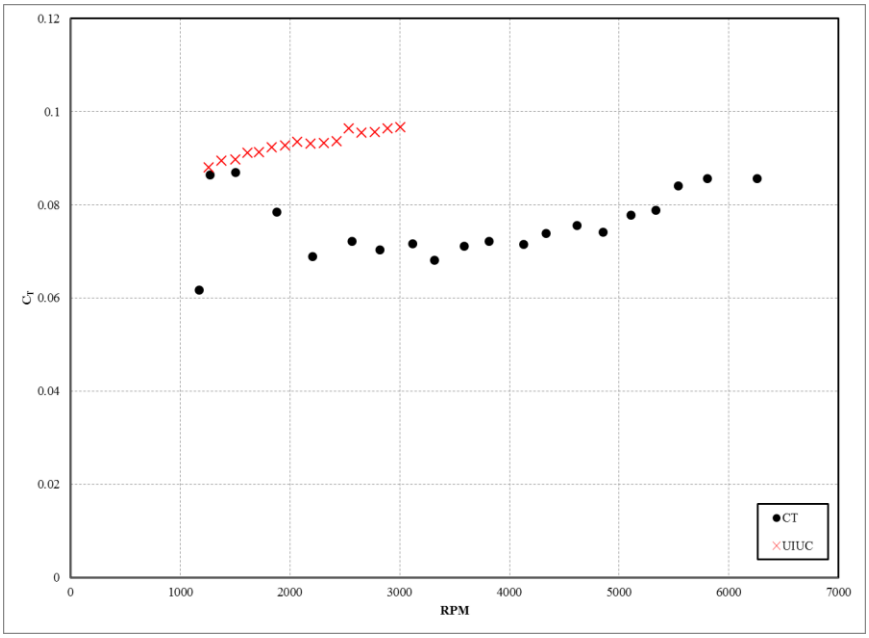

Figure 21-Wind Tunnel and UIUC, C_T vs. RPM Statically

When looking at the C_P plot, the wind tunnel results approach infinite as rpm approaches zero. Instead, C_P should stay at a constant value throughout the rpm range much like the UIUC data. The UIUC data has been compared to an OSU propeller code that utilizes blade-element momentum theory and the results prove to be very similar. This can only be caused by the thrust values leveling out on a constant value instead of returning to zero at zero rpm. To try and assess the problem with the data, we can look at thrust and torque plots.

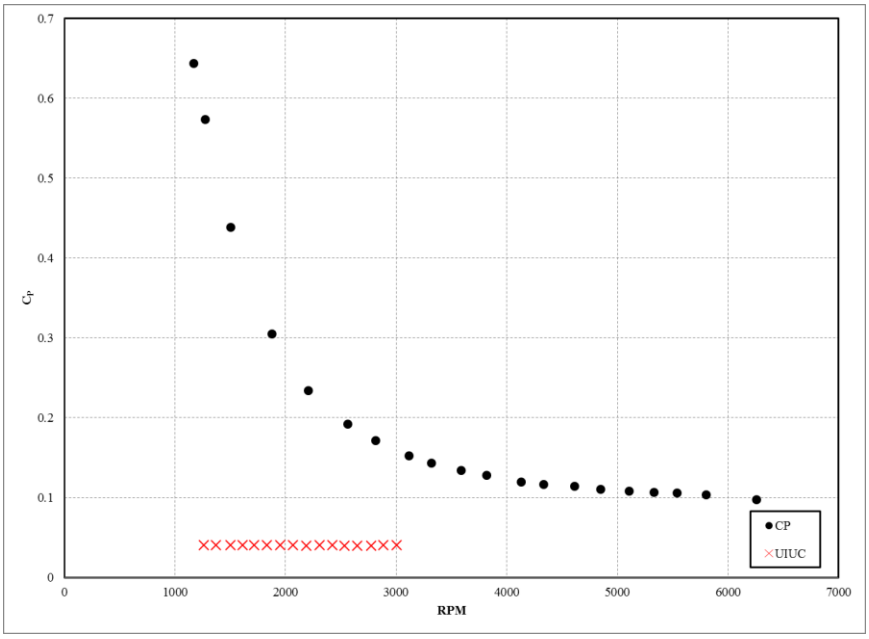

Figure 22- Wind Tunnel and UIUC, C_P vs. RPM Statically

On 7/22/13, a test run on the wind tunnel dyno with a 2-blade APC 14x12E thin electric was performed to attempt to discover the wind tunnel dyno problems. The results are only static checks and are shown in Figure 23 and Figure 24. The thrust does not collapse to zero at 0 rpm as, in theory, it should. This causes our large errors in the thrust and power coefficients, making the coefficients of thrust and power go to infinite as the rpm approaches zero.

This is obviously not the case and can be corrected by making the data follow the theoretical path by subtracting a large percentage of the lowest rpm data point from each data point and causing the graph to shift down and intersect with zero. This experiment is shown in the next four graphs. The recorded data are solid symbols, while the open symbols show the corrected results.

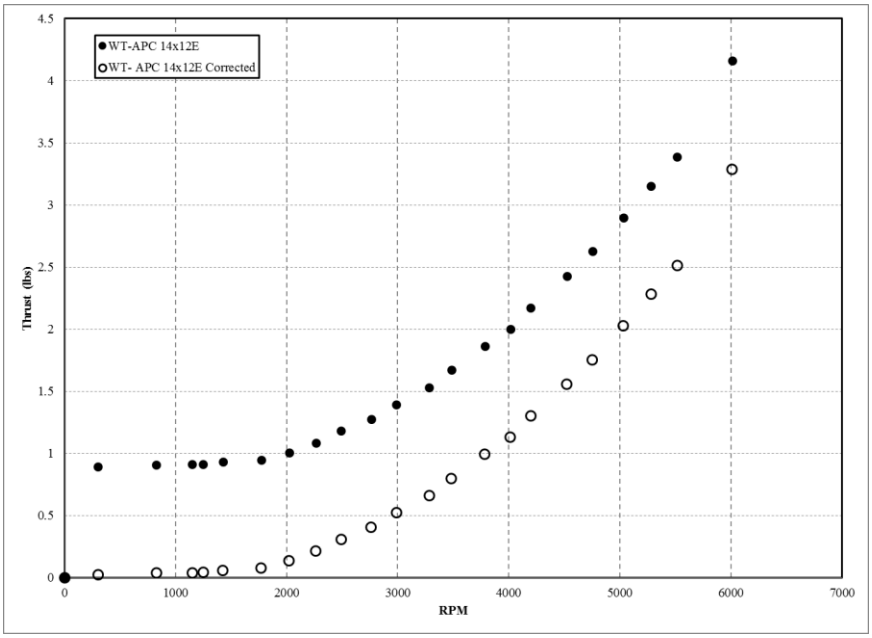

Figure 23-Making Data Corrections for Thrust on the Wind Tunnel Dyno

The data seems to show drift in both thrust and torque load-cells, but this is not the case as the readings would return to zero at 0 rpm. However, these errors show up in the coefficient of thrust and power plots as rpm approaches zero both thrust and power coefficients go to infinite. When plotting the corrected version of C_T, the results are improved, but still have problems that will need to be addressed. Conversely, the corrected C_P results look much more comparable to the UIUC data.

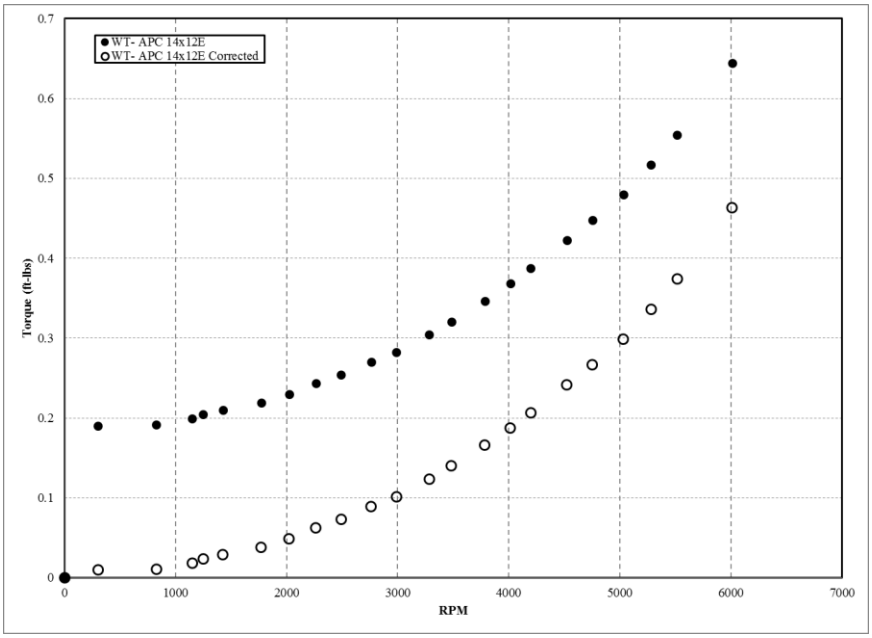

Figure 24- Making Data Corrections for Torque on the Wind Tunnel Dyno

The errors have also shown to be repeatable when testing the same system on different days, which is shown by looking at results in the Appendix. While the results from the other wind tunnel tests can be corrected the same way, this may be futile. In the end, the wind tunnel will need renovation to produce more accurate results at lower thrust and torque values. The data looks as if there is a constant load that is applied once the propeller starts to spin and stays constant until the propeller can produce enough load to overcome this value.

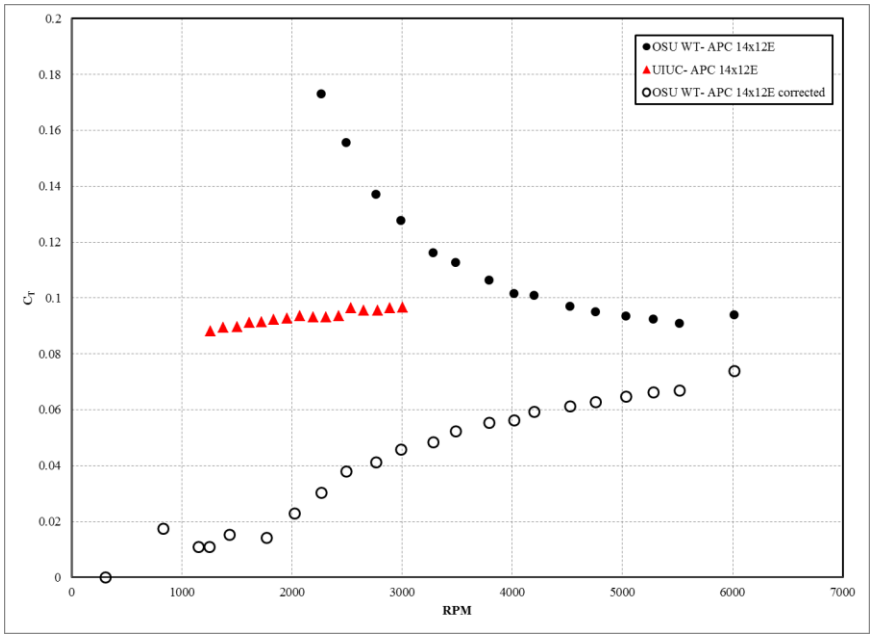

Figure 25- C_T vs. RPM with UIUC Compared to Recorded Results and Corrected Results

I propose that multiple problems cause the errors. One problem being the use of a large and heavy Hacker motor to power the propeller. Over time the dyno has developed large amounts of slack in the hinges, load-cell mounts, and worst of all the joints where motor mount head is attached. Another problem is that the dyno is not perfectly level; as a result the propeller plane is not perpendicular to the oncoming flow. The additional mass of the larger propulsion system being at an inclined angle causes the four-bar system to have larger amounts weight transmitted onto the thrust load-cell. Unfortunately, time constraints did not allow investigation and correction of these problems.

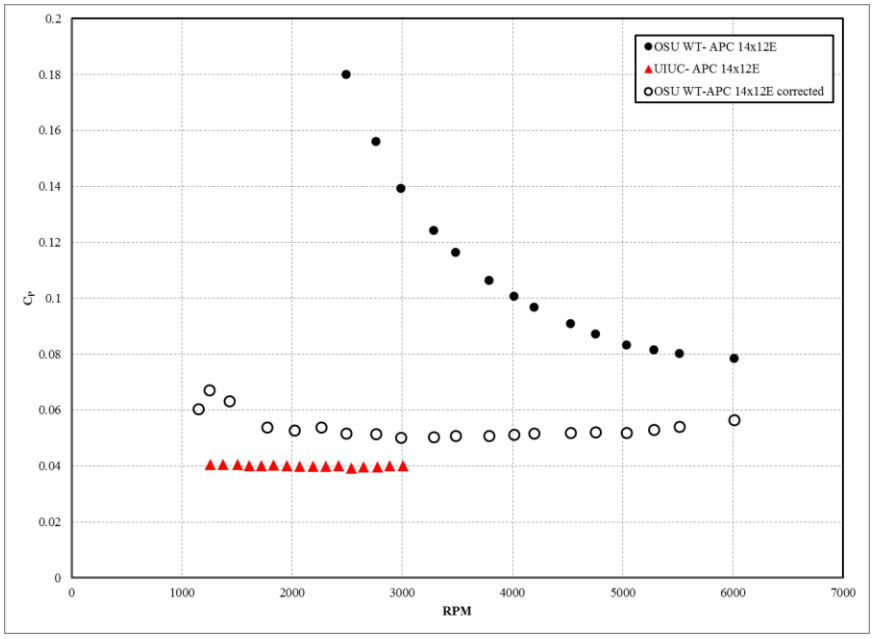

Figure 26- C_P vs. RPM with UIUC Compared to Recorded Results and Corrected Results

CHAPTER IV

VEHICLE AERODYNAMICS EXPERIMENTAL SETUP AND RESULTS

When measuring the boundary layer over the truck, two methods were used to adequately characterize the flow. First being a full-scale test using several pitot-tubes in a line also known as a pitot-rake. The pitot-rake is a device that allows you to get several pressure measurements created from the oncoming air flow velocity and works great for boundary layer measurements because each probe gets different velocity measurements as each probe of the rake leaves the boundary layer.

Another method used a $1/8^{th}$ scale model of the truck and dyno system inside the OSU wind tunnel to get qualitative information about the flow. The qualitative method was attained by using a smoke generator to input smoke into the wind tunnel while taking high speed images.

Each test was run with the $1/8^{th}$ scale plastic shell truck model with the dyno installed and without the dyno installed. These methods proved to be adequate in characterizing the flow over the truck and in determining what impact the flow has on the propeller's performance measurements.

Full-Scale Testing

The setup for this testing was designed to be a very cheap, efficient, and effective way to measure the vehicle's boundary layer. While a much more elaborate setup uses stepper motors to automatically adjust the rake position, this testing was to be done inexpensively. The

experimental setup for this testing is square tubing that can slide inside of each other for adjustability, a hole drilled into the tubing and a nut welded over the hole to allow the tubing to be fixed in a desired test position by tightening the bolt and essentially clamping the square tubing in place. A piece of strut channel is welded vertically to the end of the square tubing to allow pitot-tube mounting. The square tubing is mounted to the mobile dyno unit for ease and to ensure that the dyno does not impact the flow into the propeller plane as well. The adjustability of the tubing allows you to move the pitot-rake forward/backward and left/right above the truck cab from the driver's point of view. This way all the testing can be done in one position, then easily moved to the next test position, allowing for quick and efficient data collection of a very fine mesh of the velocity profile data.

Two different types of pitot-rakes were assembled to get the information needed. The first pitot-rake consisted of ten Eagle Tree pitot-probes mounted to rods using small hose clamps and mounted the length of the strut channel using strut channel tubing mounts as shown in Figure 27. The second rake was custom made from 1/16 inch stainless steel tubing allowing for a more definite boundary layer measurement. The pressure measurements are taken from a 16-port Scanivalve at 500 samples per data point. The speeds for testing were 20, 30, 40, 50 and 60 mph using the truck's speedometer as a reference. Also, note that the truck's speedometer was only used as a reference, and there could be a variation of ±5mph along with variations in wind speeds of up to 20-25mph, depending on the day. However, this is not a problem since there is always a true airspeed pitot-probe mounted much higher than the rest of the probes to assure a free-stream velocity measurement.

Figure 27-Full-Scale Test #1 Pitot-Rake Arrangement and Pitot Mounting

Three different tests were run on three different days allowing characterization of the flow over the truck. Full-Scale Test #1 was a very coarse mesh and went several feet above the cab to determine that the majority of the flow into propeller plane is, in fact, free-stream flow and not accelerated flow around the vehicle. Full-Scale Test #2 uses the same probes as the first test, but they are condensed and moved closer to the truck to get a finer mesh in an attempt to find the boundary layer. Full-Scale Test #3 used a custom pitot-rake that had even finer spacing and was closer to the truck cab to actually quantify the boundary layer.

When going through boundary layer calculations, the flow is treated as flat-plate boundary-layer flow. So when measuring the Reynolds number, the characteristic length is made up of three different distances, each treated as flat plates, then added together to create a simulated flat plate length like that shown in Figure 28 below. The hood, windshield, and top of the truck cab length to the pitot-rake are the three distances measured to get a total characteristic

length. The time of each test is recorded in order to check the weather history after testing to get pressure and temperature so that air density can be correctly calculated.

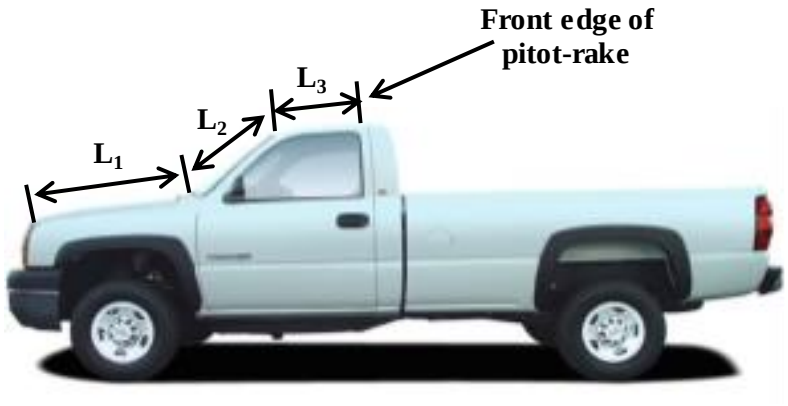

Figure 28-Reynolds Number Characteristic Length Definition

All three days of testing were conducted on the same stretch of road which is shown on the map in Figure 29. This road is located on the outskirts of Stillwater, Oklahoma, a few miles northeast of Oklahoma State University.

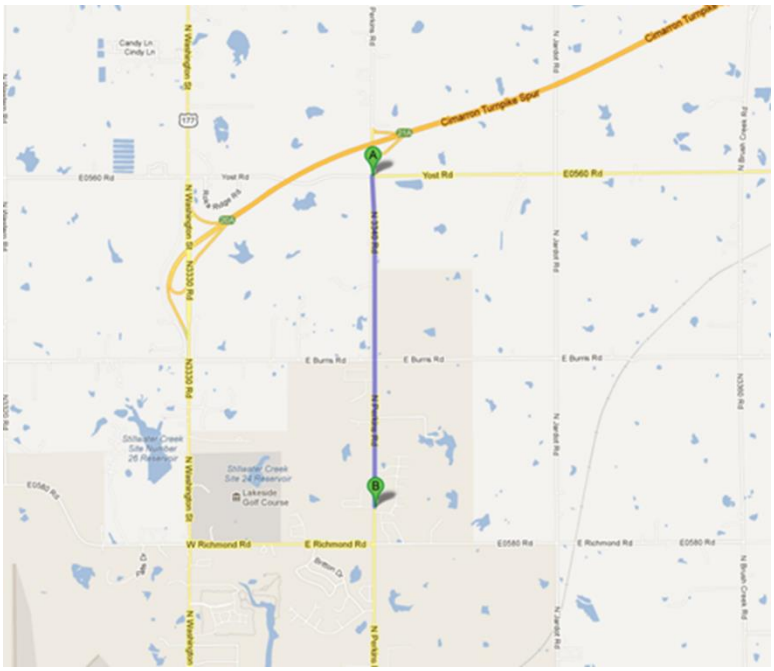

Figure 29-Full-Scale Testing Location

Full-Scale Test #1

As seen from the following figures, the spacing between each pitot probe was 4 inches with the lowest probe almost 5 inches from the cab of the truck. The tests were at four different locations above the truck cab to show how the profile differs at the different locations above the cab. However, this full-scale test was only done in one plane above the cab, so the rake was only moved left and right, and was not moved in the longitudinal direction.

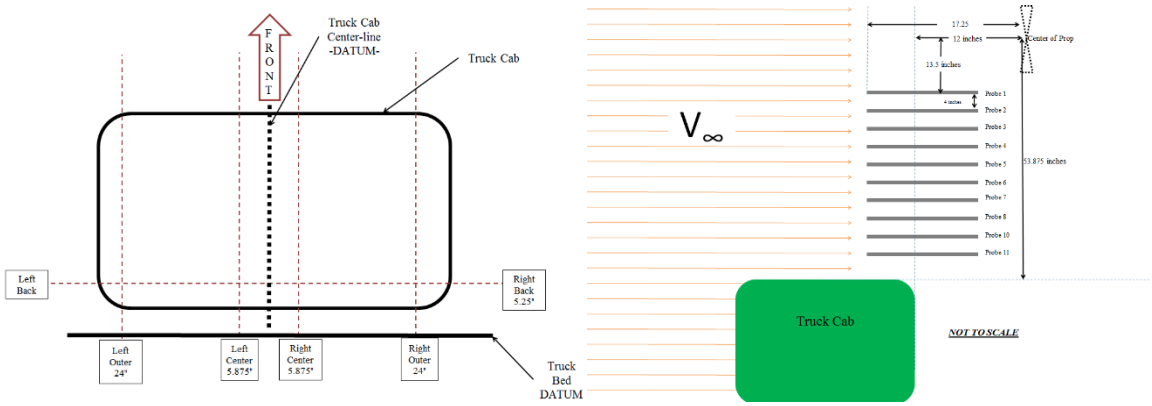

Figure 30- Pitot-Rake Layout for Full-Scale Test #1

The testing was done on March 20, 2013 around 3:00-4:00p.m., and the winds speeds throughout the day are plotted in Figure 31. The data is taken from the Oklahoma Mesonet weather reports for the Perkins, Oklahoma weather site. The green diamonds represent the maximum winds or gusts while the solid circles are winds measured at 10 meters off the ground and the open red circles are winds measured at 2 meters from the ground.

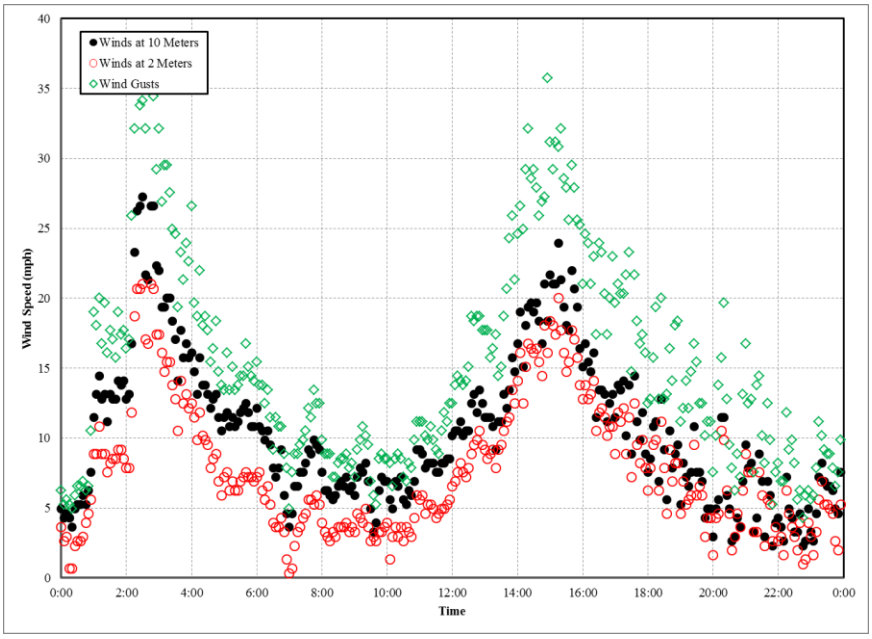

Figure 31- Winds Plotted vs. Time for 3-20-13 (Mesonet)

After the data is collected and consolidated, it is helpful to plot as distance above the truck cab vs. Reynolds number to make it easier to see all of the different positions on one graph to allow for all the different speeds in one dimensionless term. Plotting in this manner shows boundary layer growth as a function of Reynolds number, if there is a boundary layer. However, in this first test Figure 32 shows that the flow does not reveal any signs of boundary layer or accelerated flow over the truck cab for any of the speeds or locations.

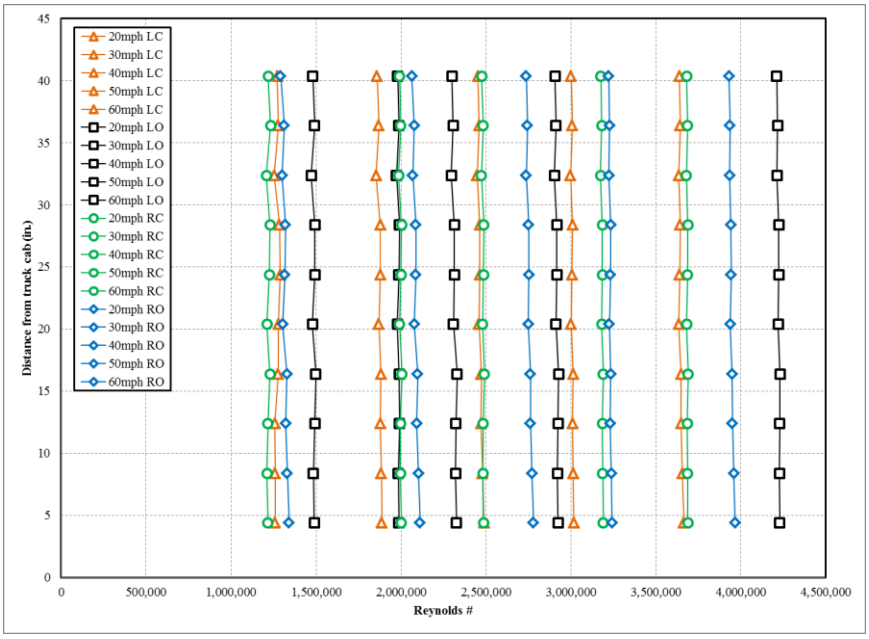

Figure 32- Distance above the cab vs. Reynolds # for all speeds and locations

It also proves useful to see the data plotted as distance from truck cab vs. the dimensionless term $\frac{u}{U_{ref}}$ to see how the flow varies from the free-stream. This data is more easily deciphered having a graph for each position above the cab to reduce clutter. This helps us determine if the flow is accelerated above the cab at the different positions above the cab. If the flow is accelerated, the values will be greater than 1, or less than 1 if the flow is decelerated. Plotting this way also proves useful when finding a function for your boundary layer profile, which is shown in later testing. Figure 33 shows that all of the flow for the Left Center position falls very close to 1. The data also shows the instability of the airflow at 20 mph. The air becomes much more uniform as the speeds are increased; but with the scale being very fine in this plot, these fluctuations are very small overall. Looking at the graphs in the appendices, the other positions follow very close to this trend as well.

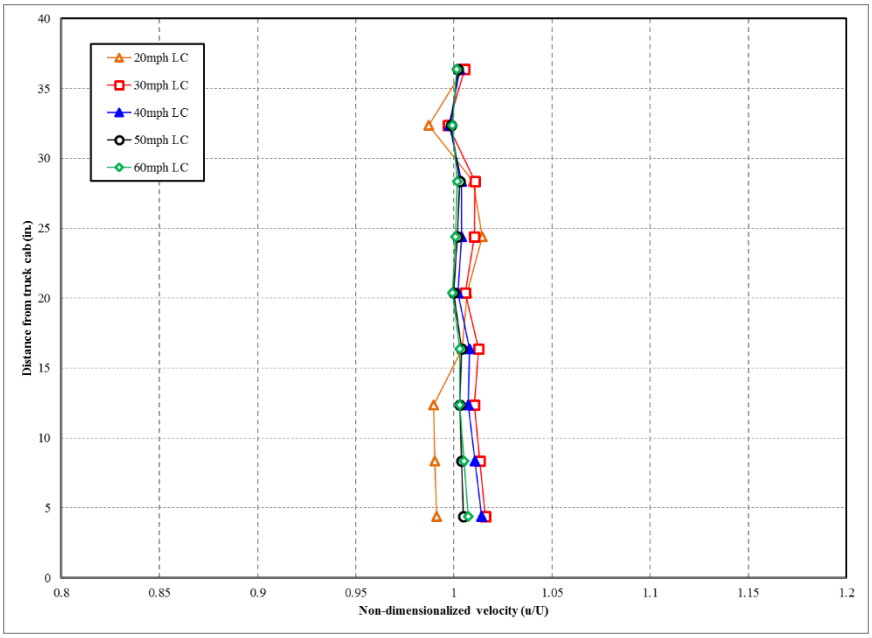

Figure 33-Nondimensionalized Flow of the Left Center Position at All Speeds

Full-Scale Test #2

Since the first test does not show any indications of boundary layer flow, the second test is designed to help find the boundary layer by shifting our focus closer to the vehicle surface. There were only four positions tested on the right side of the vehicle, which are shown in Figure 34 and Figure 36. Once an approximate location of the boundary layer is found, a more diligent assessment is used to get a finer mesh of the flow.

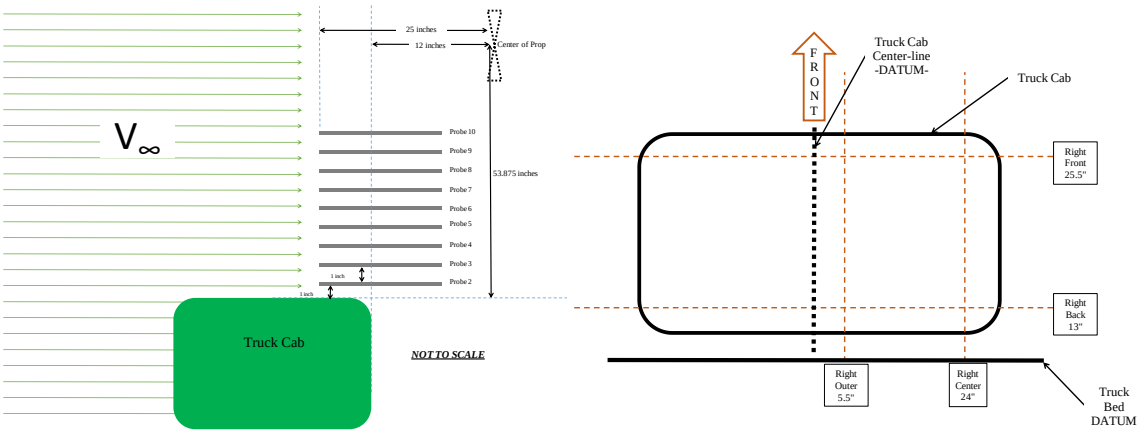

Figure 34-Full-Scale Test #2 Layout

This testing was done on September 15, 2013 between 2:00 to 3:00p.m., and the wind speeds throughout the day are plotted in Figure 35.The data is taken from the Oklahoma Mesonet weather reports for the Perkins, Oklahoma weather site. The green diamonds represent the maximum winds or gusts while the solid circles are winds measured at 10 meters off the ground and the open red circles are winds measured at 2 meters from the ground.

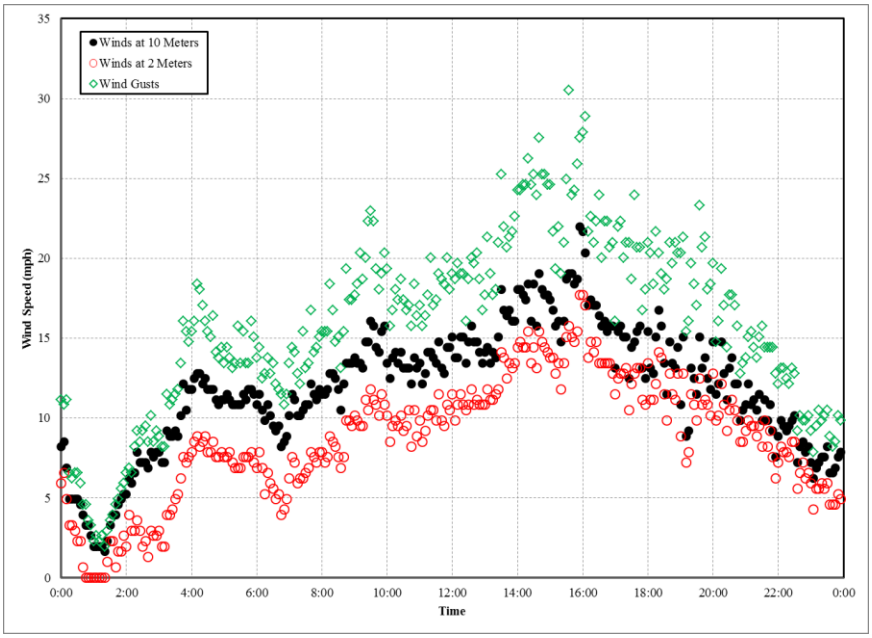

Figure 35-Winds Plotted vs. Time for 9-15-13 (Mesonet)

The second configuration used the same probes previously described with a spacing of 1 inch, much closer to the truck cab. To get this close to the cab, the propeller safety shield was removed. This allows us to see the boundary layer along with the accelerated flow over the truck cab. The distance the lowest probe is from the cab varied by position x-y position over the cab since the cab is not uniform.

Figure 36-Pitot-Probe mounting for Full-Scale Test #2

Once data was collected it was once again plotted as distance above the truck cab vs. Reynolds number for each position in the traversal direction. This shows how the boundary layer changes as the flow moves further downstream from front to back of the truck cab and higher velocities by using Reynolds number. Looking at data in Figure 37, the boundary layer is shown to be roughly 1 to 2.5 inches above the truck at the furthest back position. The graph also shows that there is accelerated flow over the vehicle since the velocity has a slight decrease in Reynolds number at the upper probes around 7 to 9 inches.

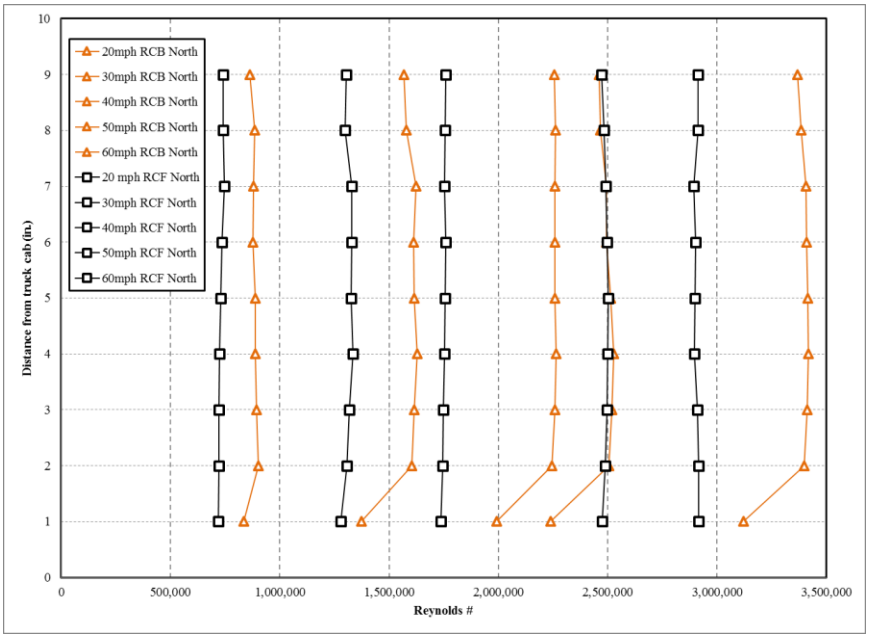

Figure 37-Right-Center-Back Location Heading North for Distance above Cab vs. Reynolds # for All Speeds

An even more interesting and helpful plot is plotting distance above the truck cab versus $\frac{u}{U_{ref}}$. Looking at this plot confirms that the boundary layer is from 1 to 2.5 inches and that the accelerated flow over the vehicle is from 2.5 to roughly 7 inches, depending on free-stream velocity. The interesting part of this graph is how the flow is shown to be more uniform and stable at the higher velocities, particularly above 30mph. The ratio of accelerated flow is not as high at the higher velocities when compared to the slower velocities. Also, notice that the graph shows the flow returning to the free-stream velocity, but not reaching free-stream until above the height of this pitot-rake. Although this is only showing the Right Center Back position, graphs for the other positions shown in the appendices indicate the same trend.

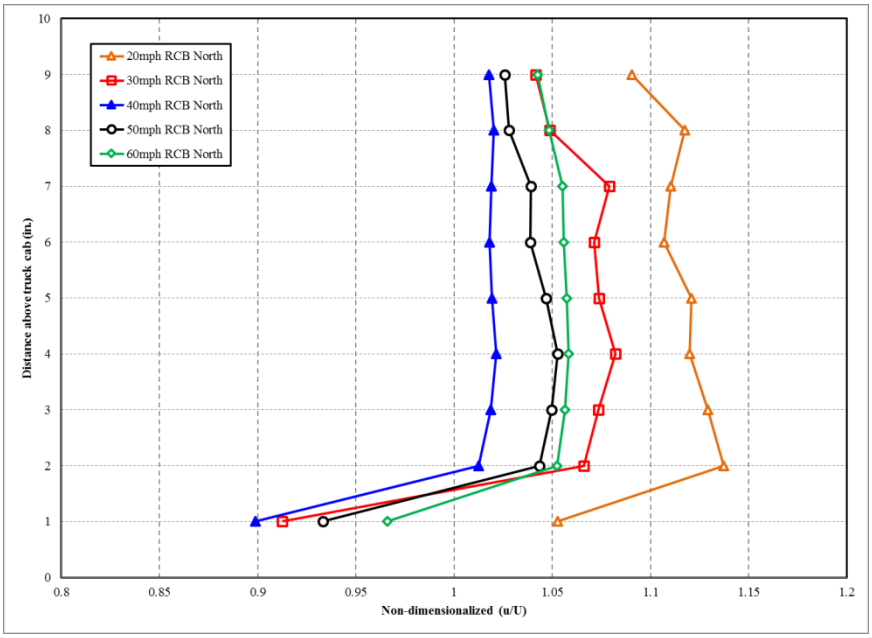

Figure 38- Right-Center-Back Location Heading North for Distance above Cab vs. u/U for All Speeds

Unfortunately, looking at the results of this test will not prove useful for any boundary layer calculations since the boundary layer is not well-defined. There will need to be more probes within the boundary layer to allow an accurate curve fit of the velocity profile. This test does allow us to distinguish where the boundary layer is located and how to move forward with the next test.

Full-Scale Test #3

When designing the last full-scale boundary test, we noted the boundary layer location obtained from the previous test and designed a pitot-rake that allowed more probes in the boundary layer. It was apparent that the testing needed to have a finer mesh of the boundary layer for further boundary layer calculations. This was achieved by making a different pitot-rake, as the probes used in the previous two tests were unable to be moved closer to the cab or have a finer spacing due to the size of the strut mounts mounting the probes to the strut channel.

The custom-made pitot-rake is shown in the Figure 39. This probe has fifteen stainless steel tubes epoxied together with ½ inch spacing between each probe. A sixteenth probe made of the same stainless steel tubing and was mounted several feet higher as a reference velocity. This allows a finer mesh of data points within the boundary layer. With this setup, there were 18 different positions of ½ inch spacing above the cab tested to give a good representation of the airflow. A schematic of the different positions tested is shown in Figure 40. Using this data we can get a boundary layer profile and calculate the displacement thickness δ* and momentum thickness θ.

Figure 39-Custom Fine Spacing Pitot-Rake

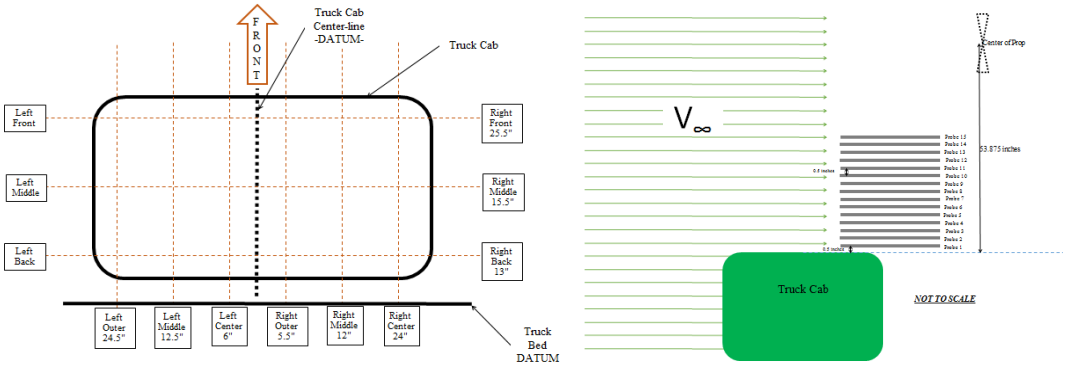

Figure 40-Full Scale Test #3 Layout

This testing was done on October 20, 2013 between 12:00 to 2:00p.m., and the winds speeds throughout the day are plotted in Figure 41.The data is taken from the Oklahoma Mesonet weather reports for the Perkins, Oklahoma weather site. The green diamonds represent the maximum winds or gusts while the solid circles are winds measured at 10 meters off the ground and the open red circles are winds measured at 2 meters from the ground.

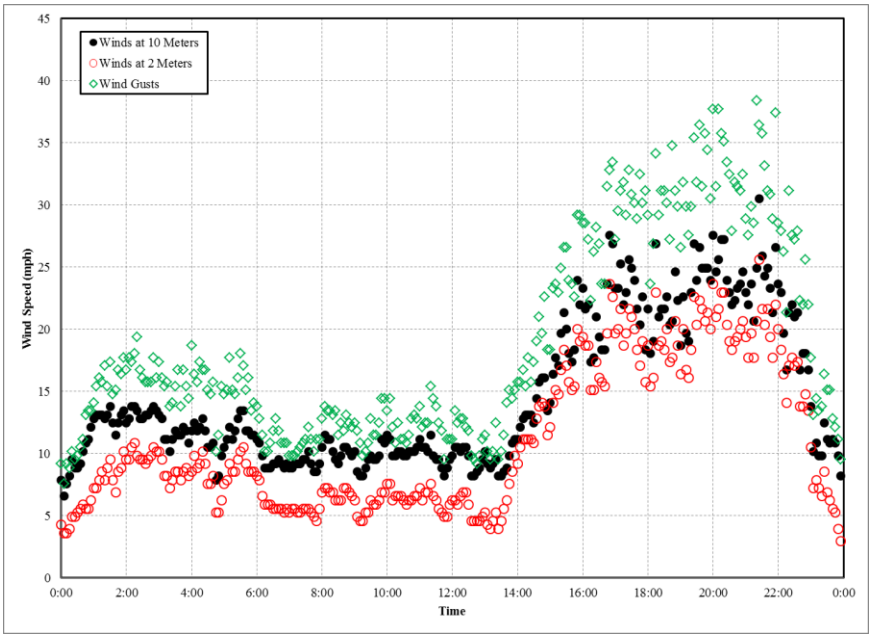

Figure 41-Winds Plotted vs. Time for 10-20-13 (Mesonet)

The data was once again plotted as distance above the cab versus Reynolds number to allow the data to demonstrate how the boundary layer changes with Reynolds number. As shown in the graph in Figure 42, the boundary layer is within the first 2.5 inches from the cab and grows with Reynolds number, as expected. It is also very interesting to see that the flow at very low Reynolds number seems to have less stability in the flow. This is assumed to be due to not having the momentum of the oncoming flow to make the flow follow a smoother, consistent path/pattern.

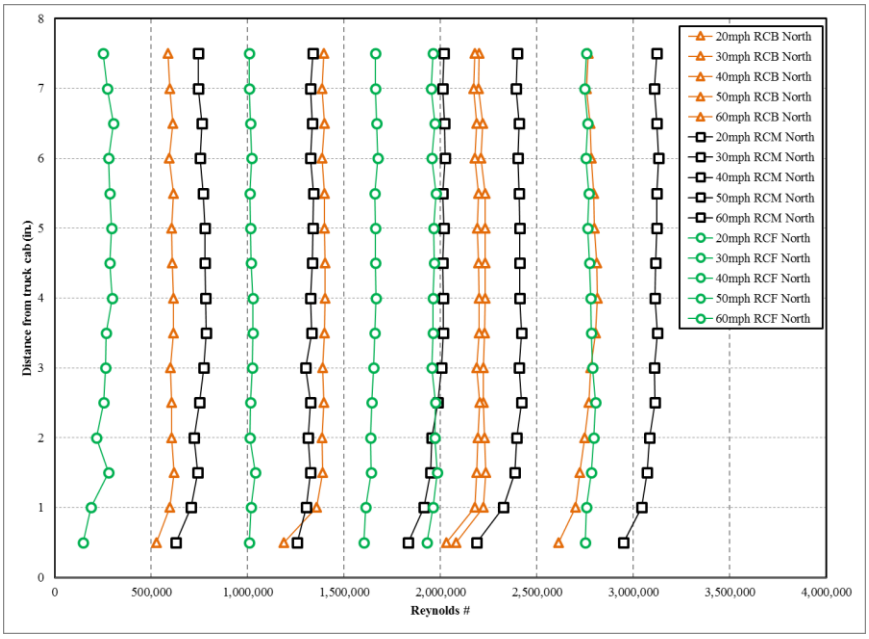

Figure 42-RCB Location Heading North, Distance above Cab vs. Reynolds # for all Speeds for Full-Scale Test #3

When plotting the non-dimensionalized velocity versus distance above the cab, the trends are the same. There is accelerated flow above the boundary layer and instabilities in the airflow at lower speeds. However, this data is important since it will allow us to curve fit the boundary layer velocity profile used to determine the boundary layer parameters.

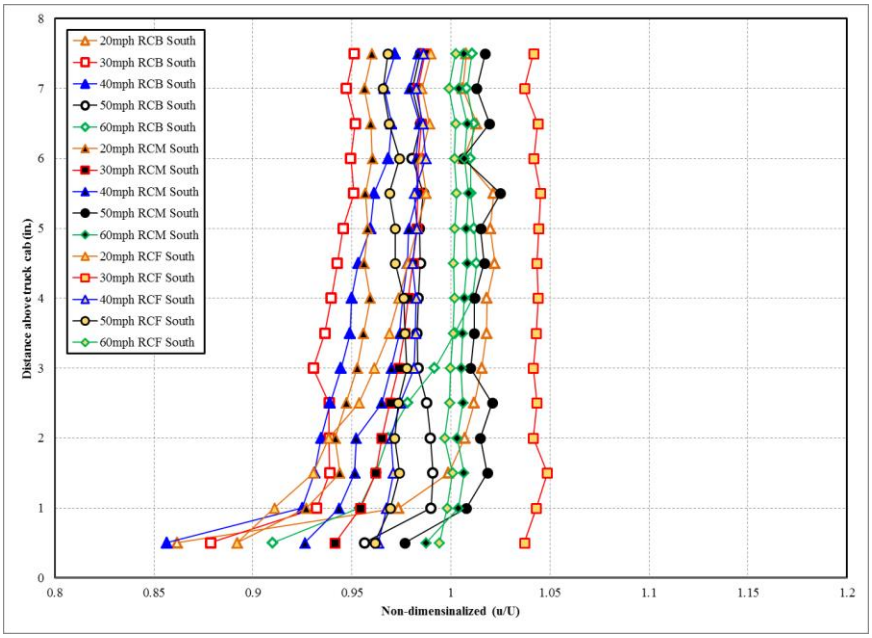

Figure 43-Nondimensionalized RC Locations Southbound vs. Distance above Cab

This data can be now be used to further investigate the boundary layer. Using the Flat Plate Integral Analysis to find displacement thickness we must find $\frac{u}{U}$ as a function of y so that we can solve the following integrals for δ* and θ.

$$\delta^* = \int_0^\infty \left(1 - \frac{u}{U}\right) dy \qquad \theta = \int_0^\infty \frac{u}{U}\left(1 - \frac{u}{U}\right) dy \qquad H = \int_0^Y \frac{u}{U} dy = \frac{\delta^*}{\theta}$$

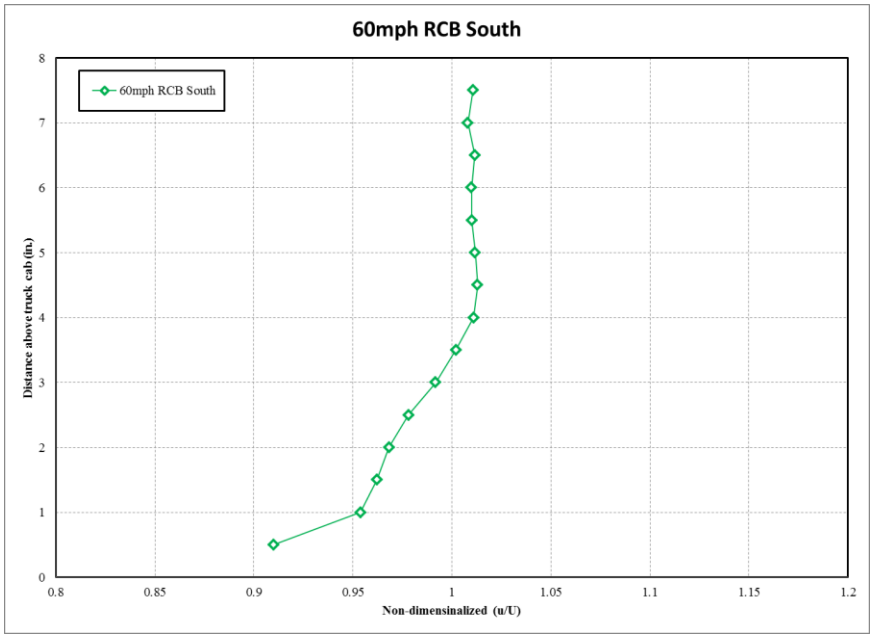

Figure 44-Velocity Profile from One Position Speed Used for Boundary Layer Calcs

By taking the non-dimensionalized data and singling out a stable boundary layer curve, in our case the 60 mph RCB South curve, we can re-plot it as shown in Figure 44. Looking at the graph, the boundary layer thickness shows to be roughly 4 inches. First, create a boundary condition so that the velocity at the wall or cab surface is zero for no slip at the wall. Curve fitting only the portion of the curve that is considered to be the boundary layer like that shown in Figure 45, will allow us to get the ratio of velocities as a function of y. Another important note is that the boundary layer portion will be plotted as the velocity at each distance above the cab up to 4 inches over the local velocity which will be in the accelerated flow over the truck directly above the boundary layer. Plotting this way will allow the flow to return to a ratio of one at the very top of the boundary layer. The power-law shown below shows to give a good fit and can be used to calculate the displacement and momentum thickness.

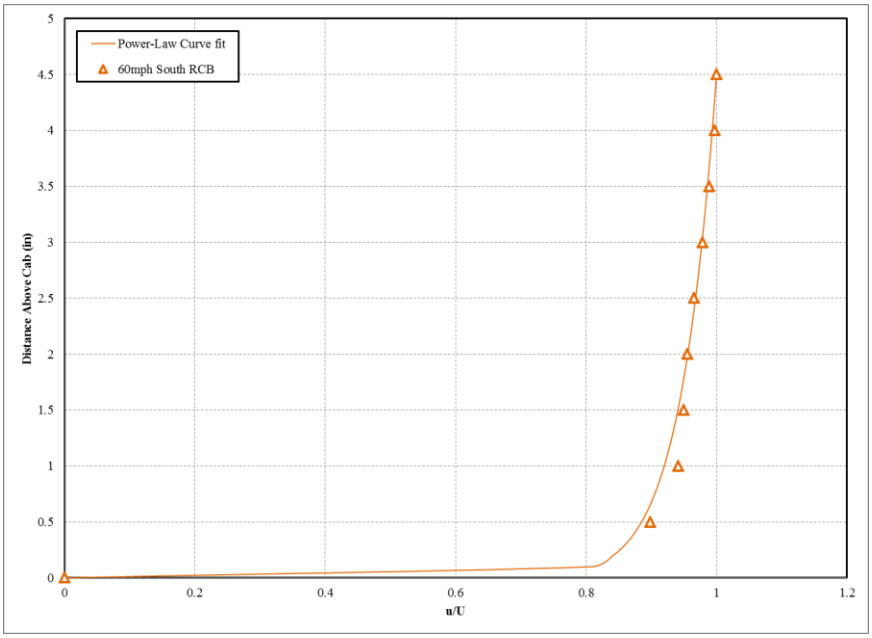

Figure 45-Power-Law Curve fit of Boundary Layer Profile

$$\frac{u}{U} = \left(\frac{y}{\delta}\right)^{\frac{1}{18}}$$

$$\delta^* = \int_0^{\delta} \left(1 - \frac{u}{U}\right) dy = \delta - 0.9474 \left(\frac{1}{\delta}\right)^{\frac{19}{18}} * \delta^{\frac{37}{18}} = \delta \frac{1}{19}$$

$$\theta = \int_0^{\delta} \frac{u}{U}\left(1 - \frac{u}{U}\right) dy = \frac{18y \left(\frac{1}{\delta}\right)^{\frac{19}{18}} * \delta^{\frac{37}{18}}}{19} - \frac{9\delta}{10} = \delta \frac{1}{21.1}$$

While this exercise can be performed for any of the boundary layer profiles, it is shown here just to show the process, and the profiles can be assumed to be the same at all of the positions.

Propeller-Plane Full-Scale Testing

Once the boundary layer was characterized, a test was run to assure that the flow directly into a 6-foot propeller plane would be uniform. The same set-up from both Full Scale Test #1 and

#2 was used, with 10 Eagle Tree pitot probes spread over a 6-foot span where the propeller would be located. The layout is shown in Figure 46. This test was only ran at one position for roughly 30 seconds for each test. This test was ran at the highest and lowest speeds from previous testing, 20 and 60 mph, for both Southbound and Northbound directions.

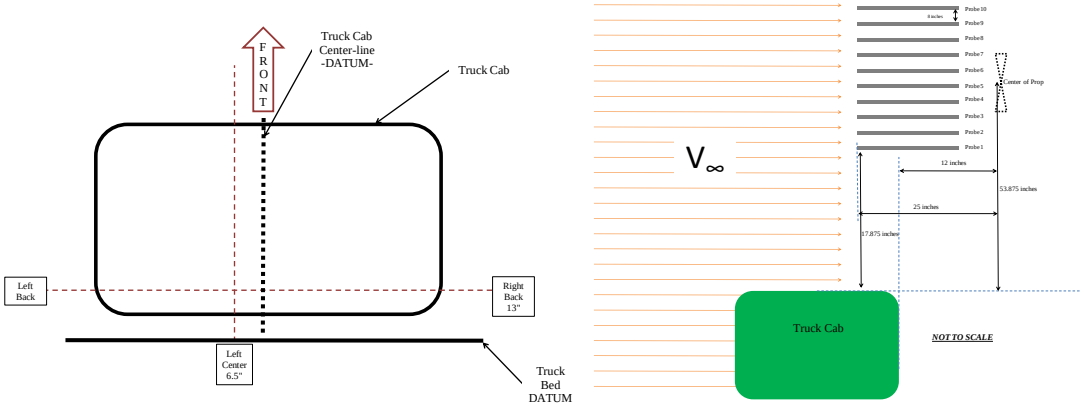

Figure 46-Propeller-Plane Full Scale Testing Layout

This testing was done on November 26, 2013 around 4:30p.m., and the winds speeds throughout the day are plotted in Figure 47. The data is taken from the Oklahoma Mesonet weather reports for the Perkins, Oklahoma weather site. The green diamonds represent the maximum winds or gusts while the solid circles are winds measured at 10 meters off the ground and the open red circles are winds measured at 2 meters from the ground.

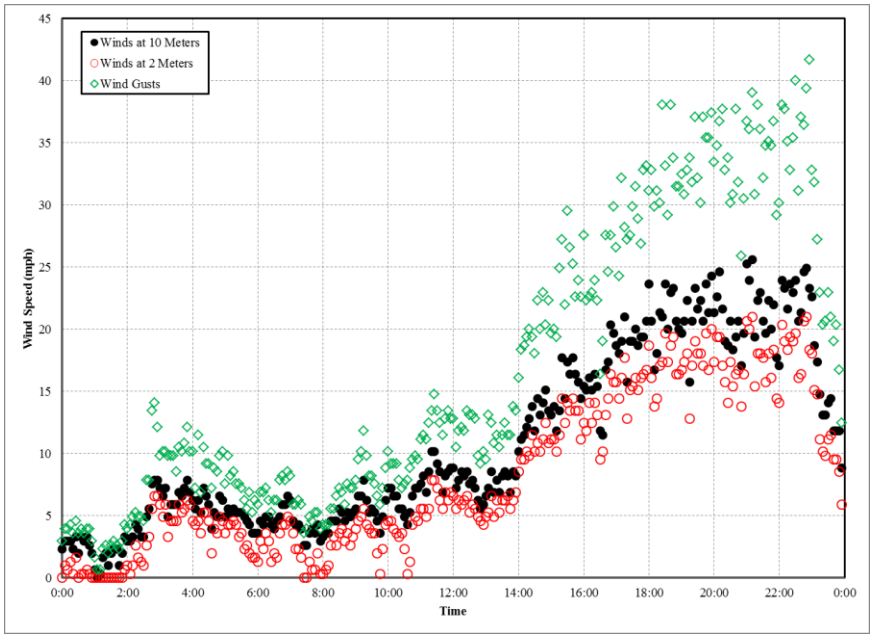

Figure 47-Winds Plotted vs. Time for 11-26-13 (Mesonet)

The data shown in Figure 48 is non-dimensionalized using the topmost probe as the reference. At 20mph, the flow is mostly smooth and uniform with a standard deviation of roughly 0.04. The errors in the measurements are not only created by the data acquisition system but also by wind gusts and unsteadiness in the truck velocity. As shown in the wind plot the winds were steady at roughly 15mph with gusts around 25-30mph which largely influenced the standard deviation calculations. The data shows a slight increase in speeds as you go up in distance from the truck cab.

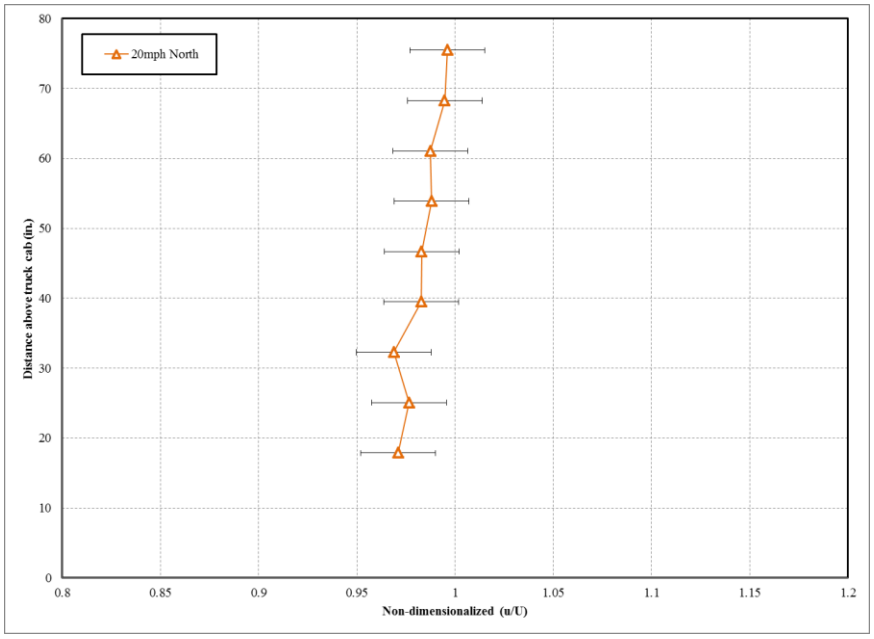

Figure 48-Nondimensionalized Northbound at 20mph with Error Bars

The data at 60mph shows to be more uniform than 20mph, as expected when comparing to previous tests. A very important point to notice when comparing the two speeds is how the error in the measurements is reduced at higher speeds due to the stability in the flow at higher speeds much like the previous tests. The airspeed still accelerates slightly as the distance above the truck cab increases. The other southbound tests show much of the same trends and can be seen in the appendix. The main difference is the error in the measurements for the southbound test at 20mph and how unstable the flow is compared to the other three plots. This is because the winds were coming from the North at roughly 10mph, so the true airspeed was approximately 13mph. As mentioned in the other full-scale testing the lower the speed the more instability in the airflow.

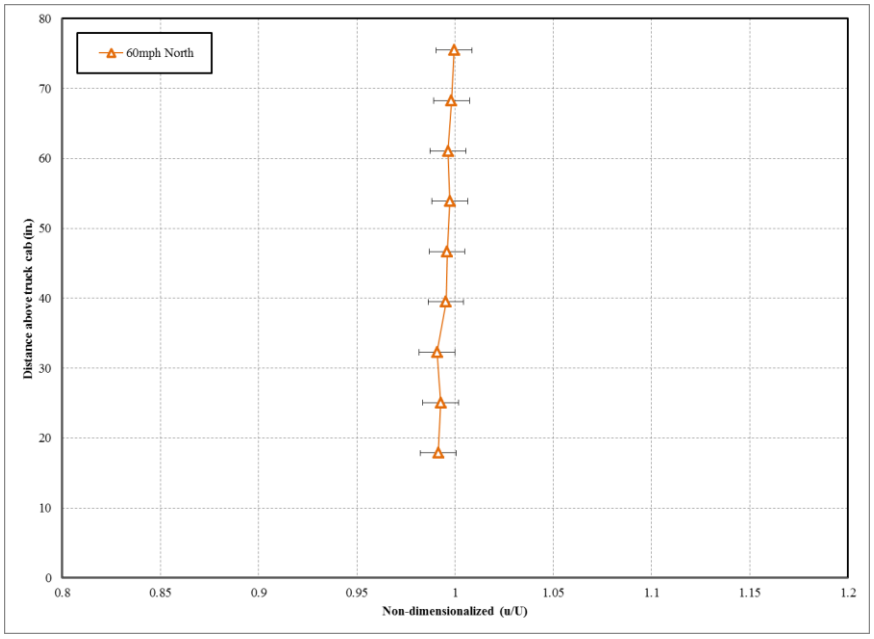

Figure 49-Nondimensionalized Northbound at 60mph with Error Bars

Wind Tunnel Testing

To help further evaluate the flow over the truck, experiments of the flow over a 1/8th scale model of the truck with and without the mobile dyno installed were conducted. The model truck was a plastic shell used for remote control trucks, along with an 1/8th scale model of the fairing that was rapid prototyped using a 3D printer then epoxied to four 1/8th inch square rods to create the dyno legs. The model assembly was attached to a large acrylic sheet with a rounded edge and mounted to the wind tunnel floor. A high-speed camera was mounted to the side of the wind tunnel to capture high-speed images to help with the flow visualization.

Since the model did not represent the actual vehicle perfectly, the distance the dyno was above the truck cab was measured to make sure the model was scaled accurately.

Qualitative Test

The first test was purely qualitative flow visualization using a smoke machine installed at the bottom of the wind tunnel inlet to inject a smoke stream into the tunnel and allowing the smoke to be straightened in the honeycomb section of the tunnel. Trial and error found the position that allowed a good seeding of smoke over the model was conducted. Once the smoke was positioned correctly, the tunnel was run at speeds from 20, 30, 40, 50, and 60 mph with smoke injection and images were taken at a rate 30Hz for 5 seconds allowing a total of 150 images for each airspeed. The test was run with the truck model only then repeated with the dyno model installed. There were even a few runs with the smoke only going over the dyno model to see how the flow goes around the fairing. The images were viewed and only images that showed good streamlines and could be evaluated were chosen to be shown in this paper.

While the model is not an exact replica of the full-scale vehicle, it has very similar shape and allows us to examine the flow around this type of vehicle. Reynolds number matching is a very important part of the scale model testing, but is nearly impossible to perfectly match without changing the test fluid density from air to something like water. However, since the Reynolds number for the actual truck is $3.5x10^6$-$1x10^7$, using the full truck length as the characteristic length and the scale model Reynolds number at $5x10^5$-$1.5x10^6$, both Reynolds number ranges are for the most part, within the same order of magnitude. Also, there are no other options readily available.

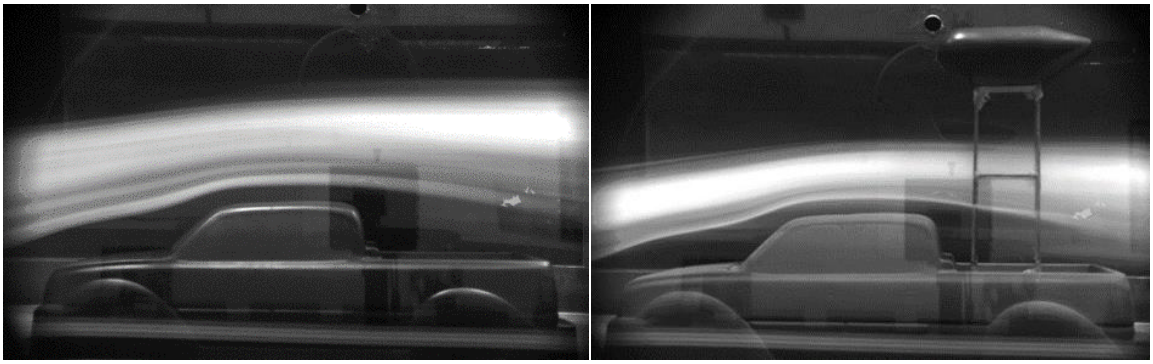

Figure 50-Flow Visualization With and Without Dyno with Reynolds Number of $7.3x10^5$ (30mph)

Several things can be taken from the flow visualization images. For example, when looking at Figure 51 the red arrows show the gap between the airflow and the surface represent the boundary layer shape. The gap becomes thinner as the flow has to accelerate over the vehicle, which feeds more energy in the flow to resist the fluid pushing back on the model. This helps with our case since we want a boundary layer that is as thin as possible so that it does not influence the propeller. The orange arrows show how the smoke stream becomes thinner the more the fluid has to change direction to go around the object. We can assume that the stream has constant area, and create the relation, $(VA)_1=(VA)_2$ where velocity and stream cross-sectional area are V and A respectively. This relation is created by using control volume analysis and mass flow rate of the stream and allows us to relate the height of the orange arrows to the velocity of the stream. Using this information you see that the flow in the stream has to roughly double its velocity from the front of truck to the top of cab to move over the vehicle. Another important note is the areas of separation created by the flow not being able to follow the surface, such as in the truck bed. The flow dispersion shows mixing which results in the turbulent flow encountered behind the truck cab. Separation is shown to only happen behind and below the propeller plane.

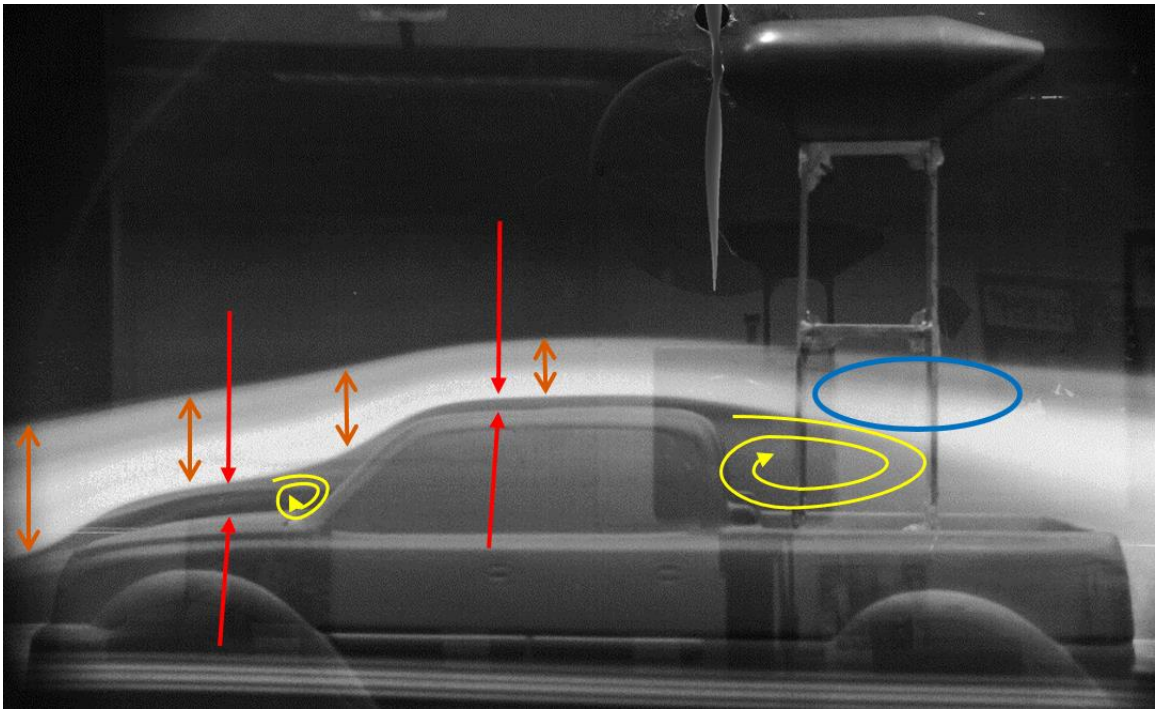

Figure 51-Flow Visualization with Dyno with Reynolds Number of $1.2x10^6$ (50mph)

When comparing the flows with and without the dyno installed, the results from Figure 50 show that the dyno did not have any impact on the flow above the truck cab. These show to be the results for all of the speeds tested as can be seen in the Appendix. The dyno did in fact affect the flow downstream as can be seen in the above figure. The flow is not a smooth streamline while passing the legs of the dyno like they are in the model without the dyno. The flow is tripped turbulent, but this is not a concern for propeller testing since all testing will be ahead of this point in the flow. Also, speeds around 20mph showed to be less stable than higher speeds. This cannot be seen by the images, but the flow would fluctuate in y-direction more easily, but this was only due to flow instability, not the model.

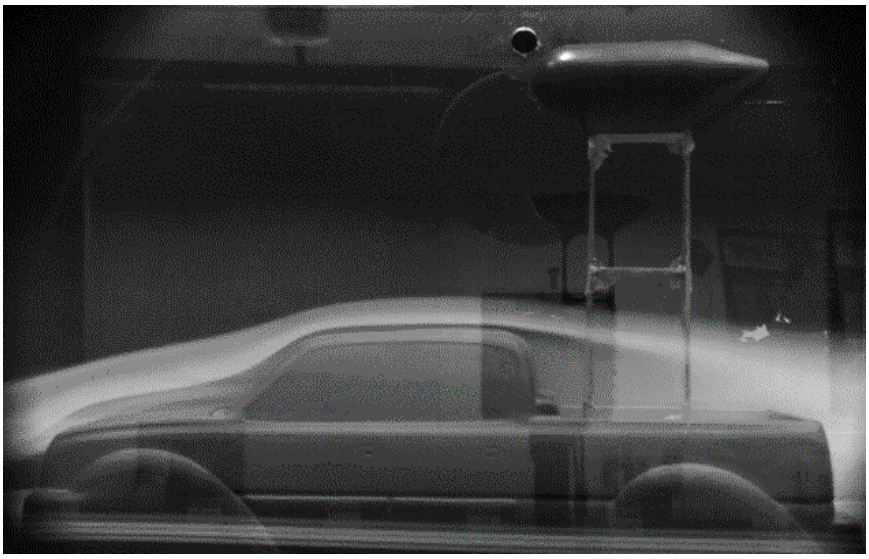

Figure 52-Flow Visualization With Dyno with Reynolds Number of $1.5x10^6$ (60mph)

Another very interesting and expected observation of the flow is how the gap between the smoke flow and the model gets thinner as the velocity is increased. This is even more easily seen when comparing the images in order of increasing velocity. Overall the flow is shown to be a very smooth and consistent flow in the plane of the propeller and not affecting the propeller's aerodynamics.

CHAPTER V

CONCLUSIONS

While the validation results for the mobile dyno are not finished, the results obtained to this point have proven that the mobile dyno is capable of producing accurate dynamic propeller tests. However, the wind tunnel dyno must be renovated to allow for better results than are available at this time. Also, a larger propeller that has published data could be purchased and ran on the dynamic dyno and then compared against the manufacturer's results for further validation.

The inclinometer measurements show to have a lot of noise, but the moving average results could be used to remove errors in thrust measurements. However, installing a more accurate inclinometer would be beneficial to acquire more accurate data overall. In addition to the inclinometer, a GPS system could be used to record the location of the dyno during testing and running a few test runs with no propeller can be recorded to get the errors in thrust due to inclines. The GPS data can be used to match up the data with no propeller and used to subtract the errors in thrust measurement. The inclinometer validation results also exposed problems with thrust not returning back to zero due to hysteresis. The testing shows thrust to follow the same trends, but not actually follow the same values. This is probably due to the small amount of friction in the bearings being amplified by the angle produced thrust errors.

After evaluating the full-scale vehicle aerodynamic results, it has been shown that the airflow over the vehicle will not influence the propeller performance data collected by the mobile

dyno. Carefully looking at all of the data, the largest propeller that can be properly evaluated on the dyno can have a radius no larger than 42 inches or 3.5 feet. This allows the dyno to test propellers up to 7 feet in diameter, which is more than the dyno's original design requirements. In the end, any propeller being tested that is at least 12 inches away from the top of the truck will not be influenced by accelerated flow over the truck.

The scaled model wind tunnel testing proved to be very useful to see how the air flows around the vehicle; however, you must be careful, since the flow is three dimensional, it may not follow the same two dimensional trends that you see in the images. PIV testing will be needed to assure that the flow is actually behaving as you would expect. Unfortunately, a shortage in time did not allow this testing to be completed for this paper. The model may also need to be altered to allow a ground-effect so that the results will be similar to the full-scale pickup truck flow.

Overall, Oklahoma State University has designed and manufactured a mobile propeller/propulsion system dyno that is capable of making accurate performance measurements. The dyno will allow OSU to conduct "simulated flight" tests on larger propulsion units without the use of a large and expensive wind tunnel, allowing important performance parameters to be collected.

Future Work

Making the mobile propulsion dyno more accurate through future improvements will be an ongoing process, especially when different propulsion units are fitted. Once propellers become too large to run on the existing brushless Hacker motor, an internal combustion engine will have to be mounted, along with fuel tanks and the appropriate controls. A combustion engine will allow larger propellers to be evaluated due to the larger amount of available power.

Accuracy

Adding a multi-hole pitot-probe will assist in making corrections to the data when testing during winds that are not perpendicular to the propeller plane and will also serve as a true airspeed during testing. When adding the multi-hole probe, additions will have to be made to the Labview program to allow all of the pressures to be recorded using the Scanivalve.

Additional validation of the dyno is needed after the wind tunnel dyno is fixed or by finding an alternative method of validation. Before validating the mobile dyno, the wind tunnel dynamometer will have to be restored to produce more accurate data which matches published data from the UIUC database, along with propeller performance calculated from Blade-Element/Momentum Theory.

Vehicle Aerodynamics

For additional assurance of the flow over the vehicle, turbulence measurements over the truck cab and in the propeller plane would be beneficial to assure that the flow is laminar or at least near laminar. Full scale flow visualization would prove useful to compare to the wind tunnel results by installing a smoke generator and using a smoke wand mounted to the front of the vehicle.

While the wind tunnel model proved to be good for the uses of this project, the accuracy of the model can be enhanced by making several adjustments. Adding a gap underneath the model and simulated tires would allow the vehicle to simulate the flow underneath the truck. Also a treadmill system could be added or a simpler approach of blowing or sucking flow under the model would allow a simulated ground effect. A propeller will change the flow patterns over the vehicle and could be studied by adding a small motor to the fairing model and mounting a propeller.

Automation

As mentioned in the previous work, the truck dyno should be made more autonomous by allowing the Labview program to control the propeller rotational rate. The operator would hold constant truck velocity while the program runs through a specified range of rpm to allow a full sweep of propeller performance data. Once data is collected for that speed, simply accelerate or decelerate to a new speed and repeat the test.

Additional Uses

Oftentimes experimental aircraft can use further testing before actual flight tests. The propulsion dyno could serve as a simulated flight test bed for full size UAVs or scaled aircraft. This would allow the user to test vehicle lift, drag, and installed thrust without the risk of flying and damaging the aircraft. As you can see in the figure below, the dyno can be retro-fitted to allow the installation of an experimental VTOL (Vertical Take-off and Landing) aircraft. This allows the user to test the unknown transition from vertical to horizontal flight on the dyno without compromising the aircraft. The retrofit is easily done by adding a specialized mount for the aircraft and adding load cell for lift built into the mount.

Figure 53-VTOL Aircraft Installed to Allow Dynamic Tests of Transition

REFERENCES

Conner, J. and Arena, A., "*Advanced Dynamometer Designed to Fully Characterize the Propulsion System for a UAV*," SAE Technical Paper 2002-01-2921, 2002.

Gamble, D. E. "*Automated dynamic propeller testing at low Reynolds numbers*", M.S. Thesis, Oklahoma State University, 2009.

Hays, T. "*High energy density propulsion systems and small engine dynamometer*" , M.S. Thesis, Oklahoma State University, 2009.

White, F. M. (2006). *Viscous fluid flow*. New York, NY: McGraw-Hill Higher Education. "Viscous Fluid Flow" , M.S. Thesis, Oklahoma State University, 2009.

University Mulitspectral Laboratories. "*Unmanned Aerial Systems Engine Studyr*" , Technical Study, Oklahoma State University-UML, 2009.

Theodorsen, T. (1948). *Theory of propellers*. New York: McGraw-Hill Book Co

McGovney,G and Otto, J. and Smith, B. "*Propeller Test Module*", B.S. Project Report, Oklahoma State University, 2010.

Mesonet, 2013. Perkins Past Weather Data Files.URL http://www.mesonet.org/index.php/weather/local

Abdullah M. Al-Garni, Luis P. Bernal, Experimental study of a pickup truck near wake, Journal of Wind Engineering and Industrial Aerodynamics, Volume 98, Issue 2, February 2010, Pages 100-112, ISSN 0167-6105, http://dx.doi.org/10.1016/j.jweia.2009.10.001.

Youngren, H. and Chang, M., "*Test, Analysis and Design of Propeller Propulsion Systems for MAVs",* AIAA 2011-876, 49th AIAA Aerospace Sciences Meeting, January 2011.

Brandt, J. and Michael, S., "*Propeller Performance Data at Low Reynolds Numbers",* AIAA 2011-1255, 49th AIAA Aerospace Sciences Meeting, January 2011.

Adkins, C. and Robert, L., "*Design of Optimum Propellers"*, Journal of Propulsion and Power Vol. 10, No. 5, Sept.-Oct. 1994.

Chattot, J., "*Optimization of Propellers Using Helicoidal Vortex Model"*, Computational Fluid Dynamics Journal Vol. 9, July 2000.

Merchant, M. "*Propeller Performance Measurement for Low Reynolds Number Unmanned Aerial Vehicle Applications*", M.S. Thesis, Wichita State University, 2005.

Koch, L. Danielle,Lewis Research Center. *Design and Performance Calculations of a Propeller for very High Altitude Flight: Microform*. 1998-206637 Vol. Springfield, Va: National Aeronautics and Space Administration, Lewis Research Center, 1998. Web. 6 Dec. 2013.

Uhlig, D. and Michael, S., "*Post Stall Propeller Behavior at Low Reynolds Numbers",* AIAA 2008-407, 46th AIAA Aerospace Sciences Meeting, January 2008.

APPENDICES

Appendix A- Inclinometer Validation Results

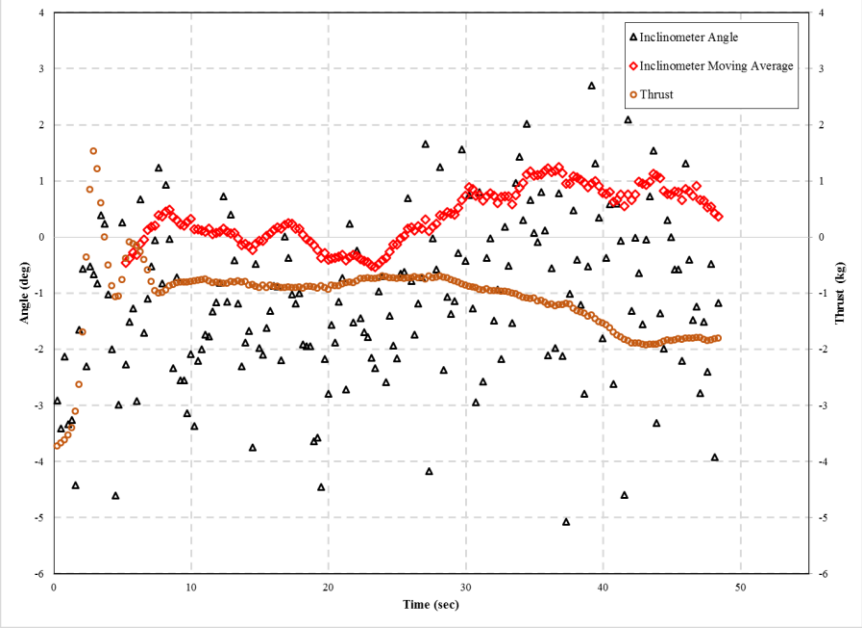

Figure 54-Northbound Inclinometer and Thrust Data with Insulator

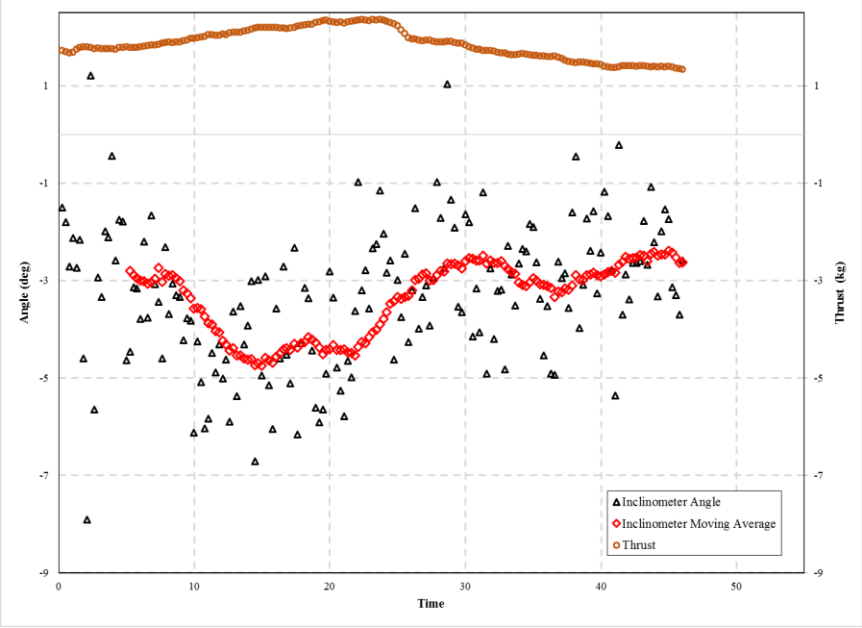

Figure 55-Southbound Inclinometer and Thrust Data with Insulator

Appendix B- Results of Mobile Dyno Validation

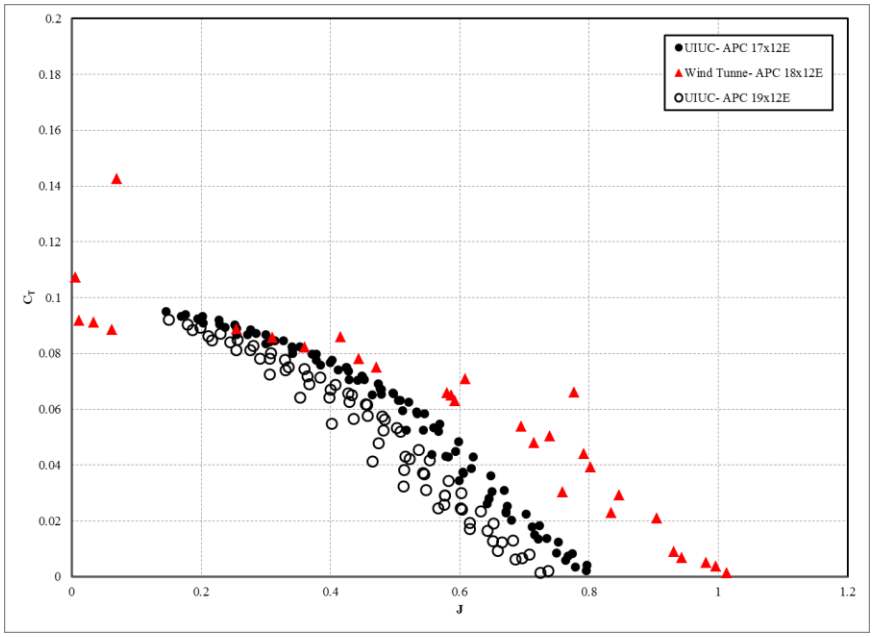

Figure 56-C_T Wind Tunnel Dyno Compared To UIUC Data

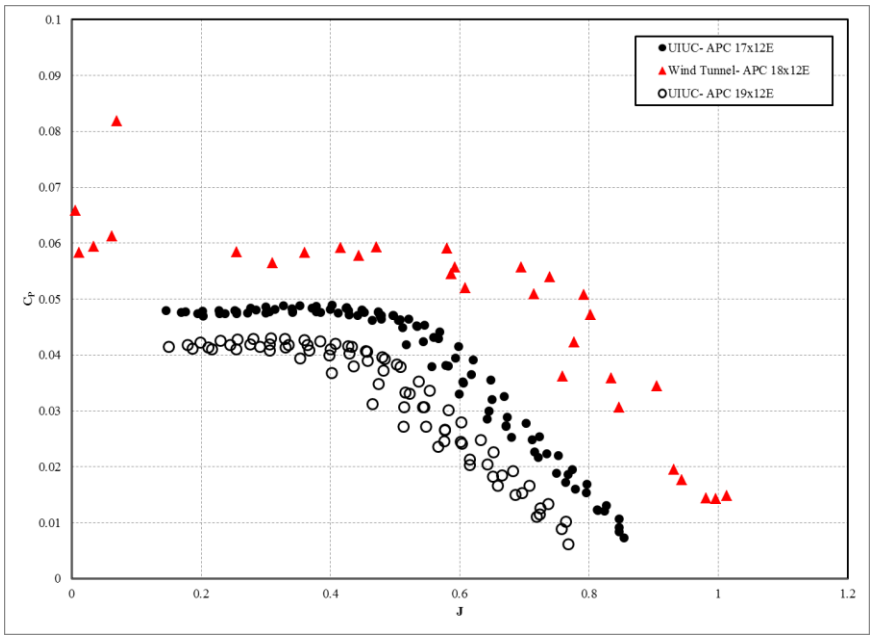

Figure 57- C_P Wind Tunnel Dyno Compared To UIUC Data

Appendix C- Results of Full Scale Tests #1

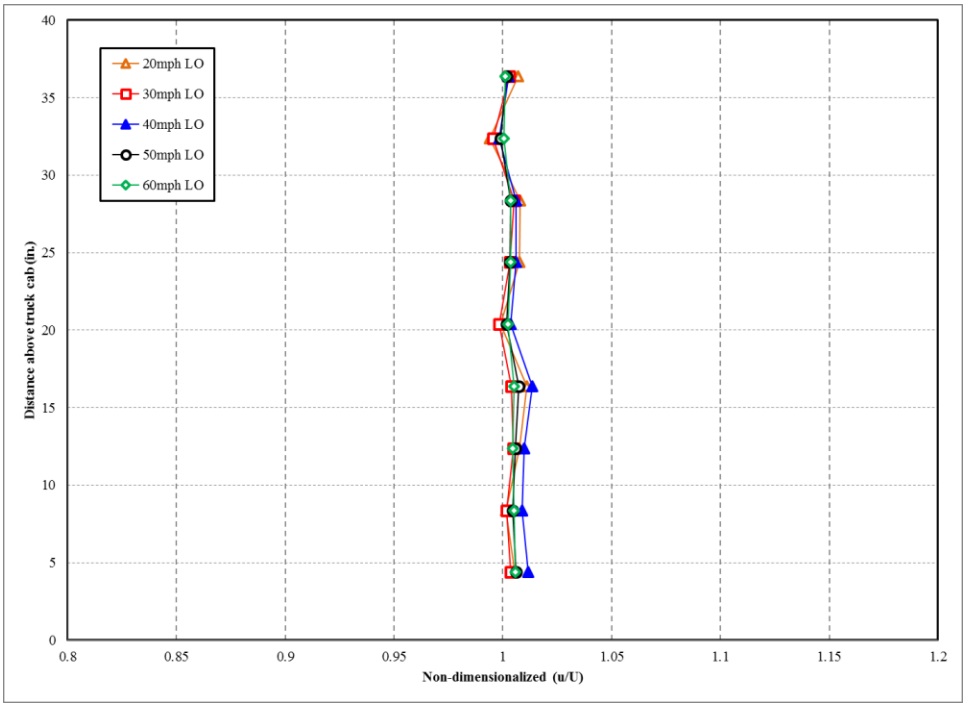

Figure 58- Non-dimensionalized Flow of the Left Outer Position at All Speeds

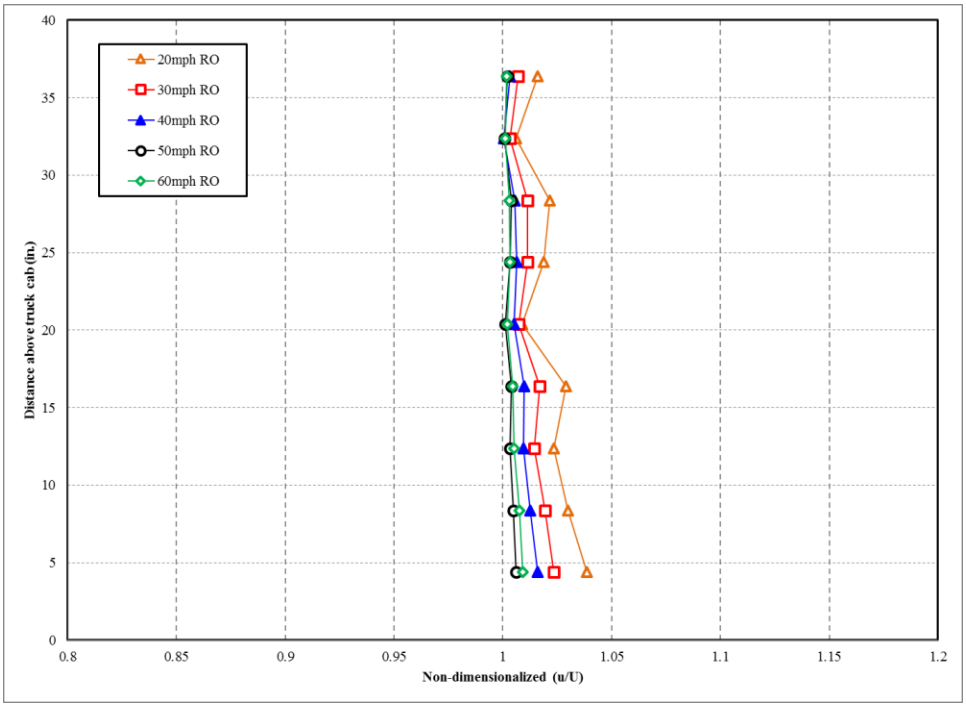

Figure 59- Non-dimensionalized Flow of the Right Outer Position at All Speeds

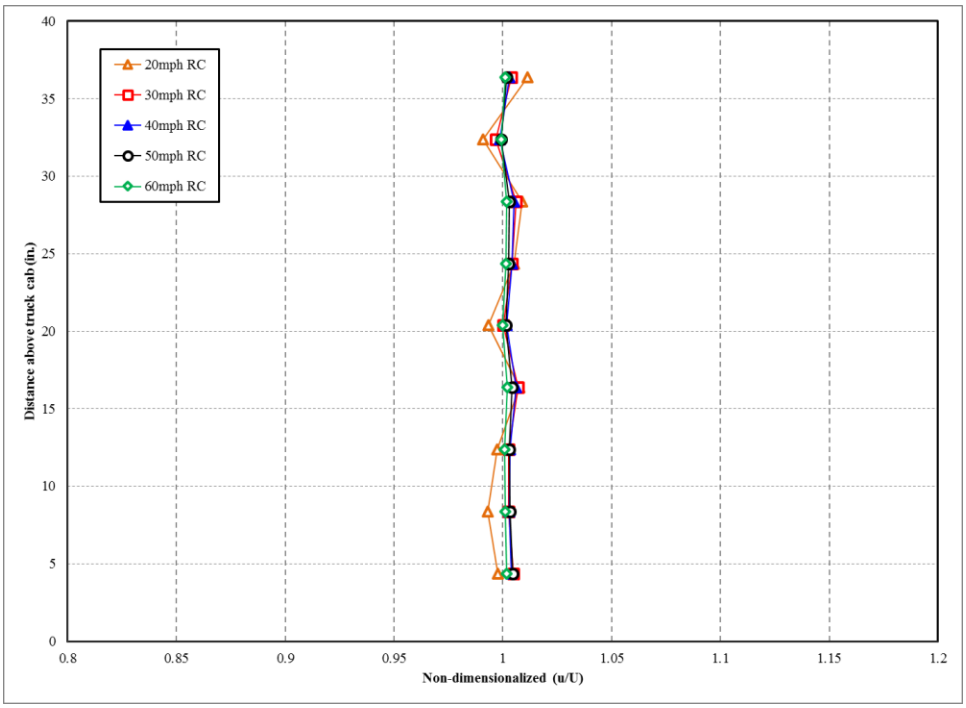

Figure 60-Non-dimensionalized Flow of the Right Center Position at All Speeds

Appendix D- Results of Full Scale Tests #2

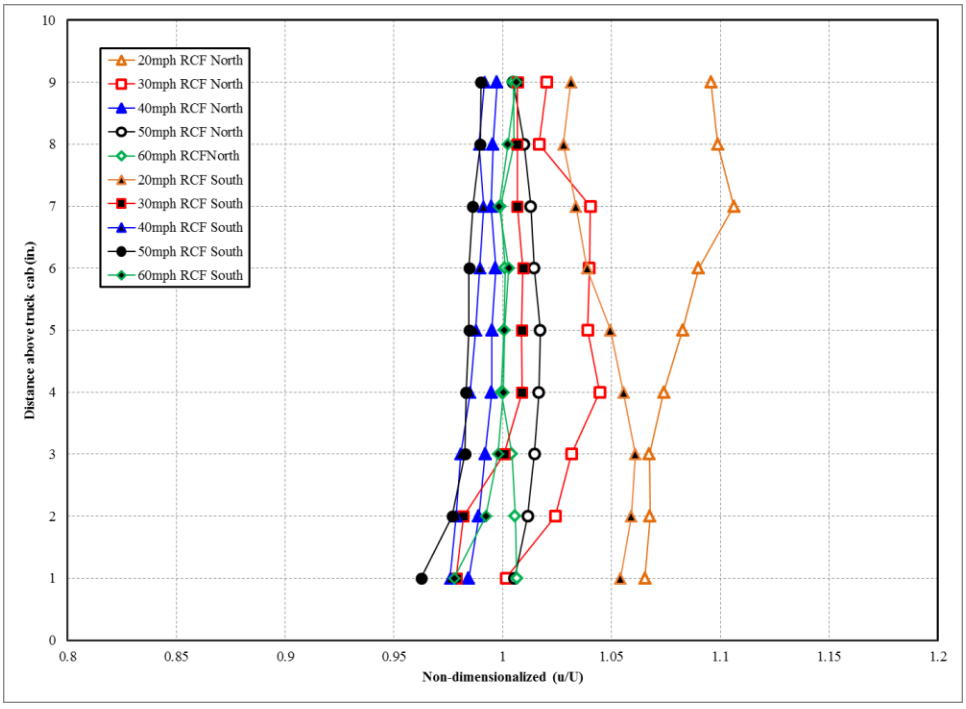

Figure 61-Non-dimensinalized Flow of the Right Center Front Position at All Speeds

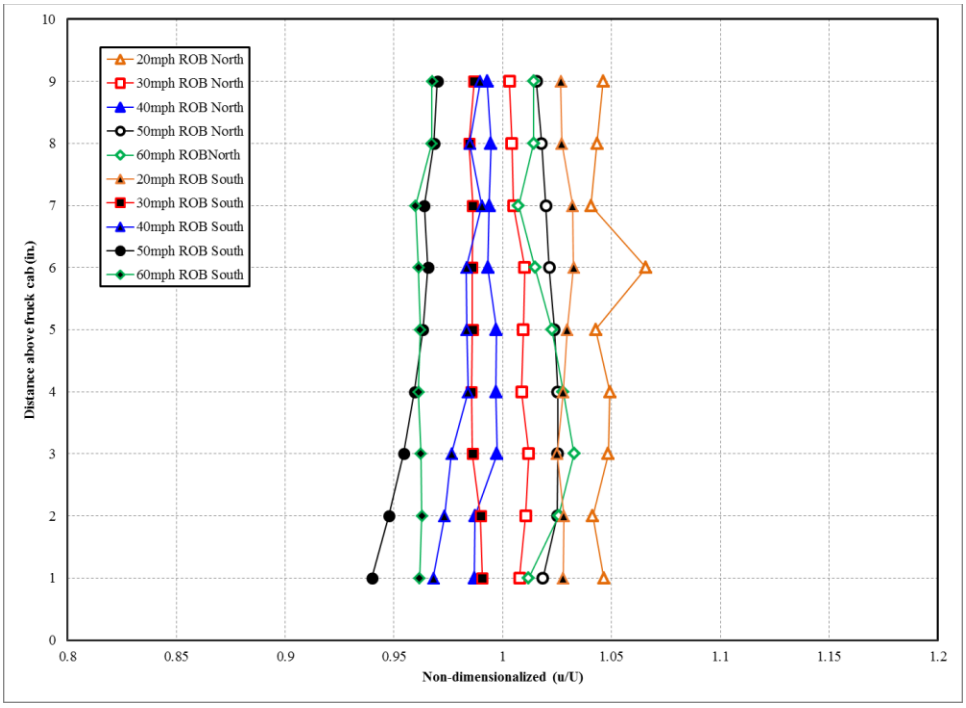

Figure 62- Non-dimensinalized Flow of the Right Outer Back Position at All Speeds for All Directions

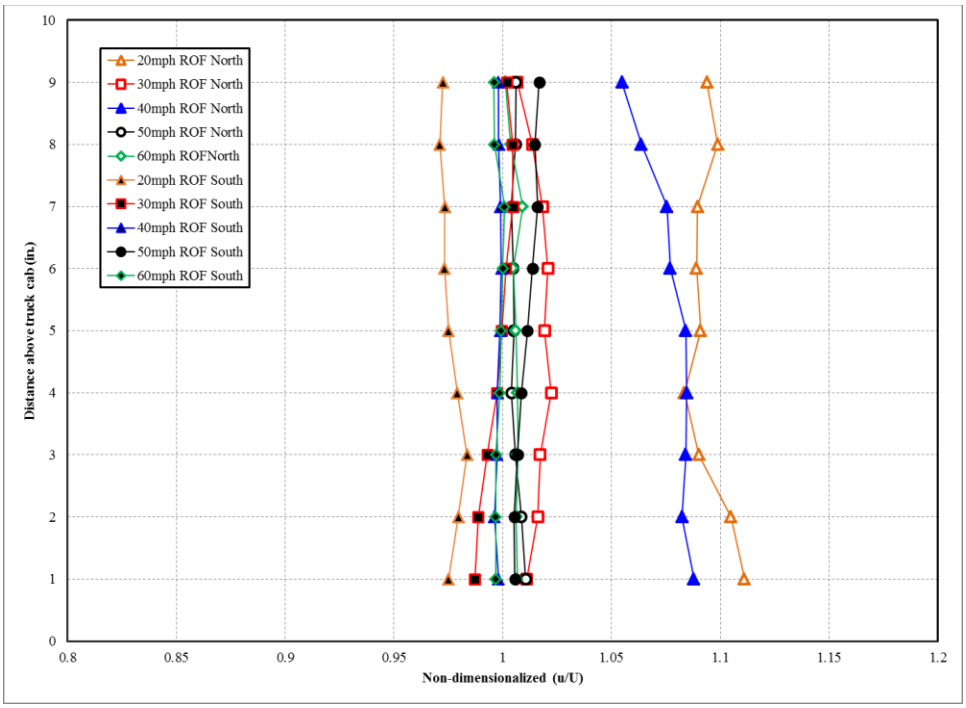

Figure 63- Non-dimensinalized Flow of the Right Outer Front Position at All Speeds for Both Directions

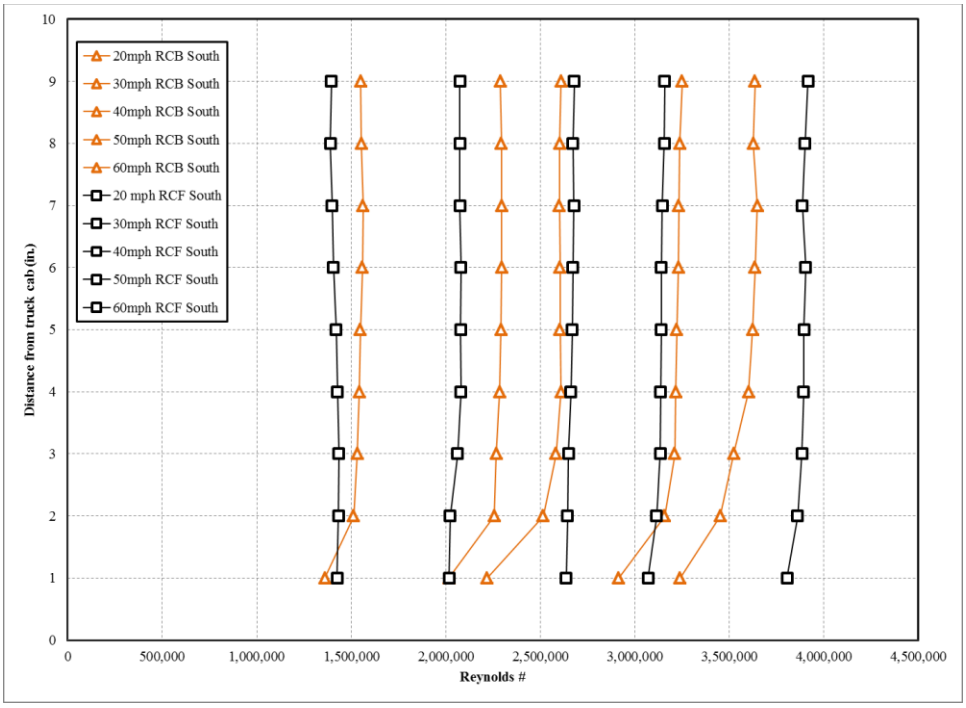

Figure 64- Right Center Positions Southbound vs. Reynolds Number

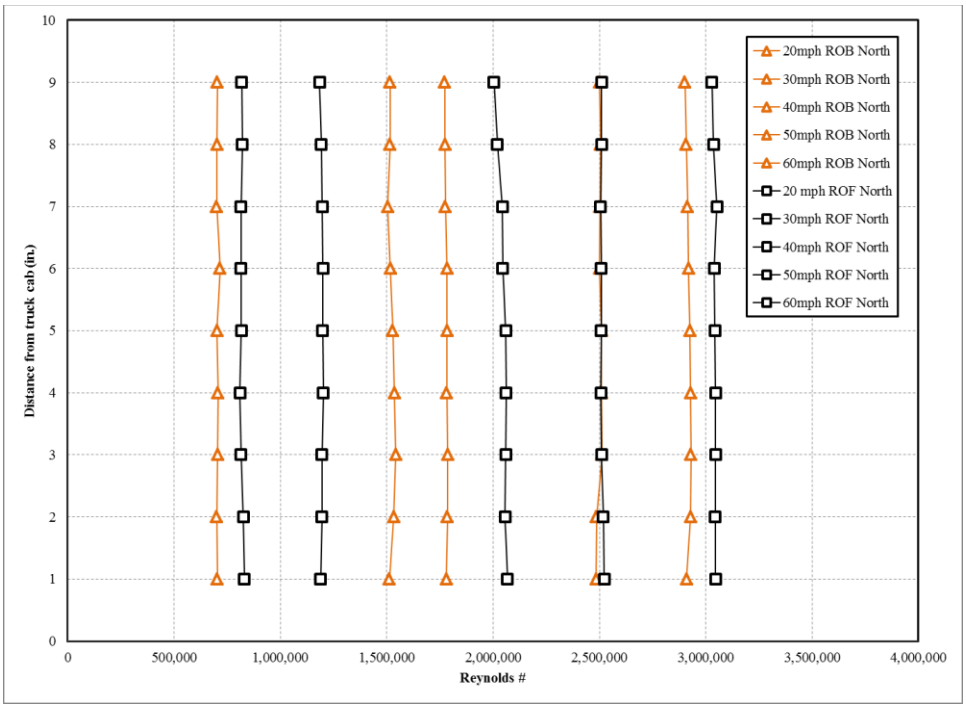

Figure 65- Right Outer Positions Northbound vs. Reynolds Number

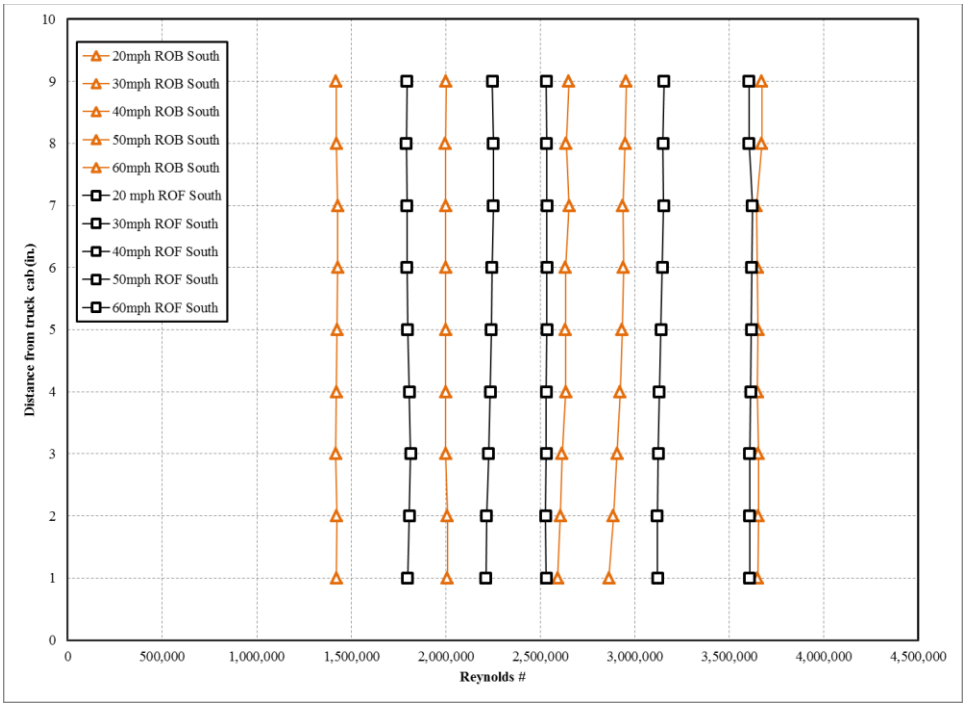

Figure 66- Right Outer Positions Southbound vs. Reynolds Number

Appendix E- Results of Full Scale Tests #3

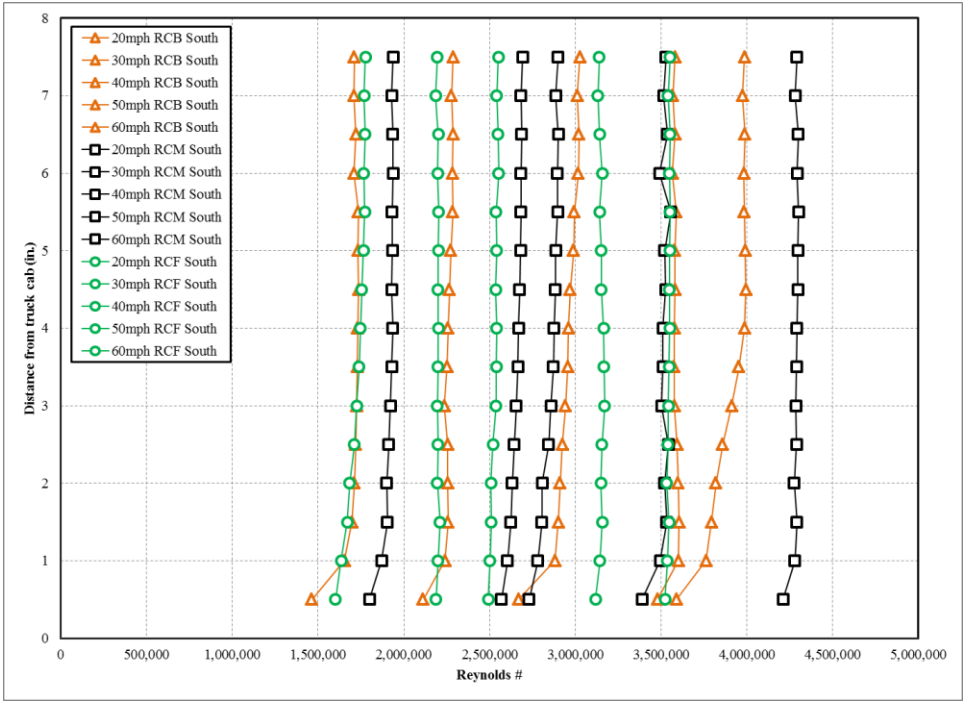

Figure 67-Right Center Positions Southbound vs. Reynolds Number

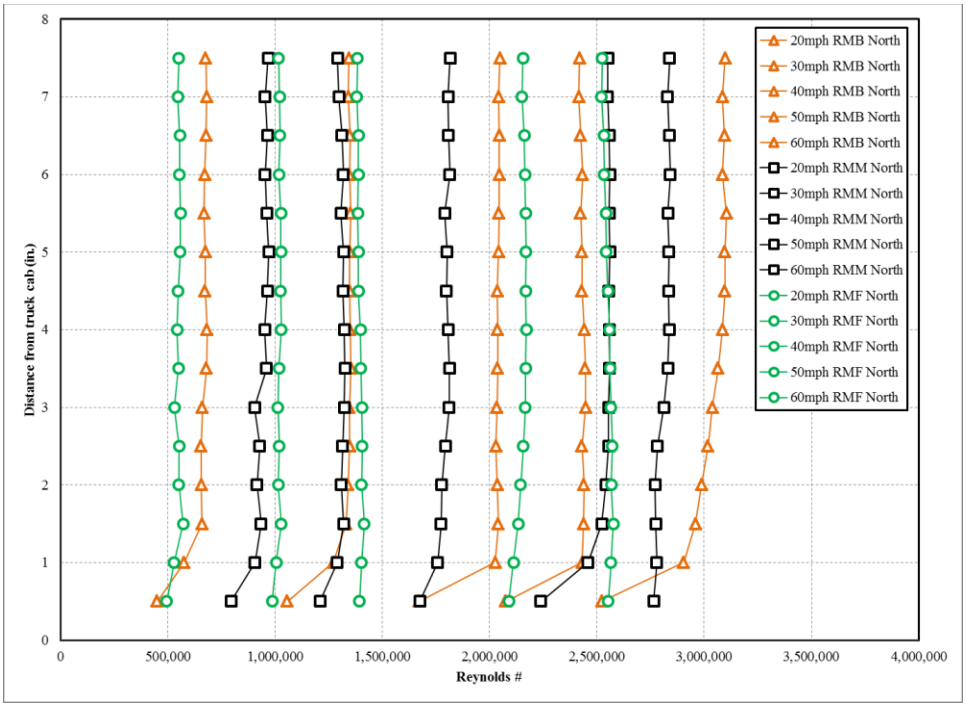

Figure 68-Right Middle Positions Northbound vs. Reynolds Number

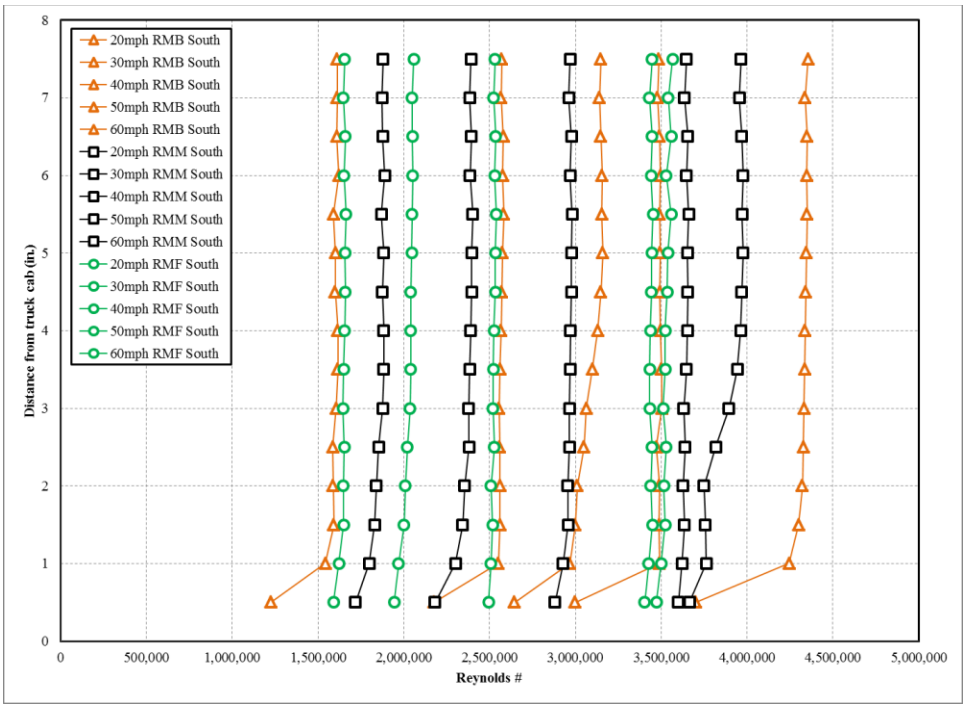

Figure 69-Right Middle Positions Southbound vs. Reynolds Number

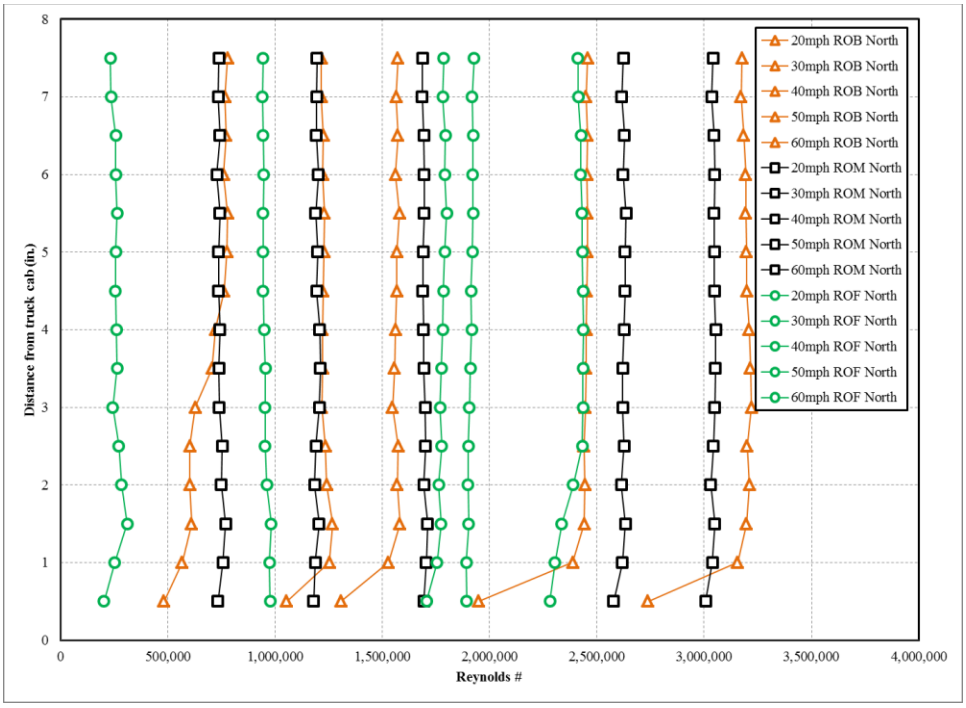

Figure 70-Right Outer Positions Northbound vs. Reynolds Number

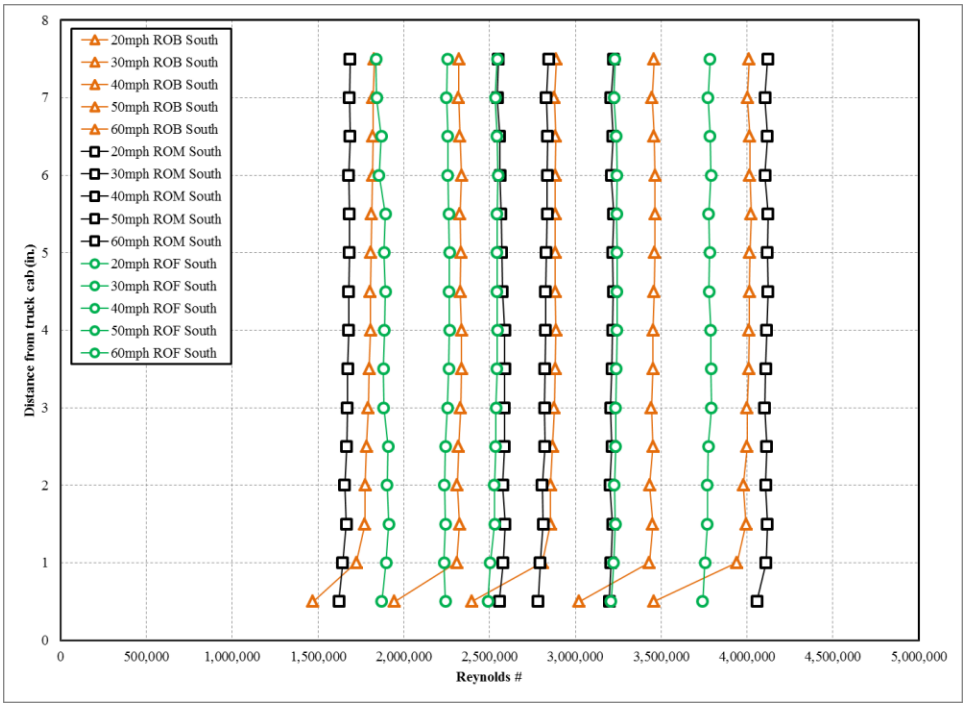

Figure 71- Right Outer Positions Southbound vs. Reynolds Number

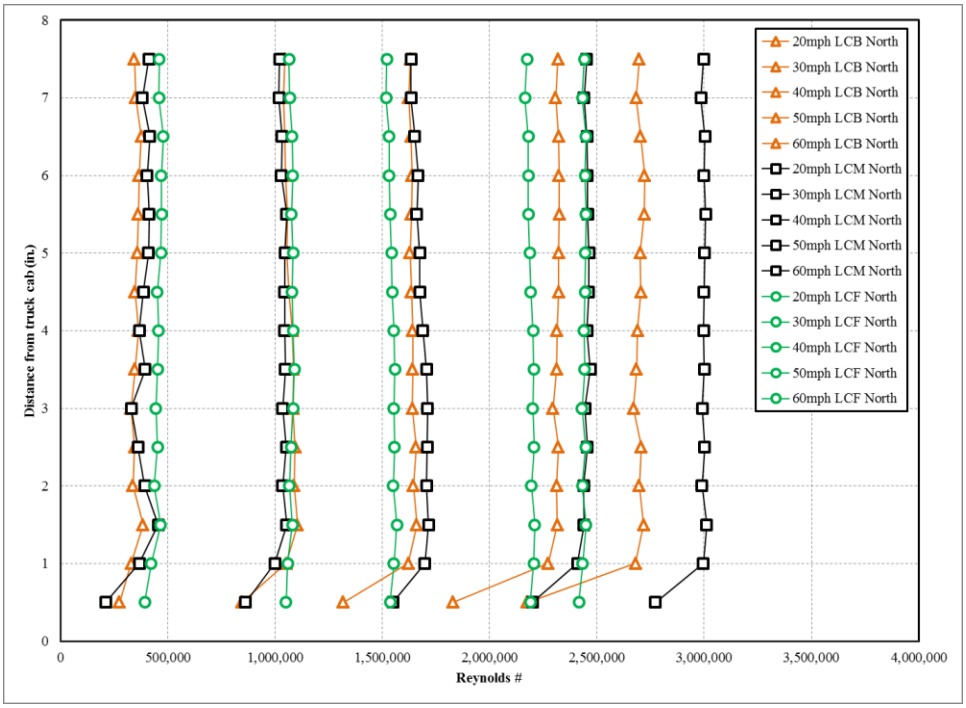

Figure 72- Left Center Positions Northbound vs. Reynolds Number

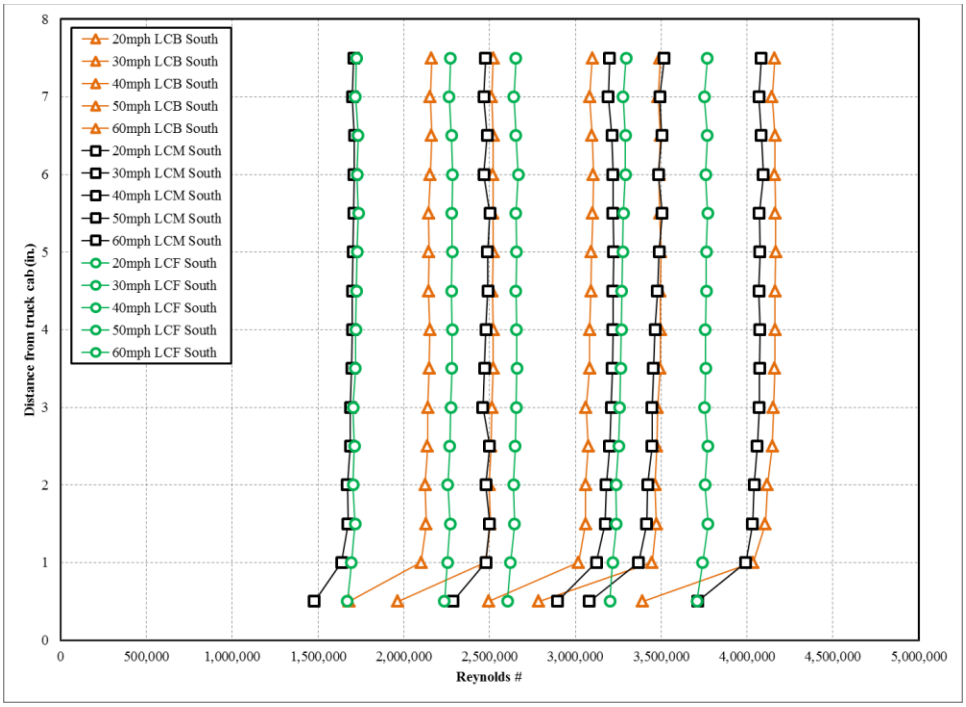

Figure 73- Left Center Positions Southbound vs. Reynolds Number

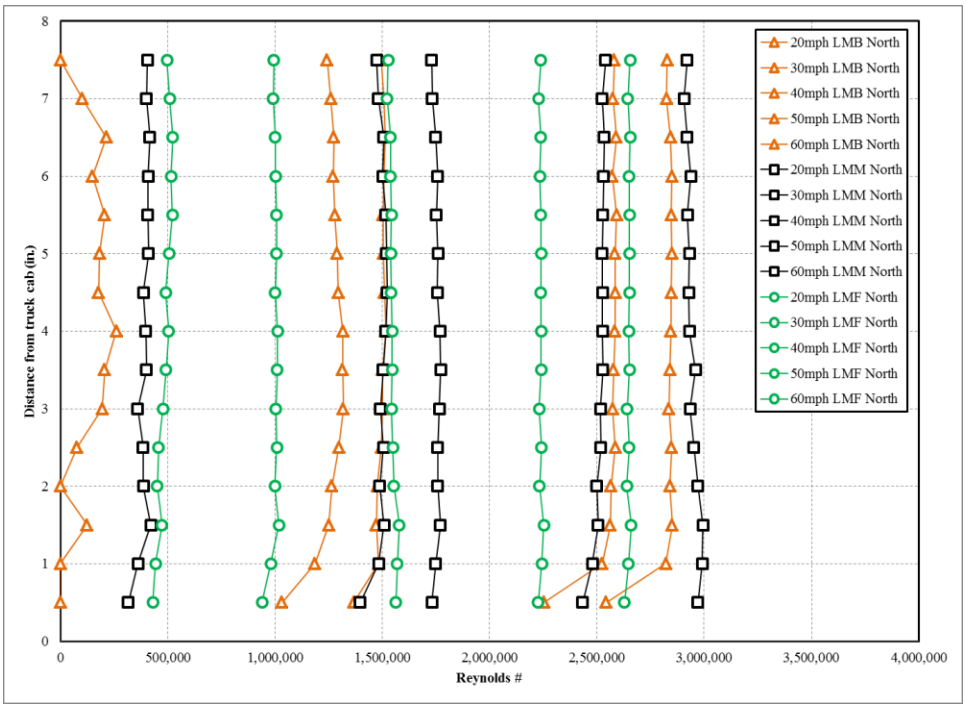

Figure 74- Left Middle Positions Northbound vs. Reynolds Number

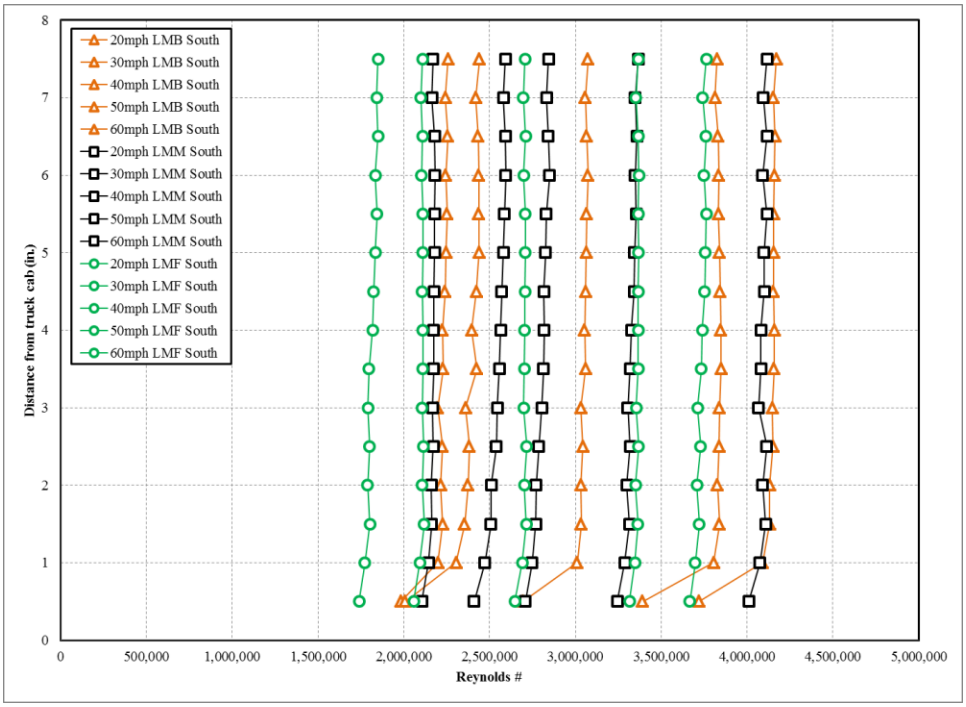

Figure 75- Left Middle Positions Southbound vs. Reynolds Number

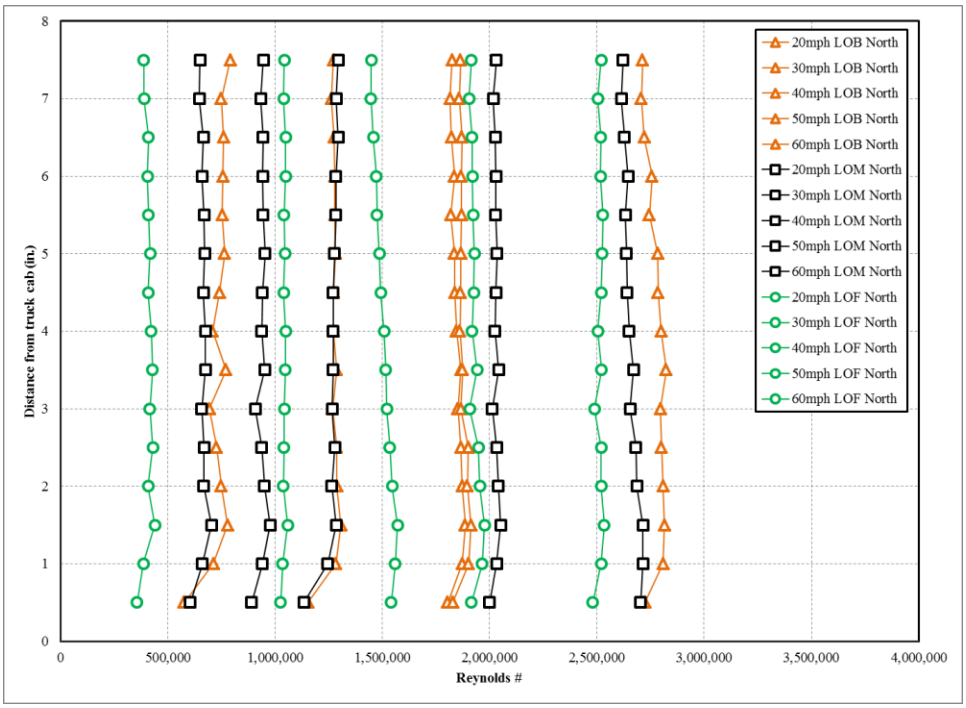

Figure 76- Left Outer Positions Northbound vs. Reynolds Number

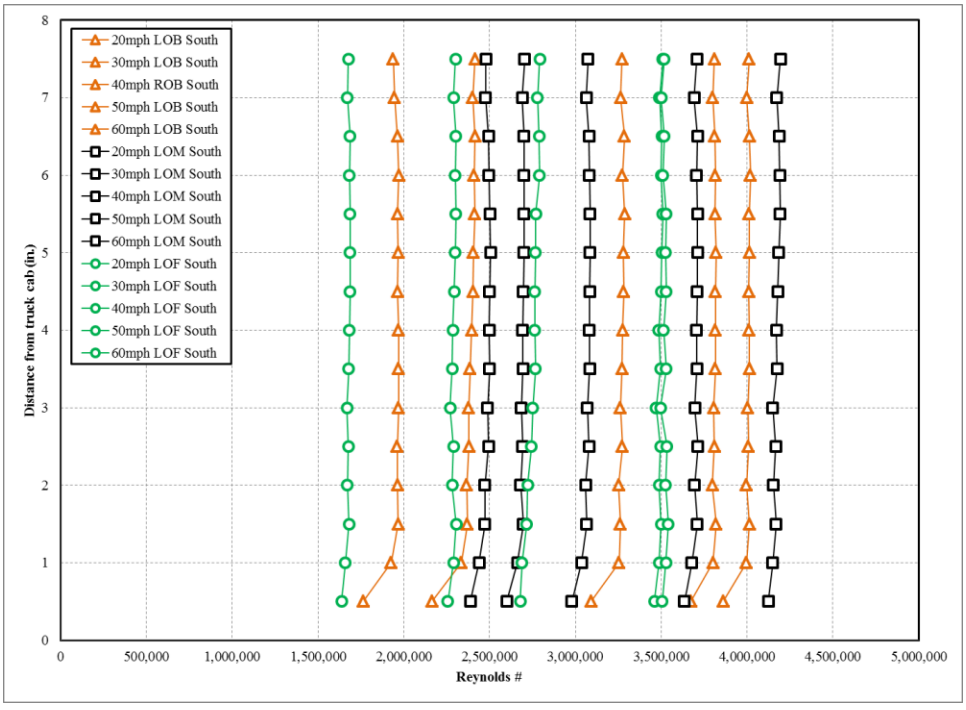

Figure 77- Left Outer Positions Southbound vs. Reynolds Number

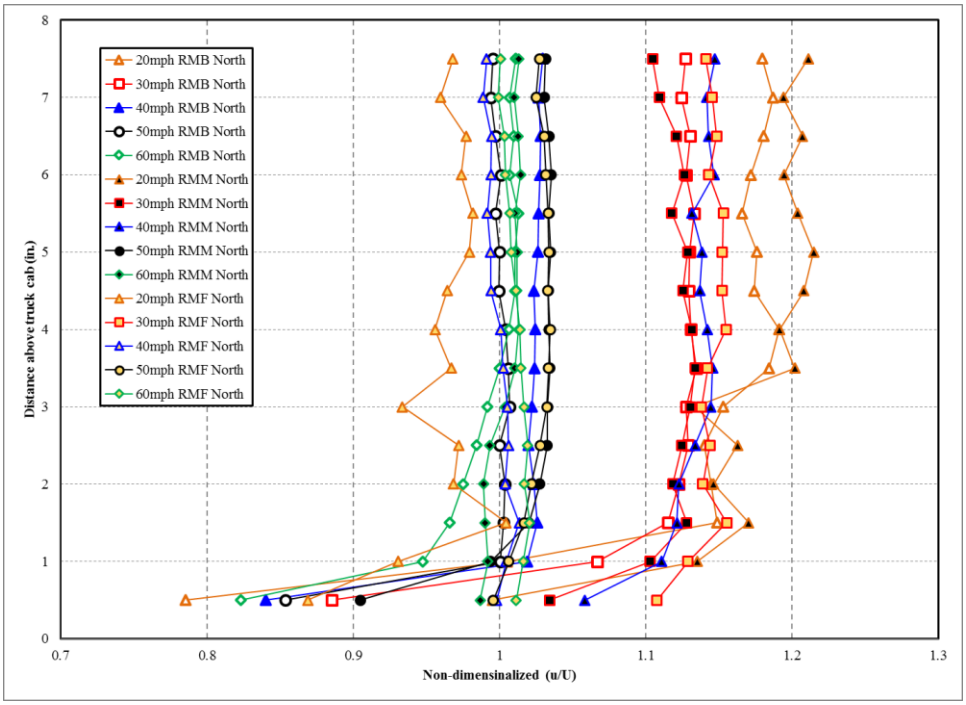

Figure 78-Right Middle Positions Northbound Non-dimensionalized

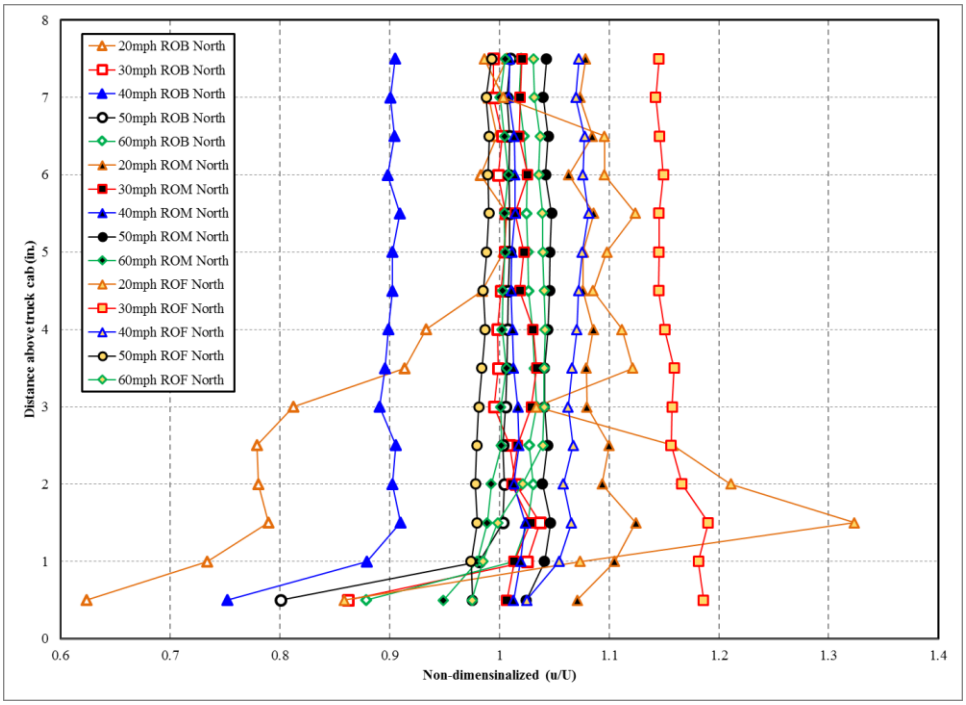

Figure 79-Right Outer Positions Northbound Non-dimensionalized

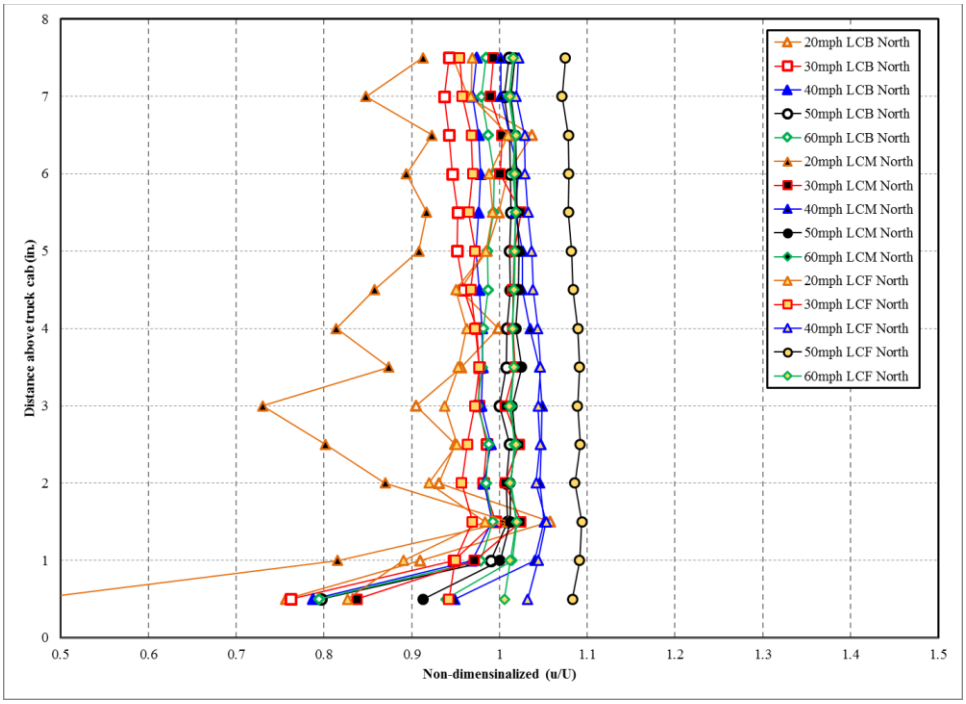

Figure 80-Left Center Positions Northbound Non-dimensionalized

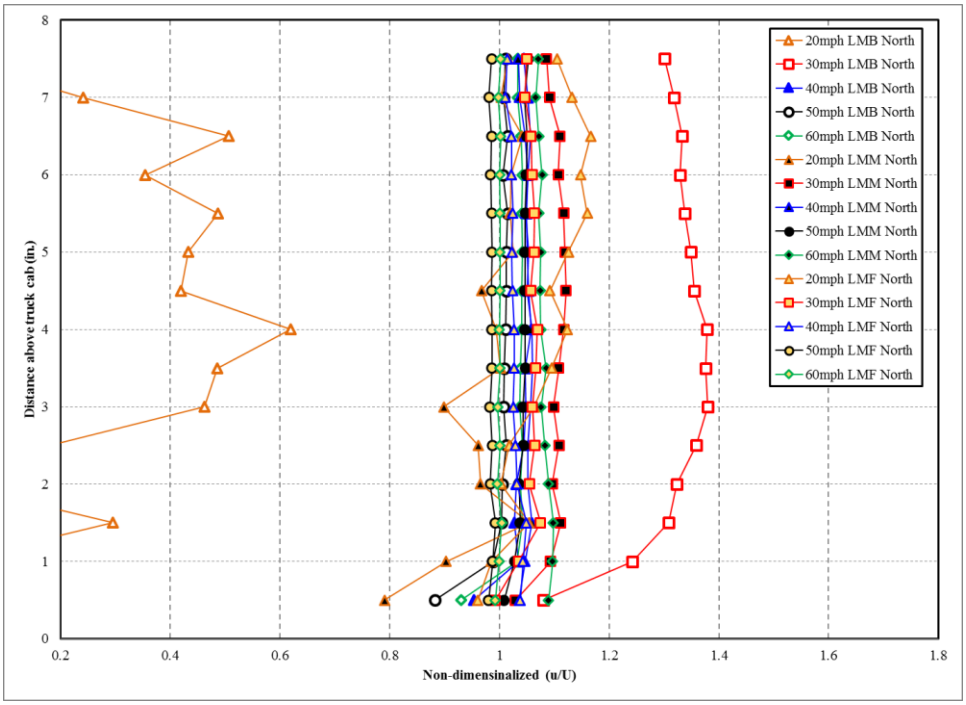

Figure 81-Left Middle Positions Northbound Non-dimensionalized

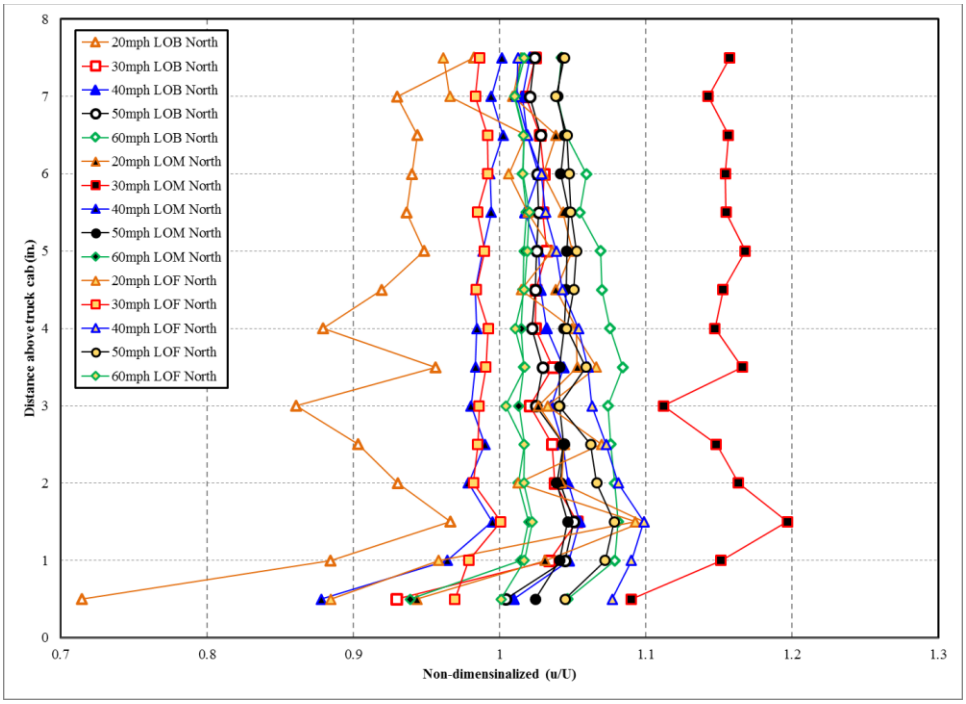

Figure 82-Left Outer Positions Northbound Non-dimensionalized

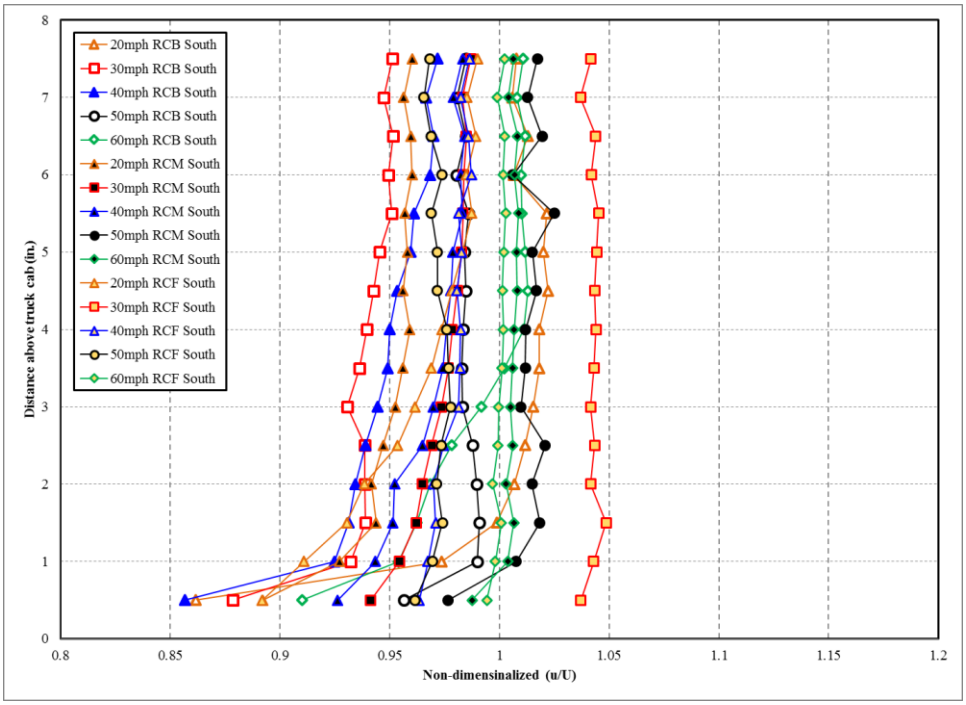

Figure 83-Right Center Positions Southbound Non-dimensionalized

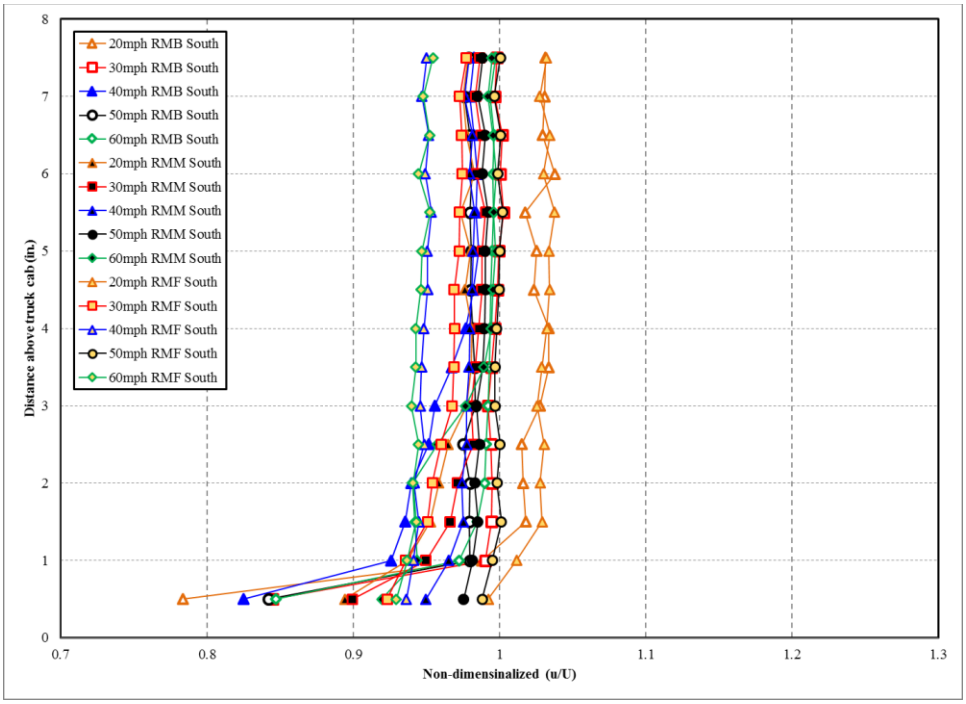

Figure 84-Right Middle Positions Southbound Non-dimensionalized

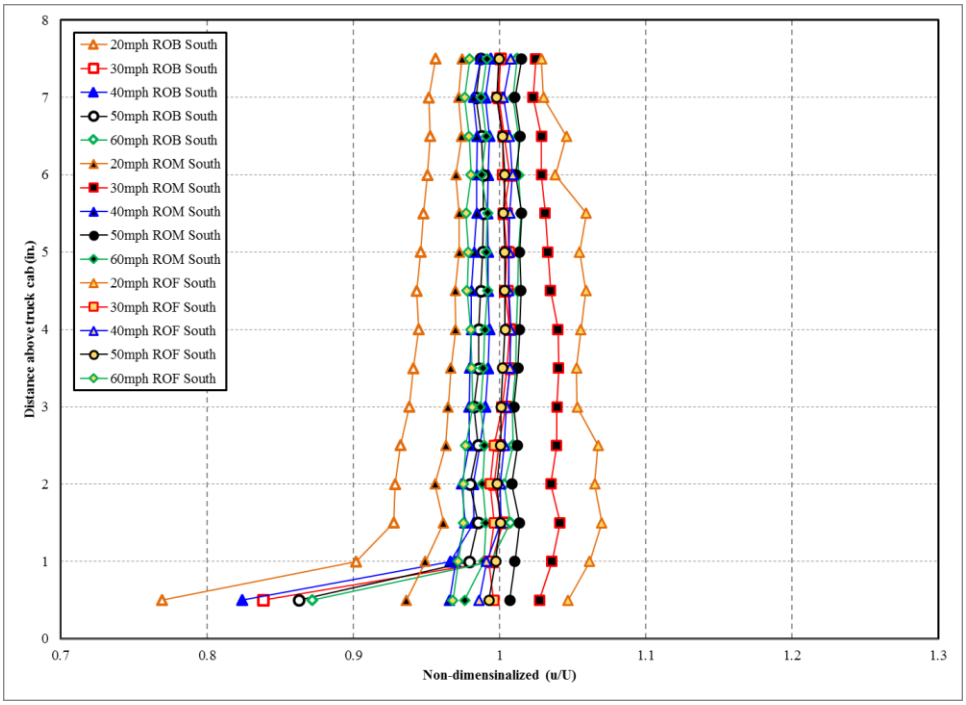

Figure 85-Right Outer Positions Southbound Non-dimensionalized

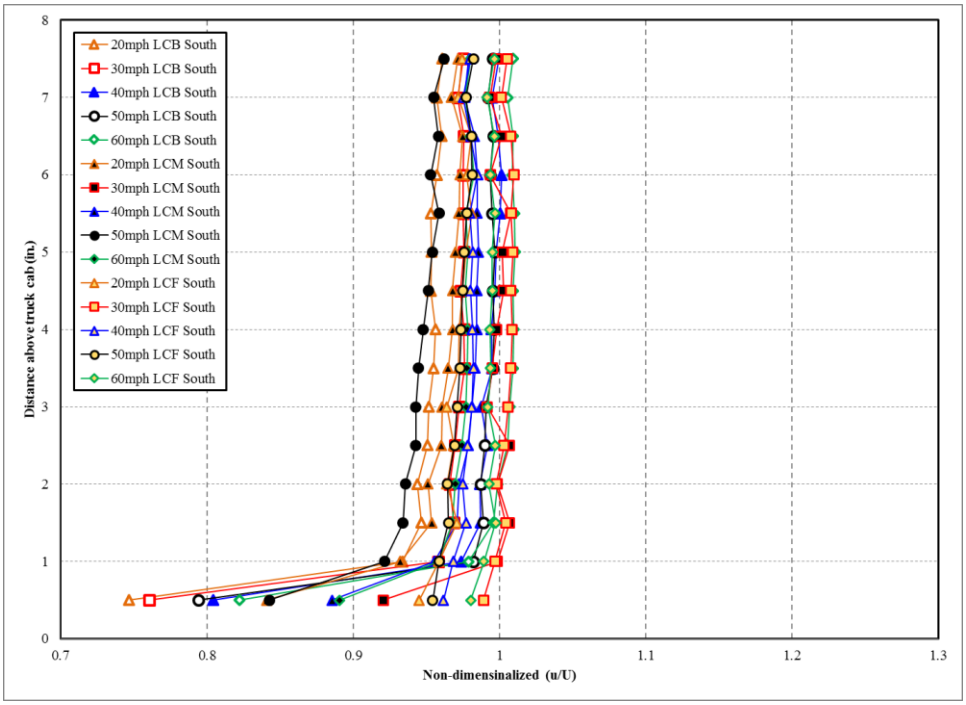

Figure 86-Left Center Positions Southbound Non-dimensionalized

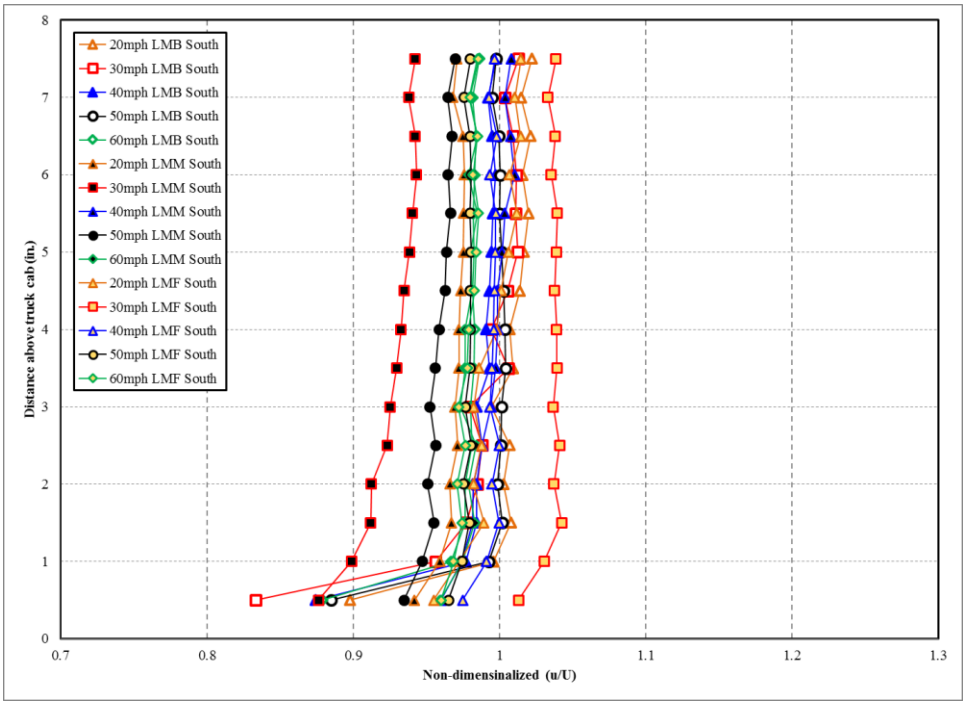

Figure 87-Left Middle Positions Southbound Non-dimensionalized

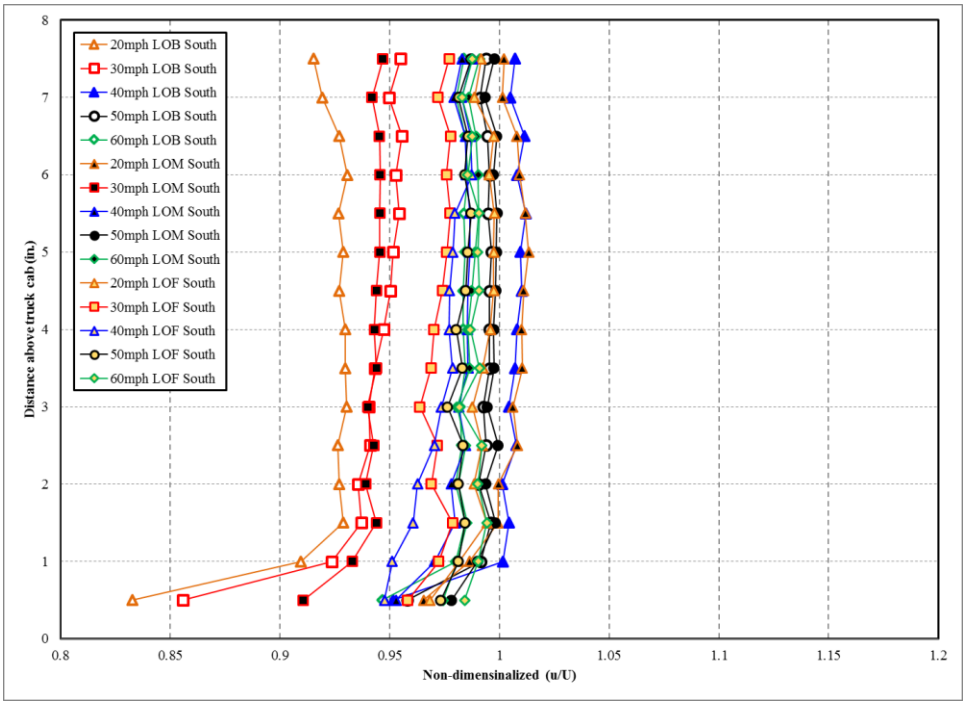

Figure 88-Left Outer Positions Southbound Non-dimensionalized

Appendix F- Results of Full Scale Tests #3

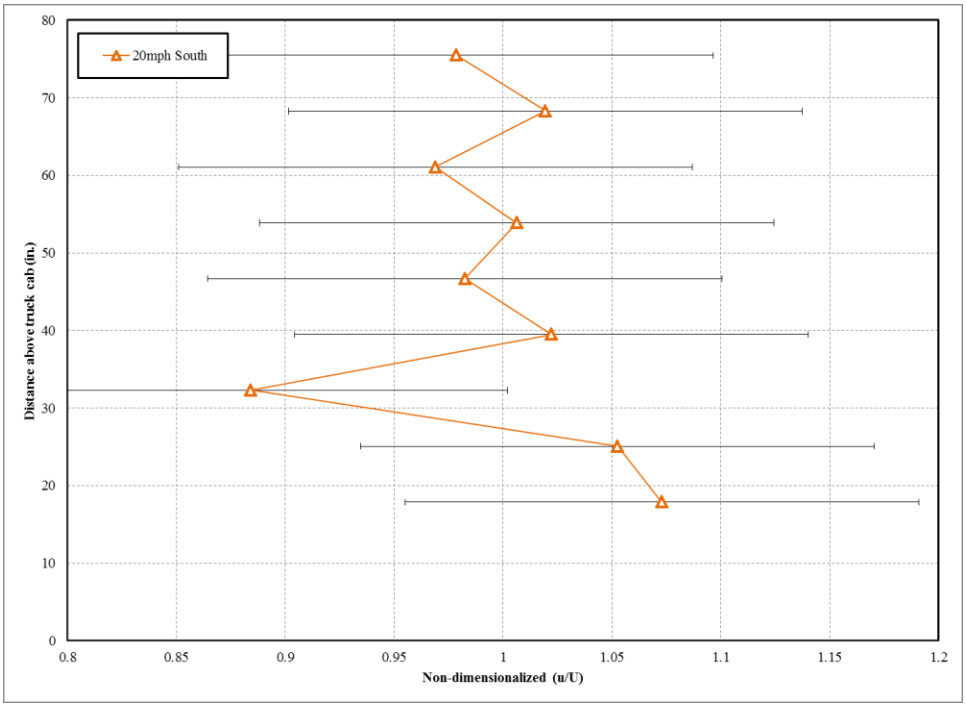

Figure 89-Nondimensionalized Southbound at 20mph with Error Bars

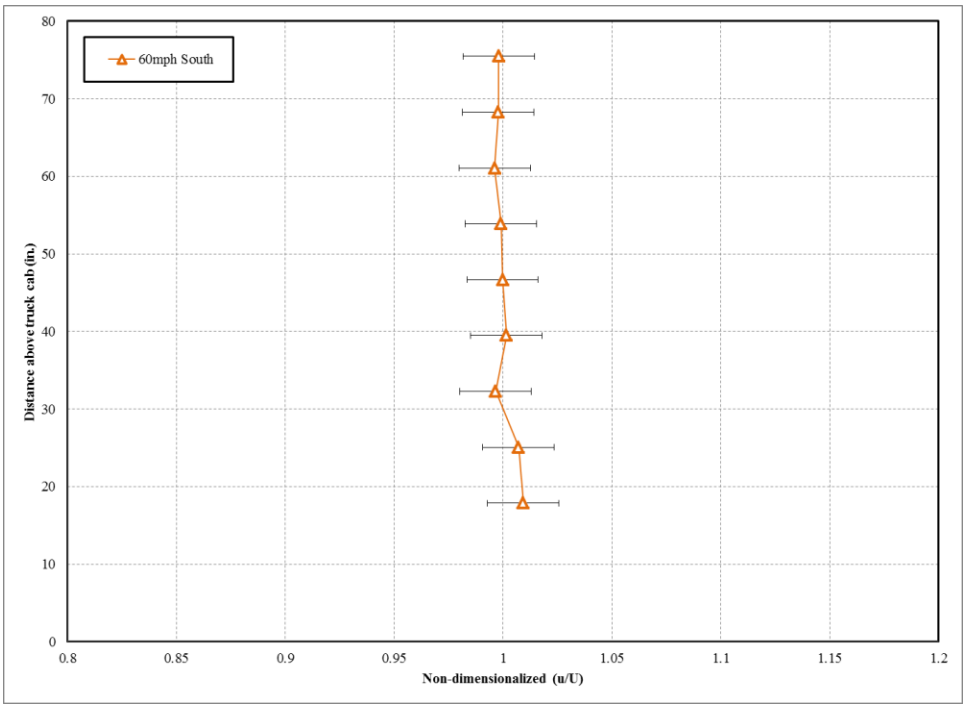

Figure 90-Nondimensionalized Southbound at 60mph with Error Bars

Appendix G- Results of Qualitative Wind Tunnel

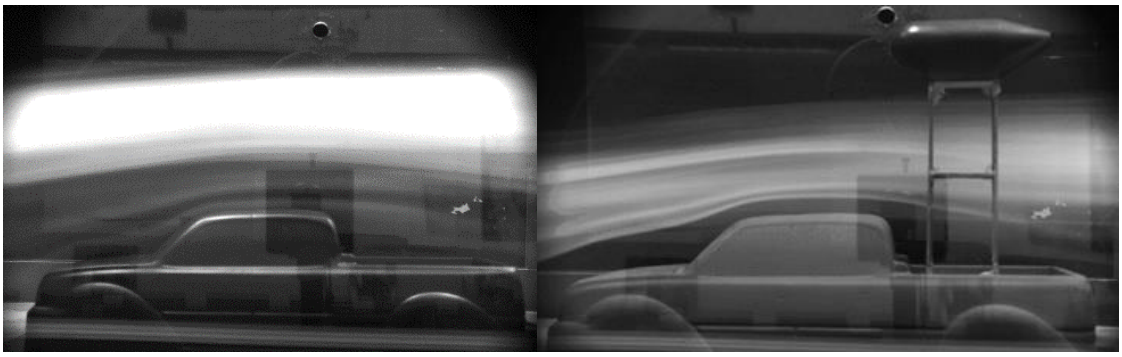

Figure 91-Flow Visualization With and Without Dyno with Reynolds Number of 4.9×10^5 (20mph)

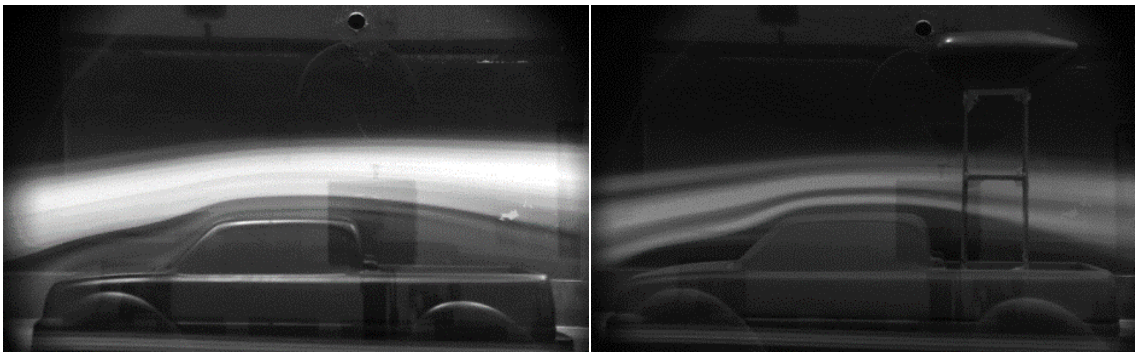

Figure 92- Flow Visualization With and Without Dyno with Reynolds Number of $9.8x10^5$ (40mph)

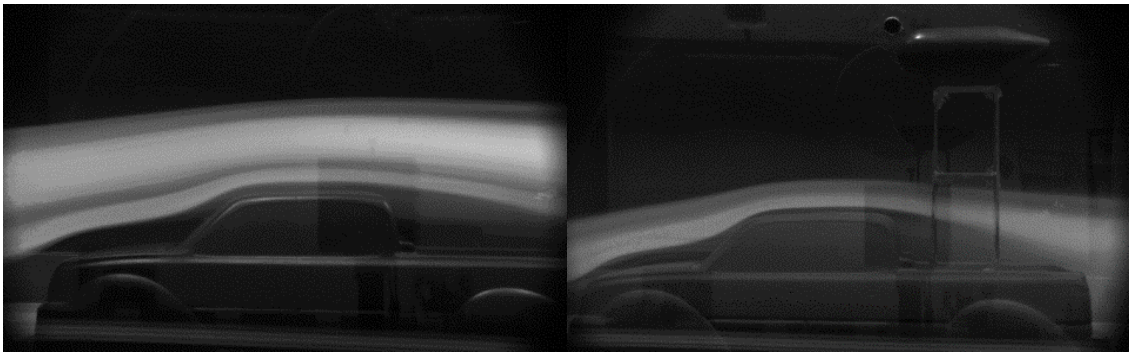

Figure 93- Flow Visualization With and Without Dyno with Reynolds Number of $1.2x10^6$ (50mph)

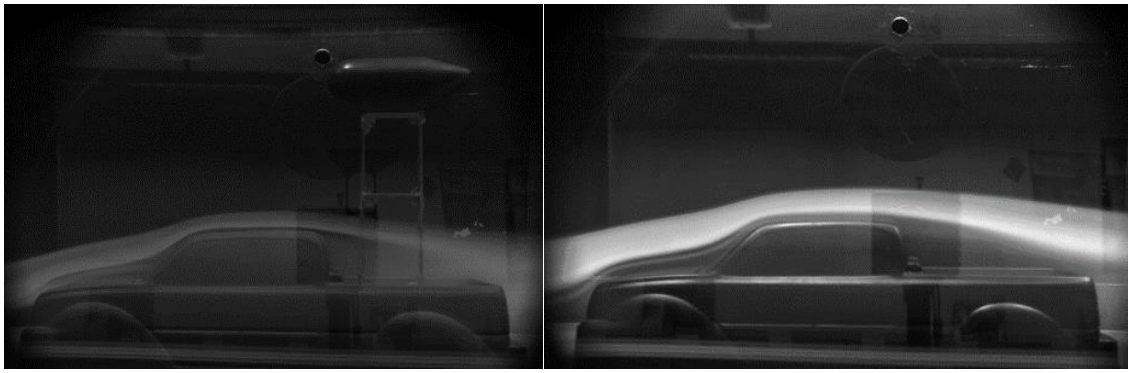

Figure 94- Flow Visualization With and Without Dyno with Reynolds Number of $1.5x10^6$ (60mph)

VITA

Mason Wade Morris

Candidate for the Degree of

Master of Science

Thesis: MOBILE PROPELLER DYNAMOMETER VALIDATION

Major Field: Mechanical and Aerospace Engineering

Biographical:

Education:

Completed the requirements for the Bachelor of Science in Aerospace Engineering at Oklahoma State University, Stillwater, Oklahoma in May, 2012.

Completed the requirements for the Bachelor of Science in Mechanical Engineering at Oklahoma State University, Stillwater, Oklahoma in May, 2012.

Experience:

Graduate Research Assistant, Department of Mechanical and Aerospace Engineering, Oklahoma State University, Stillwater, Oklahoma for Summer of 2012 and 2013, Fall of 2012.

Graduate Teaching Assistant, Department of Mechanical and Aerospace Engineering, Oklahoma State University, Stillwater, Oklahoma for Fall of 2012 and 2013, Spring of 2012 and 2013.

Summer Internship, Michelin North America, Ardmore, Oklahoma, 2008

Summer Internship, East Jordan Iron Works, Ardmore, Oklahoma, 2010

Summer Internship, Zeeco, Broken Arrow, Oklahoma, 2011

Professional Memberships: AIAA, ASME, AUVSI